ABSORPTIVE CORRECTIONS AND HIGHER SYMMETRIES FOR PRODUCTION PROCESSES.

by

KEVIN MICHAEL MORIARTY

A thesis presented for the Degree of
Doctor of Philosophy of the University of London
and the Diploma of Imperial College.

Department of Theoretical Physics,
Imperial College of Science & Technology,
LONDON.

April, 1971.

ABSTRACT

The elementary and Reggeized Absorption models are applied to the reaction $0^-\frac{1}{2}^+ \to 1^- \ {}^3/_2{}^+$. U(6,6) symmetry is used to predict all couplings for spin-0 and spin-1 exchanges. In the Reggeized version the spin-2 exchanges are obtained by the assumption of strong exchange degeneracy. There are no drastic failures of the model and some considerable successes. Of course, the better fit to the experimental data is obtained by the Reggeized version of the model, due to the improved energy dependence of the vector and tensor exchanges.

PREFACE

The work described in this thesis was carried out under the supervision of Professor P.T. Matthews in the Department of Physics, Imperial College, London between October 1965 and September 1970. The material presented in the text is original, except in so far as explicit reference is made to the work of others, and has not been submitted for a Degree in this or any other university.

The author wishes to thank Professor P.T. Matthews for his encouragement and advice. He also expresses his gratitude to many members of the Theoretical Physics Department, in particular to Dr. R.W. Moore and B.J. Hartley with whom he collaborated for parts of this and similar work.

The financial assistance of the National Research Council of Canada from May 1966 to April 1969 and of the Science Research Council of Great Britain from May 1969 to September 1970 is gratefully acknowledged.

I would finally like to thank my parents for their continued help and my wife Mavis who typed this thesis. But for her enthusiasm and rapid typing of this thesis it might have taken longer to complete.

CONTENTS

Page.

APPENDICES

CHAPTER I

INTRODUCTION

1.1 Characteristic Features of Two-Body Scattering.

Experimental information on hadron-hadron collisions exist in great abundance for two-body and quasi-two-body processes. (The term quasi-two-body is applied to those processes in which resonances living long enough to be treated as particles are produced). These processes may be represented in the centre-of-mass frame of the incoming particles 1 and 2 as a collision yielding particles 3 and 4 at an angle θ with respect to the incoming direction. This is shown schematically in Fig. 1.

For multiparticle production processes initiated by collisions of elementary particles at high energies (say above the resonance region ~ 3 GeV/c) we can make the following observation. Dalitz plots of these reactions show that a large part of the final state proceeds through the formation of one or more resonances, which subsequently decay[1]. In Fig. 2 we show the Triangle plot for the reaction[2]

$$K^+P \rightarrow K^+ \pi^-\pi^+ P \ .$$

In Fig. 3 we show the $M(K^+ \pi^-)$ and $M(P \pi^+)$ projections of the Triangle plot. It is clear that a large proportion of the events proceed through the two reactions

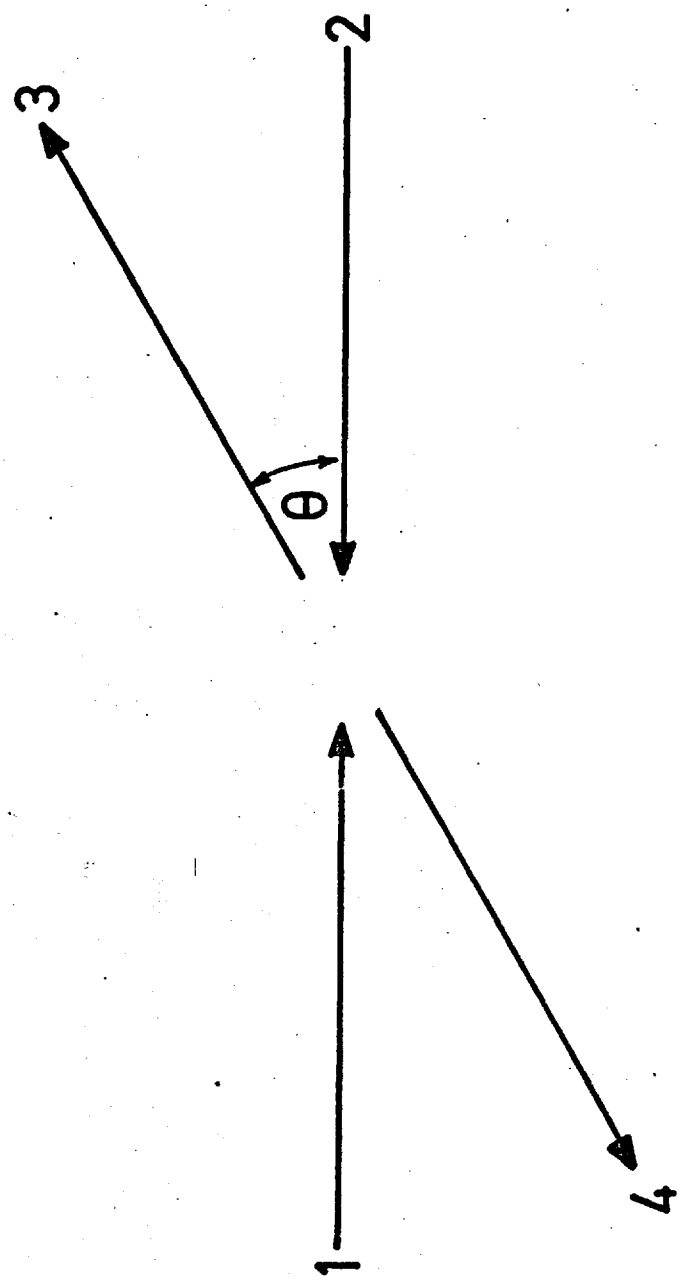

FIG. 1.

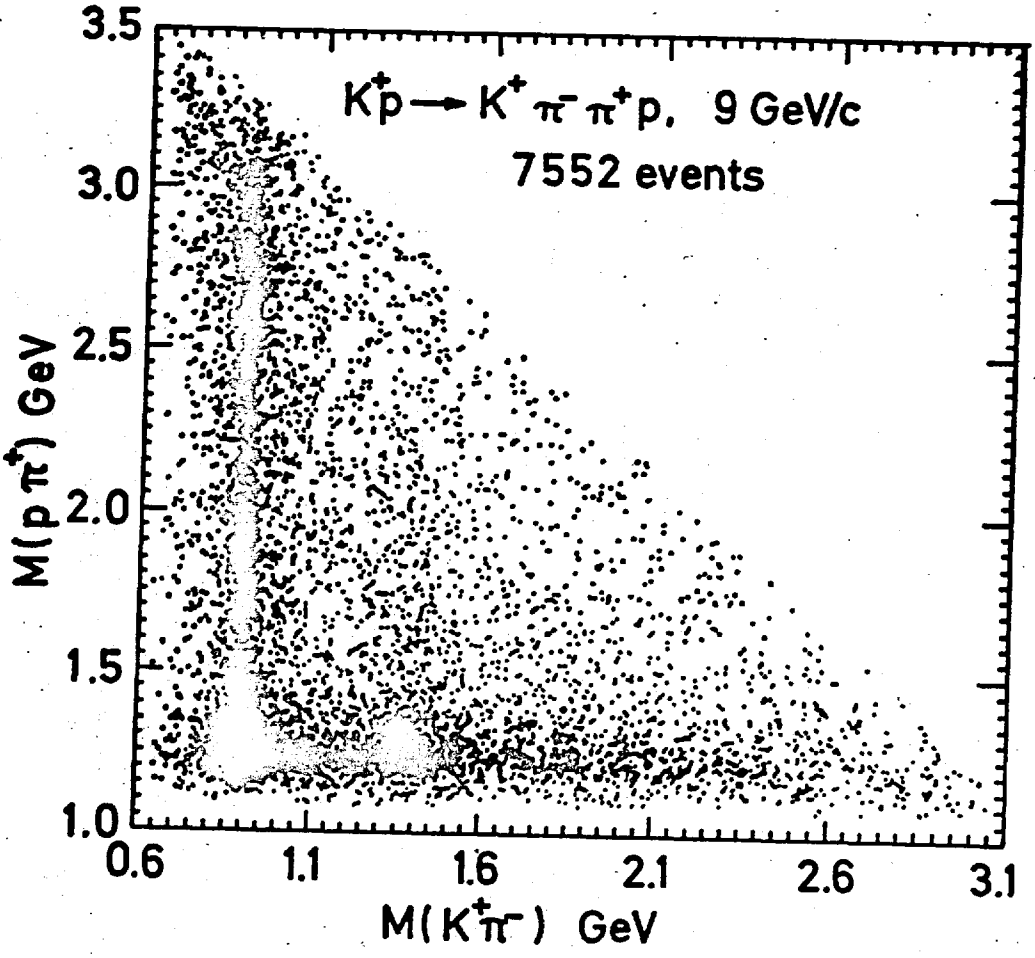
$K^+p \rightarrow K^+\pi^-\pi^+p$, 9 GeV/c
7552 events
3.5
3.0
2.5
2.0
1.5
1.0
$M(p\pi^+)$ GeV
0.6
1.1
1.6
2.1
2.6
3.1
$M(K^+\pi^-)$ GeV

FIG. 2.

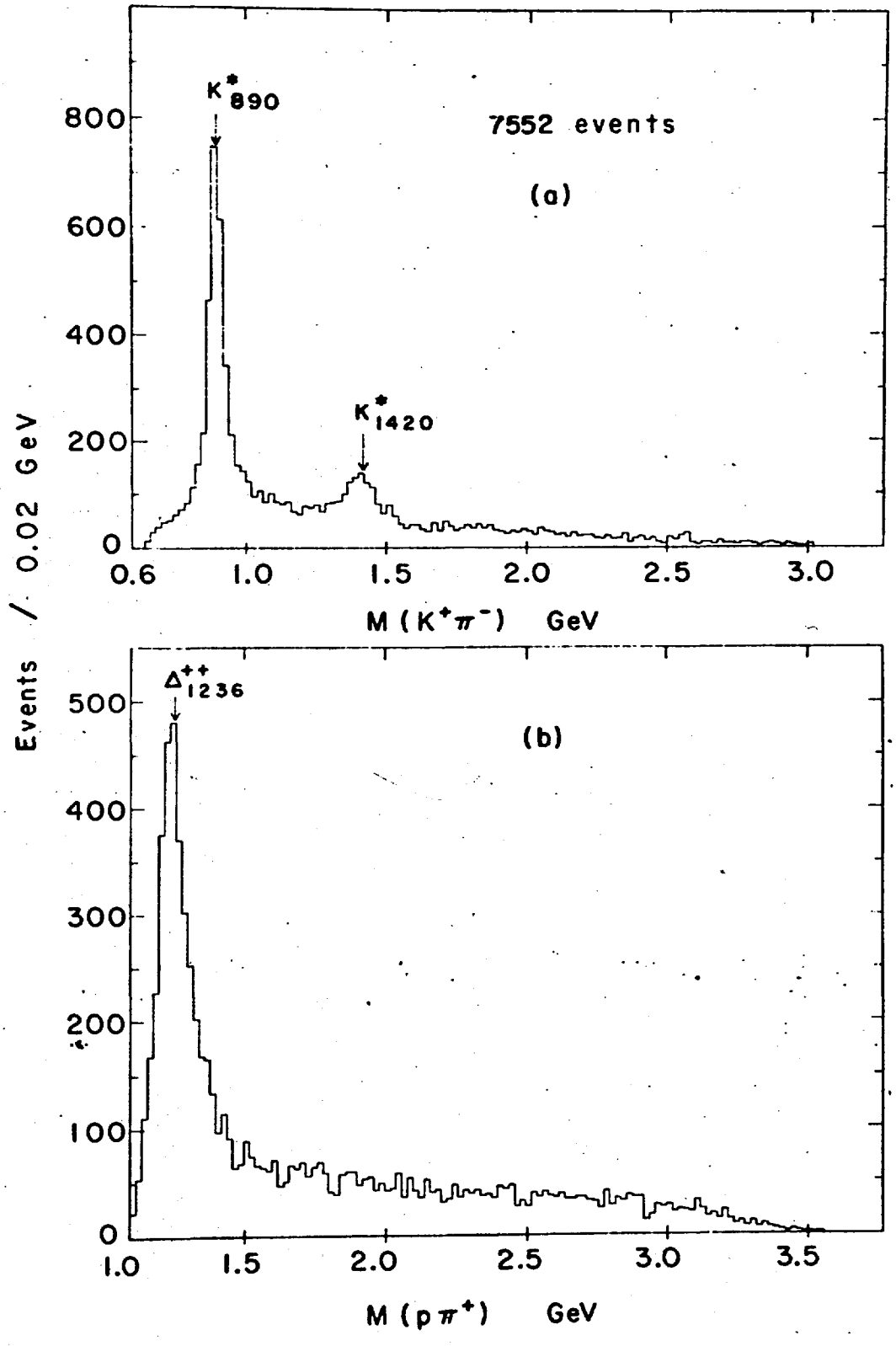
K*890
7552 events
(a)
K*1420
800
600
400
200
0
0.6
1.0
1.5
2.0
2.5
3.0
Events / 0.02 GeV
M(K+π−) GeV
Δ++1236
(b)
500
400
300
200
100
0
1.0
1.5
2.0
2.5
3.0
3.5
M(pπ+) GeV

FIG. 3.

$$K^+P \to K^{*o}(890)\,\Delta^{++}$$
$$\quad\;\; |\to \qquad\quad |\to$$
$$\quad\;\; K^+\pi^- \qquad\quad P\pi^+ \quad ,$$

$$K^+P \to K^{*o}(1420)\,\Delta^{++}$$
$$\quad\;\; |\to \qquad\quad |\to$$
$$\quad\;\; K^+\pi^- \qquad\quad P\pi^+ \quad .$$

The two-body process of Fig. 1 will be described by the three Lorentz-invariant variables

$$s = (P_1+P_2)^2 = E^2_{c.m.}$$

$$t = (P_1-P_3)^2 = \text{square of four-momentum transfer between particles 1 and 3}$$

$$u = (P_1-P_4)^2 = \text{square of four-momentum transfer between particles 1 and 4}$$

where $P_i = (\underline{P}_i;E_i)$ is the four-momentum of particle i. These three variables satisfy the relation

$$s + t + u = \sum_i m_i^2$$

We define two-body or quasi-two-body exchange reactions as those reactions where non-vanishing intrinsic quantum numbers are

exchanged in the t- or u-channel, where we call intrinsic any quantum number other than angular momentum and associated parity. One of the empirical facts resulting from all the experimental data on such processes is that forward or backward peaks occur if, and only if, the quantum numbers allow the exchange of a member of a U(3) singlet, octet or decuplet in the t- or u-channel[3]. Here we define the forward and backward directions by following the baryon number. This is illustrated in Fig.4.

The peaking of the differential cross-sections near $t = o$ $(u = o)$ for forward (backward) scattering, suggests that the amplitudes describing these processes may be dominated by the presence of singularities which occur near $t = o$ $(u = o)$ but in the kinematically forbidden region of t and u; this region is called the crossed channel. In the case of forward (backward) scattering the crossed channel which is closest to the physical region, and therefore expected to dominate is the t-channel (u-channel). To be more explicit, if the reaction we are studying is

$$1 + 2 \to 3 + 4 \qquad \text{(s-channel)}$$

then its amplitude is related to the amplitude of the reactions

$$1 + \bar{3} \to \bar{2} + 4 \qquad \text{(t-channel)}$$

$$1 + \bar{4} \to \bar{2} + 3 \qquad \text{(u-channel)}$$

by analytic continuation. Therefore, if the t-channel S-matrix contains a singularity near $t = o$ at a value of t which is non-physical for the s-channel, such that the t-channel amplitude has a

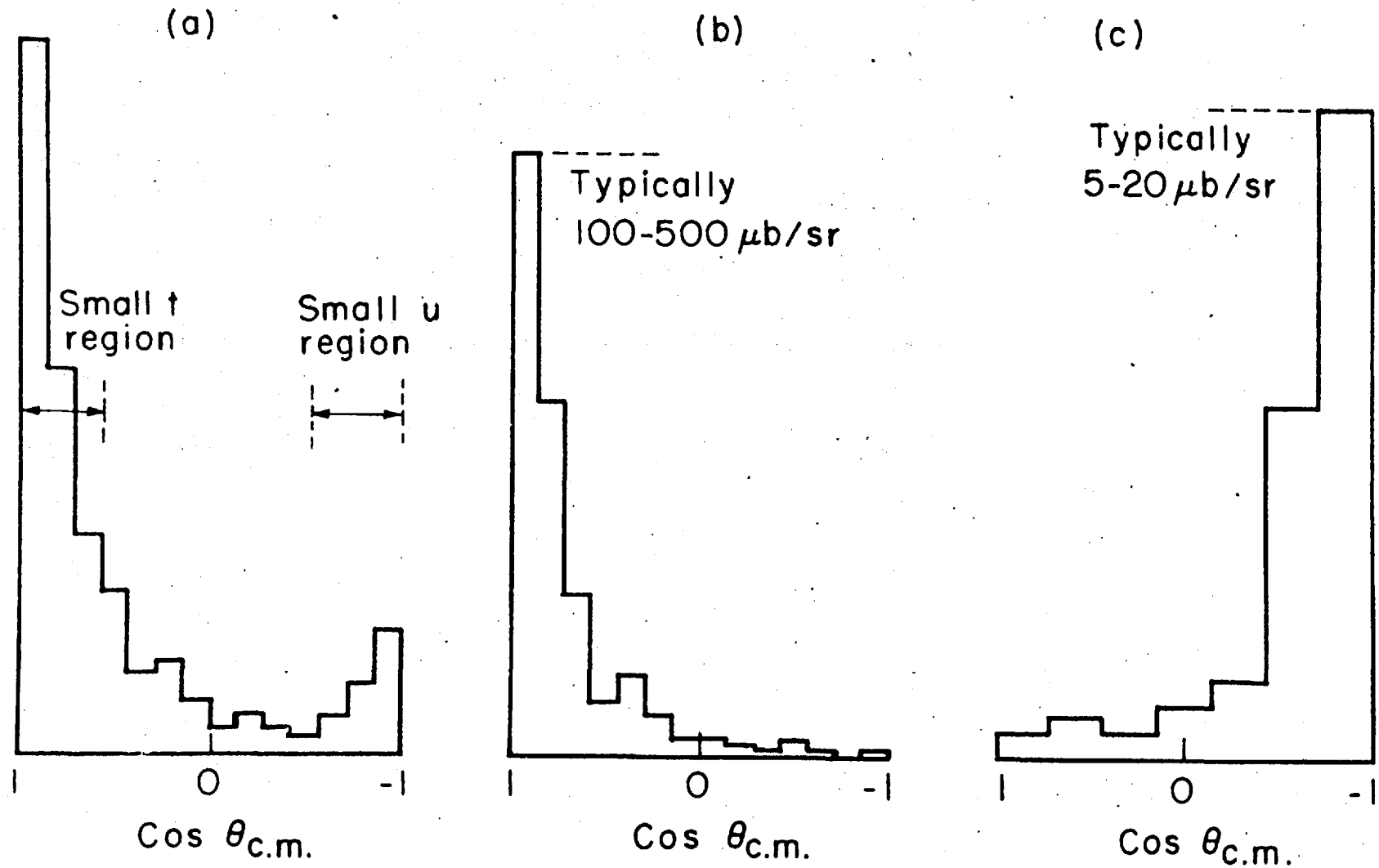
(a)
(b)
(c)
Small t region
Small u region
Typically 100-500 μb/sr
Typically 5-20 μb/sr
1
0
-1
Cos θc.m.

FIG. 4.

maximum, one expects that the analytically continued s-channel amplitude will be dominated by this t-channel singularity for small values of $|t|$.

1.2 Early History of the Model.

The theoretical formulation of the model starts from the Feynman diagram in Fig.5. The incident particles 1 and 2 interact with each other by the exchange of particle e; this interaction leads to the particle systems 3 and 4.

According to Feynman rules the matrix element M_{fi} for the process $i \to f$ which is represented in the diagram has the following general structure:

$$M_{fi} = M_{13}(t, m_3^2) \frac{1}{t - m_e^2} M_{24}(t, m_4^2)$$

where M_{13} and M_{24} are the vertex functions. On the mass-shell they are the matrix elements for the following processes

$$1 + e \to 3$$
$$2 + \bar{e} \to 4 \quad .$$

When 3 and 4 are quasi or real particles these vertex functions at $t = m_e^2$ are proportional to the appropriate coupling constants. The factor $(t - m_e^2)^{-1}$ is the propagator of the exchanged particle.

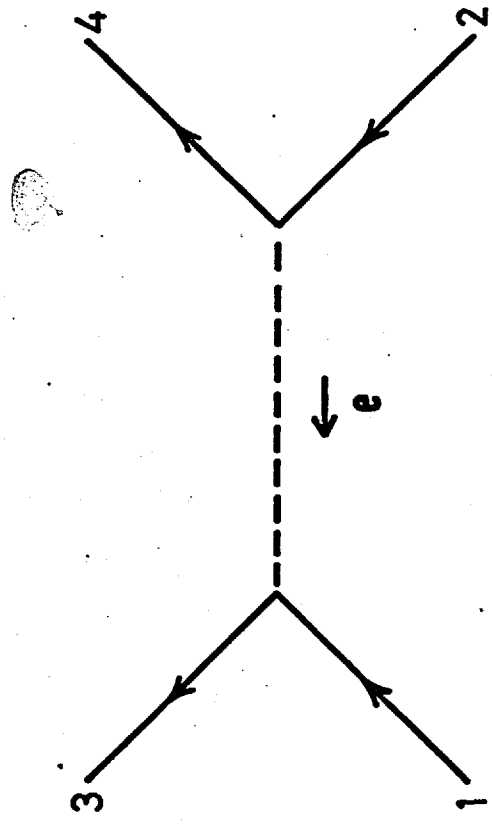

FIG. 5.

There thus exists poles in the S-matrix, in the momentum transfer, t, which correspond to the exchange of a single particle.

As an example, we consider nucleon-nucleon scattering. There is a diagram in which a pion is exchanged as shown in Fig.5. Neglecting spin, this gives a contribution to the scattering amplitude of the form

$$g \frac{1}{t - m_\pi^2} g$$

where g is the pion-nucleon coupling constant and m_π is the pion mass. We expect this pole term to dominate the NN scattering amplitude in the region $t \simeq m_\pi^2$. In the centre-of-mass system, however, $t = -2q_s^2(1-\cos\theta)$ where q_s is the s-channel centre-of-mass three-momentum, and so the singularity occurs at

$$\cos\theta = 1 + \frac{m_\pi^2}{2q_s^2} .$$

Since $\cos\theta$ is here greater than 1, the pole does not occur in the physical region. Hence in order to reach a region of $\cos\theta$ where one is sure that the pole dominates, it is necessary to extrapolate to beyond the forward direction as indicated in Fig.6. One may observe that, as the energy increases, the position of the pole moves closer to the physically accessible region. It has therefore been conjecture, as we stated previously, that at high energies the scattering amplitude in the physical region near the forward direction will be dominated by this type of pole. The approximation

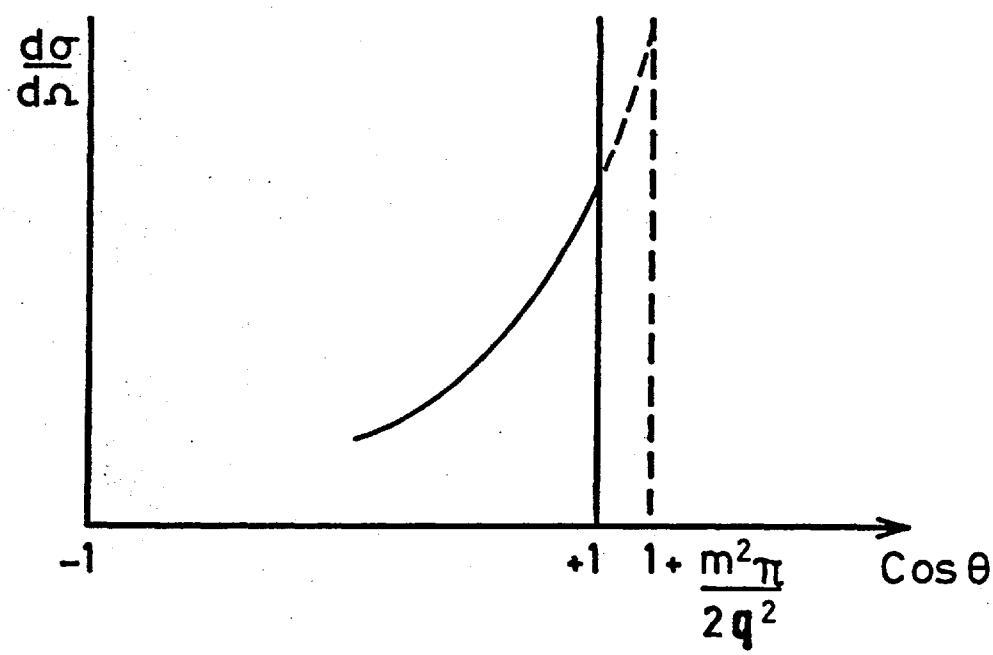

FIG. 6.

of keeping only this pole in describing the amplitude near $\cos\theta = 1$ is known (essentially) as the peripheral model and has had some success in describing high-energy experiments.

The basic assumption of the peripheral model is that the scattering amplitude is given by a sum of one-particle-exchange (OPE) amplitudes,

$$T = T_p + T_v + T_B + \ldots$$

where p = pseudoscalar, v = vector meson, B = baryon, indicate the quantum numbers of the exchanged particles. As previously indicated the motivation for this assumption arose from the fact that each term will contain the factor

$$\frac{1}{t - m^2} .$$

The function $(t - m^2)^{-1}$ is largest at the smallest value of -t and thus produces the type of peak found experimentally.

Let us consider the exchange of a particle of spin ℓ, as shown in Fig.7. Thus, we have in the s-channel

$$s = 4(q_s^2 + M^2) \quad ; \quad t = -2q_s^2(1-\cos\theta_s)$$

where $\cos\theta_s$ is the cosine of the scattering angle in the s-channel centre-of-mass frame. In the t-channel centre-of-mass, if $\cos\theta_t$ is the cosine of the scattering angle, and q_t the three-momentum,

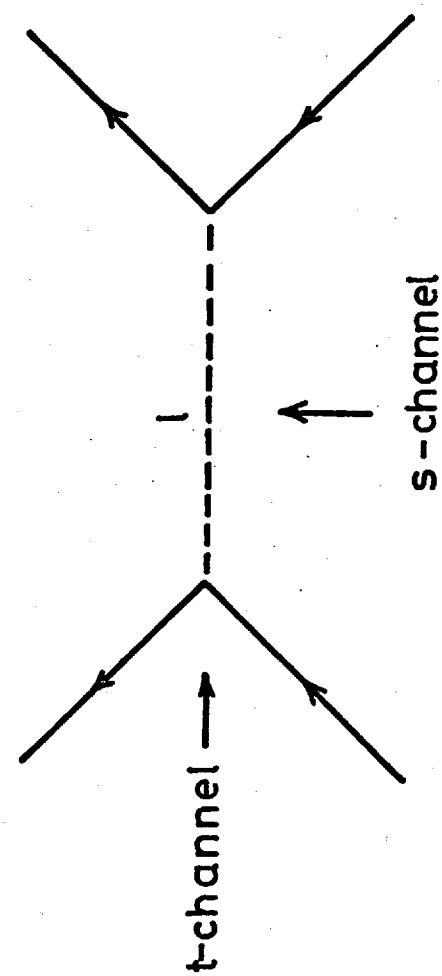

FIG. 7.

we have

$$s = -2q_t^2 (1-\cos\theta_t) \quad ; \quad t = 4(q_t^2 + M^2) \quad .$$

If we look at the process in the t-channel, by angular momentum conservation, only the ℓth partial wave can contribute. The pole term is therefore

$$\frac{g^2}{t - m^2} P_\ell(\cos\theta_t) = \frac{g^2}{t - m^2} P_\ell \left(1 + \frac{s}{2q_t^2}\right) \quad .$$

Looking now in the s-channel and letting $s \to \infty$, we see that if the pole term really dominates

$$T(t,s) \xrightarrow[\substack{s \to \infty \\ t \text{ fixed}}]{} \frac{g^2}{t - m^2} \left(\frac{s}{2q_t^2}\right)^\ell$$

where no functional relationship between m and ℓ is assumed. This means that if particles with arbitrarily large spin can be exchanged, the scattering amplitude can diverge arbitrarily fast. This is unfortunate as experiments show that cross sections do not diverge at high energy. In addition it has been shown from the axioms of field theory that there is a bound on the asymptotic total cross section called the Froissart bound which is given by

$$\lim_{s \to \infty} \sigma_{TOT}(s) < c \ln^2 (s) \quad .$$

The idea that the factor $(t-m^2)^{-1}$ is responsible for the

peaking at small $|t|$, although very attractive, is not borne out quantatively by specific calculations. Both the s- and t-dependence of the differential cross sections are found to be incorrect. Specifically the main failings are :

a) The momentum transfer distributions are not sufficiently peaked in the forward direction.

b) The absolute normalization of the momentum transfer distribution is too large, even at small momentum transfers.

c) Information about the exchange mechanism by which resonances are produced in quasi-two-body processes can be obtained from the t-dependence of the decay density matrices. The predictions of the elementary exchange model (using these exchanges) are found to be in gross disagreement with the data.

d) The s-dependence of the cross-sections is in error for all but spin-0 exchange.

1.3 Absorptive Corrections to the Peripheral Model.

In order to remedy these defects the idea of absorption was introduced. The peripheral absorption model has had some considerable success in explaining the production of resonances in quasi-two-body reactions, and the subsequent decay of resonances.

The main assumption of the peripheral absorption model, is that production amplitudes for forward or backward scattering must be modified to account for the effects of competing inelastic channels.

The absorption idea has had a long history. It originated in low-energy nuclear physics in the suggestion put forward by Butler in 1957[4]. A full exposition of this can be found in the review article by Dar[5]. In high-energy physics the model was first proposed in 1962 by Sopkovich,who treated the reactions $N\bar{N} \to K\bar{K}$ and $N\bar{N} \to Y\bar{Y}$[6]. The model was then successfully applied to a number of reactions. A complete review of this can be found in the article by Jackson[7].

The basic assumption of the peripheral absorption model is that in reactions where fixed or moving poles are exchanged, the partial wave amplitude for the process is given by the traditional Watson formula[8]

$$T'^{j}_{fi} = \frac{1}{2} \left(S^{j}_{ff} T^{j}_{fi} + T^{j}_{fi} S^{j}_{ii} \right)$$

where T^{j}_{fi} is the partial wave amplitude for the process $i \to f$, j is the total angular momentum, and S_{ii} and S_{ff} are the elastic scattering S-matrix elements in the initial and final states respectively. For practical purposes we diagonalise the elastic scattering S-matrix elements, take them to be independent of helicity and parameterize it as a pure Gaussian. This is done because elastic scattering at high energies is dominated by the forward diffraction

peak and the S-matrix is mainly diffractive and helicity preserving.

Because we are usually unable to observe the elastic scattering of the final state particles we make the additional assumption that

$$S_{ff} = S_{ii} .$$

This is strictly only true for pair-wise equal mass scattering. Then our formula becomes

$$T'^{j}_{fi} = S^{j}_{ii} \; T^{j}_{fi} .$$

This modification has the effect of making

$$T'^{j}_{fi} \simeq T^{j}_{fi}$$

for large values of j while

$$| T'^{j}_{fi} | << | T^{j}_{fi} | .$$

for small values of j, where the influence of the competing channels would be felt the most. Thus, the low partial waves are suppressed, with the s-wave almost completely eliminated. When the partial-wave series is resummed, the modified amplitude looks quite different from the original Born amplitude.

There is usually considerable freedom of manoeuvre in calculating pole graphs for peripheral collisions, which arise from three main sources : (i) there is often a wide variety of particles to be considered as intermediary; (ii) there are often alternative couplings possible at the vertices and (iii) the values of the coupling constants may usually be chosen freely.

Rather than use arbitrary D to F ratios, and relative magnitudes of vertex couplings it seems preferable to assume some higher symmetry in which the Lagrangian and the coupling constants are uniquely determined, and compare the model against experiment. In this work we assume the U(6,6) symmetry[9]. The U(6,6) effective interaction Lagrangian is given by

$$\mathcal{L} = g\,(J_5\,\phi_5 + J_\mu \phi_\mu) + h\,(J_5\,\phi_5 + J_\mu \phi_\mu)$$

where ϕ_5 and ϕ_μ are the pseudoscalar and vector nonets and g and h are the "U(6,6) coupling constants".

1.4 Criticism of the Model.

The differential cross section for the exchange of a fixed pole of spin J behaves like (see previous section)

$$\frac{d\sigma}{dt} = f(t)\ s^{2J-2}\ , \qquad s \to \infty\ .$$

It is now well known that the inclusion of absorptive effects, as in the present work, cannot effect the energy dependence of the

differential cross section[10]. Since all production cross sections decrease with energy at sufficiently high energy, only spin-0 exchange can be expected to give agreement at all energies. The use of the absorption model for the exchange of elementary particles with spin can only be expected to produce agreement with experiment over a limited range of incident momenta.

By treating the spin of the exchanged particle as virtual we are able to improve the situation for higher-spin exchange. This idea, which was first put forward by Regge[11], is to treat the spin as a function of the momentum transfer, $J \to \alpha(t)$, i.e., as a continuous variable. In this case our momentum transfer dependence is

$$\frac{d\sigma}{dt} = f(t)\, s^{2\alpha(t)-2} \quad , \quad s \to \infty \, .$$

The s-channel reaction $\pi^- p \to \pi^0 n$ has the following quantum numbers in the t-channel: Y=0, B=0, G = +1, I = +1. The only possible exchanges are the

$$\rho(.765 \text{ GeV}, \; J^{PG} = 1^{-+})$$

and

$$g(1.650 \text{ GeV}, \; J^{PG} = 3^{-+}) \, .$$

A fit to the momentum transfer data above 4 GeV/c was made by Höhler et. al.[12] Using the above equation over the range

$$-1.0 < t < 0.0 \quad (\mathrm{GeV}/c)^2$$

they obtained

$$\alpha(t) = (0.57 \pm 0.01) + (0.91 \pm 0.06)t \quad .$$

Their fit is shown in Fig.8. which is referred to in the literature as a Chew-Frautchi plot. It is interesting to note that the extrapolation of the $\alpha(t)$ determined for $t<0$ (scattering region) into $t>0$ (resonance region) intercepts $\alpha = 1.1$ at the mass of the ρ, and $\alpha = 3.03$ at the mass of the g. $J=1$ is, of course, the established spin of the ρ and $J=3$ is the preferred experimental value for the spin of the g. We have therefore reached the remarkable phenomenological conclusion that for charge-exchange scattering the t-channel singularities are not fixed in the J-plane, and that moreover they seem to be constrained to move in such a way that when projected into the resonance region they intercept integer values of J which correspond to the physical resonances which can be exchanged in the t-channel.

With the aid of Reggeization we are able to produce quite remarkable agreement with the data for the s-dependence of a large number of reactions. Thus, the problems of high spin exchange vanish with the introduction of the Reggeization procedure.

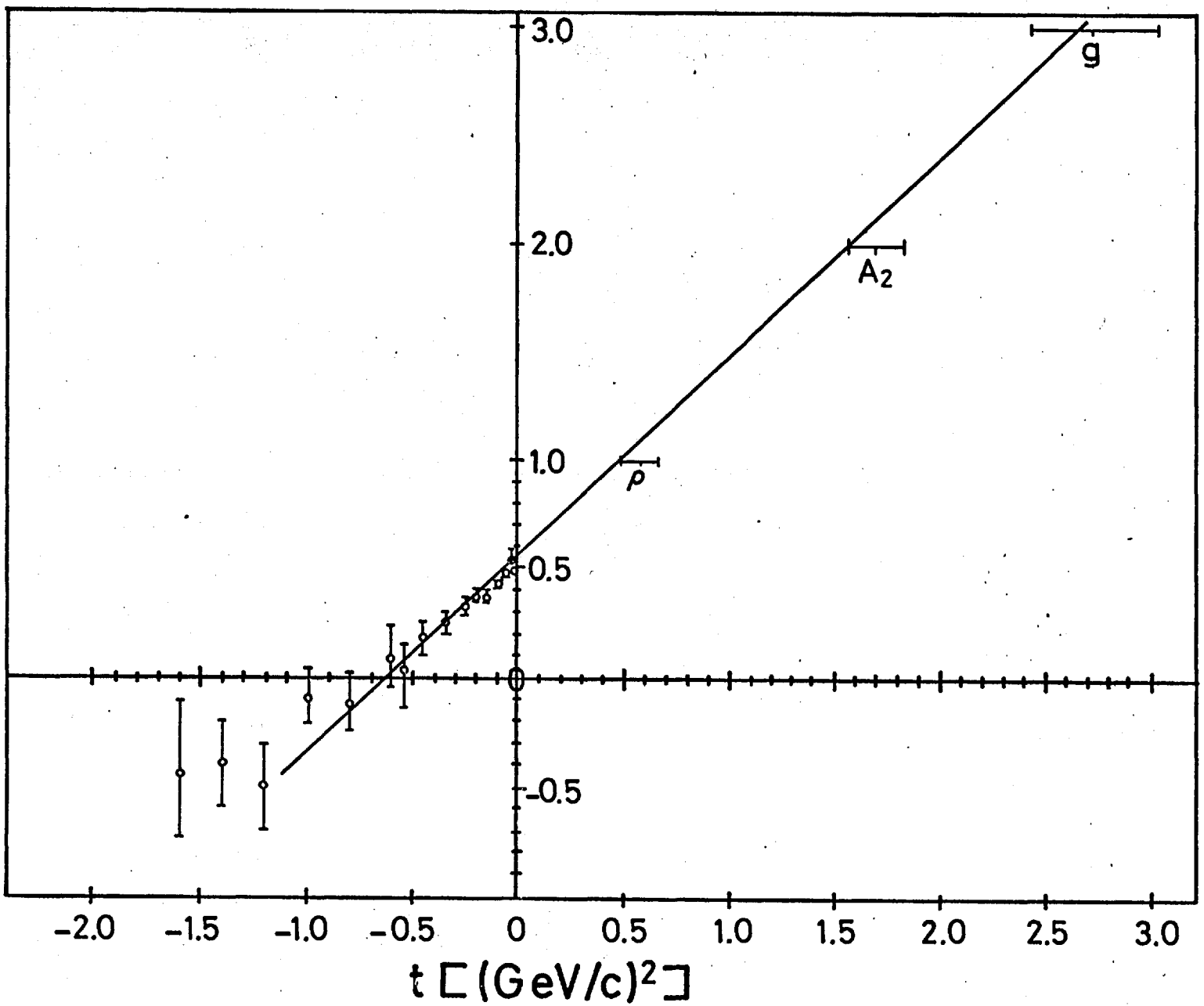

FIG. 8.

1.5 Reggeization.

In the simple Regge-pole model one assumes that the amplitude which describes peripheral processes is dominated by a crossed-channel singularity which moves in the J-plane. The locus of these poles is described by $\alpha(t)$ (or $\alpha(u)$ if we are considering the u-channel) which is called a Regge trajectory. Each trajectory possesses definite quantum numbers such as isotopic spin I, parity P, hypercharge Y, baryon number B, G-parity (in the case of non-strange mesons and baryons) and signature τ. When $\alpha(t)$ is extended to $t > 0$ it intercepts integer values of α at $t = t_R$, where t_R equals the mass squared of resonances having the quantum numbers of the crossed channel and spin $J = \alpha(t_R)$ where $(-1)^J = \tau$ (for baryon trajectories the signature is given by $(-1)^{J-\frac{1}{2}}$).

The specific result of the model for the case where there is only one trajectory and where we neglect the spin of the external particles is that the scattering amplitude for large s is given by

$$A(s,t) = \frac{\beta(t)\,\xi(t)}{\Gamma(1+\alpha)\sin\pi\alpha(t)} \left(\frac{s}{s_0} \right)^{\alpha(t)}$$

where $\xi(t) = 1 + \tau e^{-i\pi\alpha(t)}$ is the signature factor, s_0 is a scale factor traditionally taken to be $1(\mathrm{GeV}/c)^2$ and $\alpha(t)$ is the Regge trajectory.

We may now briefly examine the function of each term in the above equation. $\beta(t)$ is the residue function, which is related

to the coupling constant in the one-particle-exchange (OPE) model. For the process 1+2 → 3+4 it is assumed that

$$\beta(t) = \gamma_{1\bar{3}}(t)\ \gamma_{2\bar{4}}(t)$$

which is called factorization. The term $\{\sin\pi\ \alpha(t)\}^{-1}$ gives: poles at integer values of $\alpha(t)$ and can be compared with the propagator in the one-particle-exchange model. The signature factor $\xi(t)$ gives a zero at integer values of $\alpha(t)$, which correspond to wrong signature points (values of α such that $(-1)^{\alpha} = -\tau$) which means that in the resonance region poles occur on a trajectory in steps $\Delta J=2$ at values of α where $(-1)^{\alpha} = \tau$. The factor $\{\Gamma(1+\alpha)\}^{-1}$ compensates the poles of $\sin\pi\alpha(t)$ for negative integer values of α, which are nonsense values of the spin. The combined effect of $\xi(t)\{\Gamma(1+\alpha)\}^{-1}$ is to give a zero in the Regge amplitude at wrong signature nonsense values of α; since these values of α occur in the scattering region the differential cross section will have a dip-bump structure.

A drawback of the absorption model with moving pole input is that for proper application it requires a knowledge of the elastic scattering amplitudes in both the initial and final states. However, there are only a limited number of final states for which the elastic scattering parameters can be evaluated, e.g., $pn \to np$ and $\pi^{-}P \to \pi^{0}n$[13]. Thus, we are forced, if we want to keep the model as free as possible of arbitrary parameters, to make the assumption that the initial and final state scattering parameters are the same.

A criticism of the Reggeized absorption model is that although the absorptive correction prescription is an unambiguous parameter-free technique of introducing Regge cuts, it is probably not the complete answer on cuts. In particular, cuts other than Regge pole-Pomeron cuts are not included.

The many attempts to justify the absorption model prescription are not entirely convincing[14]. At present we must regard the absorption prescription as an ansatz which can only be tested by comparison with experiment.

In spite of these difficulties the peripheral absorption model with moving poles is able to correlate a large number of experimental facts. Thus, even though the theoretical basis of the model is very shaky we believe that the prescription predicts production amplitudes which are a good approximation to the actual amplitudes. The prescription, as we use it, is absolutely devoid of any free parameters. Thus, while making comparisons with the data on s- and t-dependences of the data we are able to compare absolute normalizations as well.

Previously we mentioned the considerable freedom of manoeuvre in calculating pole graphs for elementary particle exchange. Reggeization of such graphs gives rise to additional freedom which has three main sources: (i) the possibility of different exponential damping factors in each vertex coupling factor; (ii) a choice of various kinds of dip mechanisms at nonsense points and (iii) the impossibility of measuring some of the coupling constants for higher spins, e.g., $g_{A_2\bar{N}N}$. This freedom results in the t-dependence of the differential cross sections being essentially arbitrary.

1.6 Description of Thesis.

The present work is concerned with the application of the absorptive peripheral model with fixed and with moving poles exchanged. The particular reactions considered are of the type

$$0^-\tfrac{1}{2}^+ \to 1^- \, {}^3/_2{}^+$$

of which the only ones for which data exists are

$$\pi^+ p \to \rho^0 \, \Delta^{++}$$

$$\pi^+ p \to \omega^0 \, \Delta^{++}$$

$$K^+ p \to K^{*0} \, \Delta^{++}$$

$$K^- n \to \overline{K^{*0}} \, \Delta^- \, .$$

We present a detailed account of our method of calculation. Firstly, we calculate the pole graphs for spin-0 and spin-1 exchange and with absorptive effects included compare these with the available experimental data.

The spin is then Reggeized and the spin-2 contribution is obtained from the spin-1 exchange amplitude by the assumption of strong exchange degeneracy. These results are then compared with the experimental data.

CHAPTER II

THE U(6,6) ABSORPTION MODEL

2.1 The U(6,6) Symmetry Scheme.

In any given reaction, there are usually a multitude of possible particles which can be exchanged. Thus, the couplings at the three-point vertices must be obtained. Some of these couplings can be fixed by appealing to SU(6), universality or isospin invariance. However, we cannot fix all the couplings without using a higher symmetry scheme or by choosing the unknown couplings to be parameters to be fitted to the data[15]. We choose the former approach and use U(6,6) ⊗ O(3,1). In this section we illustrate how this group can be used to calculate the pole graphs for all reactions of the type $\underline{35} \otimes \underline{56} \to \overline{\underline{35}} \otimes \overline{\underline{56}}$ and $\underline{56} \otimes \underline{56} \to \overline{\underline{56}} \otimes \overline{\underline{56}}$ which proceed by $\underline{35}$ exchange in the t-channel and $\underline{35} \otimes \underline{56} \to \overline{\underline{35}} \otimes \overline{\underline{56}}$ which proceeds by $\underline{56}$ exchange in the u-channel in terms of $\underline{\text{two}}$ coupling constants which can be determined experimentally. Since the $\underline{35}$-plet contains the 0^- octet and 1^- nonet and the $\underline{56}$-plet contains the $\frac{1}{2}^+$ octet and $^3/_2{}^+$ decuplet, this accounts for a large section of the two-body and quasi-two-body processes on which data is presently available. In this symmetry scheme, higher multiplets can be regarded as angular momentum excited recurrences of lower ones.

The U(6,6) algebra has 144 generators

$$(J_{Ri})_A^B \equiv (J_{Ri})_{a\alpha}^{b\beta} \equiv (T_i)_a^b (\gamma_R)_\alpha^\beta .$$

$$R = 1,2,\ldots, 16 ; \; i = 0,1,\ldots,8 ; A,B = 1,2,\ldots,12$$

and the γ_R are the Dirac matrices

$$\gamma_R = 1, \gamma_\mu, \sigma_{\mu\nu} = \frac{i}{2}(\gamma_\mu,\gamma_\nu) \quad , \quad i\gamma_\mu \gamma_5, \gamma_5 = \gamma_0\gamma_1\gamma_2\gamma_3 .$$

The T_i are defined by

$$T_i = \frac{1}{2}\lambda_i \quad (i = 1, \ldots, 8) \quad ,$$

$$T_o = \frac{1}{\sqrt{6}}$$

where the λ_i are defined by Gell-Mann[16].

The basic spinor representation (quark) transforms under the group in the following way:

$$\psi_A \rightarrow S_A^B \psi_B$$

with

$$S_A^B = (\exp (i\epsilon_{Ri} T_{Ri}))_A^B .$$

By taking products of quark representations and reducing to irreducible components higher representations can be constructed. The product of quark and anti-quark gives

$$\underline{12} \otimes \overline{\underline{12}} = \underline{1} \oplus \underline{143}$$

and the product of three quarks gives

$$\underline{12} \otimes \underline{12} \otimes \underline{12} = \underline{220} \oplus \underline{364} \oplus \underline{572} \oplus \underline{572}$$

where representations are denoted by their dimensions.

Two of the above multi-spinor representations are of interest to us; (i) the traceless meson tensor $\Phi_A{}^B(143)$ and the (ii) fully symmetric baryon tensor $\psi_{(ABC)}(364)$.

Under SU(3) $\otimes$ U(2,2) these decompose as

$$\underline{143} = (8,15) \oplus (1,15) \oplus (8,1)$$

$$\underline{364} = (10,20) \oplus (8,20) \oplus (1,4) .$$

Thus the $\underline{143}$ contains the pseudoscalar meson octet and vector meson nonet and the $\underline{364}$ contains the baryon octet ($\frac{1}{2}^+$) and decuplet ($^3/_2{}^+$).

The explicit decomposition of the meson tensor is

$$\Phi_A{}^B = (\gamma_R T_i)_A{}^B \, \Phi^{Ri}$$

$$= (T_i)_a{}^b \left(\phi^i + \gamma_5 \phi_5{}^i + i\gamma_\mu \gamma_5 \phi^i_{\mu 5} + \gamma_\mu \phi^i_\mu + \tfrac{1}{2}\sigma_{\mu\nu}\phi^i_{\mu\nu}\right)^\beta_\alpha$$

for a,b = 1,2,3 ; α,β = 1,2,3,4; the trace term being included.

We restrict to the mass shell by setting $P^2 = \mu^2$, where μ is the meson mass, by application of the Bargmann-Wigner equations

$$(\not{P} - \mu)\ \Phi(P) = 0 .$$

This gives the relationships

$$\not{\phi} = 0,$$

$$iP_\mu \phi_{\mu 5} = \mu \phi_5 , \qquad i\mu\ \phi_{\mu 5} = P_\mu \phi_5 ,$$

$$iP_\mu \phi_{\mu\nu} = \mu \phi_\nu , \qquad i\mu \phi_{\mu\nu} = P_\mu \phi_\nu - P_\nu \phi_\mu .$$

With these relations and the equation of continuity of the vector field

$$P_\mu \phi_\mu = 0$$

we get

$$\Phi_A{}^B(P) = (T^i)_a{}^b(-(1+\not{P}/\mu_p)\ \gamma_5 \phi_5{}^i + (1 + \not{P}/\mu_v)\gamma_\mu\ \phi_\mu^i(P))_\alpha^\beta .$$

Then $\phi_5^i(P)$ and $\phi_\mu^i(P)$ are the nonets of pseudoscalar and vector fields (in momentum space) respectively. Here μ_p and μ_v are the pseudoscalar and vector masses respectively. In the exact symmetry $\mu_p = \mu_v = \mu$.

The decomposition of the baryon tensor is performed similarly to give

$$\psi_{(ABC)} = D_{(abc),\alpha\beta\gamma} + \frac{1}{2\sqrt{6}} \left(\varepsilon_{abd} N^{d}_{c(\alpha\beta)\gamma} + \varepsilon_{bcd} N^{d}_{a(\beta\gamma)\alpha} + \varepsilon_{cad} N^{d}_{b(\gamma\alpha)\beta} \right) .$$

Here N is the $\frac{1}{2}^+$ octet

$$mN_{(\alpha\beta)\gamma}(p) = \left((\not{P} + m)\gamma_5 C\right)_{\alpha\beta} N_\gamma(P)$$

and D is the ${}^3/_2{}^+$ decuplet

$$D_{(\alpha\beta\gamma)}(P) = (\gamma_\mu C)_{\alpha\beta} D^\mu_\gamma(P)$$

$$+ \frac{i}{2m_D} (\sigma_{\mu\nu} C)_{\alpha\beta} \{P^\mu D^\nu_\gamma (P) - P^\nu D^\mu_\gamma (P)\}$$

with C the charge conjugation matrix

$$C^{-1} \gamma_o C = - \gamma_o .$$

The three meson vertex is described by the unique effective interaction Lagrangian

$$\mathcal{L} = \Phi^A_B (-q) J_A{}^B(P,P')$$

with

$$J_A{}^B(P,P') = h\left(\Phi_A{}^C(P)\ \Phi_C{}^A(-P') + \Phi_A{}^C(-P')\ \Phi_C{}^A(P)\right) \quad .$$

In this expression h is the coupling constant, P is the 4-momentum of the incoming meson, P' the 4-momentum of the outgoing meson, and $q = P - P'$.

Evaluating the traces we find eventually that

$$\mathcal{L} = \phi_5(-q)J_5(P,P') + \phi_\mu(-q)\ J_\mu(P,P')$$

where J_5 and J_μ are the pseudoscalar and vector currents respectively.

2.2 Evaluation of Born Graphs.

The relevant Born graphs with U(6,6) symmetry are evaluated to obtain the s-channel helicity amplitudes for 0^- and 1^- exchanges in the t-channel. These pole graphs involve the exchange of $\underline{35}$ mesons, which couple uniquely through U(6,6) to $\overline{\underline{56}} \otimes \underline{56}$ and $\overline{\underline{35}} \otimes \underline{35}$. The three-particle vertices are written as

$$\mathcal{L}_{\bar{B}BM} = g\bar{B}^{(ABC)}\ B_{(ABD)}\ M_C{}^D \quad ,$$

$$\mathcal{L}_{MMM} = h\{M,M\}_A{}^C\ M_C{}^A \quad ,$$

where A,B,C and D are the U(6,6) indices.

Retaining just those parts of the currents in which we are interested, we have, for the pseudoscalar current

$$J_5 = J_5(0) + J_5(D) + J_5(V) ,$$

where

$$J_5(0) = g \left(1 + \frac{2m}{\mu}\right) \frac{P^2}{4m_B^2} (\bar{N}\gamma_5 N)_D + \frac{2}{3} F\text{-}S,$$

$$J_5(D) = g\left(1 + \frac{2m}{\mu}\right) \frac{Q_\lambda}{m_B} (\bar{D}_\lambda N)_G ,$$

$$J_5(V) = -3h\, Q_\lambda (\bar{\phi}_\lambda \phi_5)_F,$$

and for the vector current

$$J_\mu = J_\mu(0) + J_\mu(D) + J_\mu(P) + J_\mu(V),$$

where

$$J_\mu(0) = g \left\{ \frac{P_\mu}{2m_B} \left(1 + \frac{Q^2}{2m\mu}\right) (\bar{N}N)_{F+3S} + \left(1 + \frac{2m}{\mu}\right) \left(\bar{N} \frac{r_\mu}{4m_B^2} N\right)_{D+\frac{2}{3}F-S} \right\} ,$$

$$J_\mu(D) = -\frac{g}{2m_B^2} \left(1 + \frac{2m}{\mu}\right) \varepsilon_{\mu\nu\kappa\lambda} P_\nu Q_\kappa (\bar{D}_\lambda N)_G ,$$

$$J_\mu(P) = h \left(1 + \frac{Q^2}{2\mu^2}\right) P_\mu (\phi_5 \phi_5)_F ,$$

$$J_\mu(V) = \frac{3h}{2m_M} \varepsilon_{\mu\nu\kappa\lambda} P_\nu Q_\kappa (\bar{\phi}_\lambda \phi_5)_{D+2S},$$

where

$$r_\mu = \varepsilon_{\mu\nu\kappa\lambda} P_\nu Q_\kappa \gamma_\lambda \gamma_5 ,$$

P and Q are the sum and difference, respectively, of the incoming and outgoing momenta at a vertex, and F, D and S are the anti-symmetric, symmetric and singlet U(3) couplings, respectively. We have also introduced explicitly a G-coupling for the decuplet-octet-meson vertex defined as

$$(\bar{D}NM)_G = \sqrt{2}\ \bar{D}^{rst} M_t{}^u \varepsilon_{usv} N_r^v ,$$

where M,N and D are the usual meson and baryon fields. The $\sqrt{2}$ arises since we have normalised to $\bar{P}P\pi^o$. In these currents we take P^2 and Q^2 on-shell, since the three-particle vertices are derived on the assumption that all the particles are on the mass-shell.

Since there is no definitive procedure for mass splitting in higher symmetry schemes, we have adopted a simple prescription which seems physically reasonable. For the U(6,6) meson mass we take $\mu = .63$ GeV/c^2, the average of the 0^- and 1^- nonets, and for the U(6,6) baryon mass we take $m = 1.27$ GeV/c^2, the average of the $\frac{1}{2}^+$ octet and $^3/_2{}^+$ decuplet. Where shown we have used the average mass of the incoming and outgoing particles at a vertex, since these terms arise from Feynman rules rather than the symmetry scheme. In the kinematics we have used the exact physical mass of

the particles.

The two coupling constants, g and h, which appear in the currents are obtained from the known pion-nucleon coupling constant[17], giving

$$\frac{g^2_{NN\pi}}{4\pi} = 14.9 = \frac{g^2}{4\pi}\left(1 + \frac{2m}{\mu}\right)^2 \left(1 - \frac{\mu^2}{4m_B^2}\right)\left(\frac{5}{3}\right)^2 ,$$

and from the $\rho \to 2\pi$ decay width[18], giving

$$\frac{g^2_{\rho\pi\pi}}{4\pi} = 2.09 = \frac{(3h)^2}{4\pi} .$$

It is now a straightforward matter to write down the Born amplitudes in terms of these currents for the processes in which we are interested. Denoting the pseudoscalar and vector exchange amplitudes by T_P and T_V, respectively we have for

$$0^-\tfrac{1}{2}^+ \to 1^-\,{}^3/_2{}^+$$

$$T_P = J_5(D)\ \frac{1}{t - M^2}\ J_5(V) ,$$

$$T_V = J_\mu(D)\ \frac{1}{t - M^2}\left(-g_{\mu\nu} + \frac{Q_\mu Q_\nu}{M^2}\right) J_\nu(V) ,$$

where M is the mass of the exchanged particle and the metric is $g_{\mu\nu} = (+1; -1, -1, -1)$.

Explicit expressions for the helicity amplitudes are evaluated using standard techniques. The contributions from the $Q_\mu Q_\nu/M^2$ term in the spin-1 propagator, which when Reggeized would lead to $1/t$ singularities, are eliminated by appealing to pair-wise equal mass kinematics. These terms are non-leading in s.

2.3 Parameterization of Elastic Scattering.

Elastic scattering is experimentally characterized by a forward diffraction peak which is to a very good approximation exponential over the range $0 \lesssim |t| \lesssim 0.5$ $(GeV/c)^2$, i.e.

$$\frac{d\sigma}{dt} = A\, e^{-B|t|} .$$

The partial wave decomposition of the elastic scattering amplitude (see appendix A) is, in the case of spinless external particles

$$\frac{T(\theta)}{8\pi\sqrt{S}} = \frac{i}{2P} \sum_\ell (2\ell+1)\, a^\ell\, P_\ell(\cos\theta)$$

where $a^\ell = -it^\ell = 1 - S^\ell = 1 - C\, e^{2i\delta_\ell}$

$$= 1 - C\, e^{-2\,\mathrm{Im}\,\delta_\ell}\, e^{2i\,\mathrm{Re}\,\delta_\ell} .$$

For low partial waves, where there is a lot of absorption $\mathrm{Im}\,\delta_\ell$ is large and $a^\ell \to 1$. For high partial waves $\delta_\ell \to 0$ and $a^\ell \to 0$.

Thus a^{ℓ} represents the opacity of the absorbing region; $0 \leq a^{\ell} \leq 1$. Since we expect an imaginary amplitude, a^{ℓ} is largely real.

We can convert the partial wave analysis into impact parameter form using

$$\ell + \tfrac{1}{2} = Pb$$

and the approximations

$$P_{\ell}(\cos\theta) \simeq J_0\left((\ell+\tfrac{1}{2})\ 2\sin\tfrac{\theta}{2}\right)$$

$$= J_0(b\sqrt{|t|}) \quad \text{i.e.} \quad P_{pb}(\cos\theta) = J_0(b\sqrt{|t|}),$$

$$\int_{-1}^{1} P_{\ell}(\cos\theta)\, d(\cos\theta) \to \frac{1}{P^2}\int_0^{\infty} \sqrt{|t|}\ d\sqrt{|t|}\ J_0(b\sqrt{|t|}),$$

$$\sum_{\ell=0}^{\infty} \to \int_0^{\infty} P\, db$$

which are valid for $\theta \ll 1$ and $S \to \infty$. Then

$$\frac{T(\theta)}{8\pi\sqrt{S}} = i P \int_0^{\infty} a(b)\ J_0(b\sqrt{|t|})\ bdb \quad .$$

The appropriate form for $a(b)$ is a Gaussian

$$a(b) = C\, e^{-b^2/R^2}$$

since this gives

$$\frac{T(\theta)}{8\pi\sqrt{S}} = i P \int_0^\infty C\, e^{-b^2/R^2} J_0(b\sqrt{|t|}) \, bdb = i \frac{PCR^2}{2} e^{-\frac{R^2}{4}|t|}$$

$$\frac{d\sigma}{dt} = \pi \left(\frac{CR^2}{2} \right)^2 e^{-\frac{R^2}{2}|t|}$$

Thus R can be found from the slope B of the differential cross section

$$R = \sqrt{2B}$$

C is found from the total cross-section using the optical theorem

$$C = \frac{\sigma_{TOT}}{2\pi R^2}$$

Thus, we obtain

$$S(b) = 1 - Ce^{-b^2/R^2}$$

or $$S^\ell = 1 - Ce^{-(\ell+\frac{1}{2})^2/R^2p^2}$$

This is often written

$$S^\ell = 1 - C' e^{-\ell(\ell+1)/R^2p^2}$$

the values of C and C' do not differ significantly.

2.4 The Absorption Model.

This is a convenient point to examine the formalism of unitarity for two-body scattering. The unitarity of the S-matrix gives

$$S^+S = 1 \quad .$$

Putting $S = 1 + iT$

and taking T as a symmetric matrix (which is possible whenever S is time-reversal invariant), unitarity gives

$$2 \text{ Im } T = T^+ T \quad .$$

In the one-particle-exchange (OPE) model,

$$T = \sum \text{ (Born graphs)} = \sum T_{BORN} \quad .$$

Since the Born terms are real, the term ImT is identically zero. In quantum electrodynamics, the Born term T_{BORN} is proportional to α the fine structure constant, and T^+T is then, in fact, zero too, to lowest order in α . In strong interactions the coupling constants are large and so is the term T^+T. Since the perturbation theory of strong interactions does not converge, one has to modify the Born terms in order to get a unitary model.

One such unitarizer is the K-matrix which is related to the usual transition matrix T by the expression

$$T = 2K + i\pi K\rho T$$

where ρ is the density of states factor. Most authors follow Dalitz[19] and define new quantities

$$T' = (\pi\rho)^{\frac{1}{2}} T (\pi\rho)^{\frac{1}{2}}$$

$$K' = (\pi\rho)^{\frac{1}{2}} K (\pi\rho)^{\frac{1}{2}}$$

which are related by an expression

$$T' = 2K' + iK'T'$$

which has the advantage of involving only channel labels.

In terms of the usual S-matrix this gives

$$S = 1 + iT = \frac{1 + iK}{1 - iK} \quad .$$

When K is small we get

$$S = 1 + iT \simeq 1 + 2iK$$

so we identify

$$T \simeq 2K.$$

The use of the K-matrix automatically leads to a unitary S-matrix. This is so because the Born terms are real and symmetric, which are exactly the requirements that the K-matrix, with which they are identified, has to fulfill.

The expression relating T' and K' becomes, with channel labels,

$$T'_{\alpha\beta} = 2K'_{\alpha\beta} + i\sum_{\gamma} K'_{\alpha\gamma} T'_{\gamma\beta} .$$

The first term is the usual Born amplitude and the second term including the summation over all channels represents the unitary correction.

The series expansion for the T-matrix is

$$T'_{\alpha\beta} = 2K'_{\alpha\beta} + 2i\, K'_{\alpha\gamma} K'_{\gamma\beta} + 2i^2 K'_{\alpha\gamma} K'_{\gamma\delta} K'_{\delta\beta}$$

$$+ 2i^3 K'_{\alpha\gamma} K'_{\gamma\delta} K'_{\delta\varepsilon} K'_{\varepsilon\beta} + \ldots$$

where the summation over repeated indices is implied. It is the idea of the absorption model to approximate this by

$$\frac{T'_{\alpha\beta}}{2} = K'_{\alpha\beta} + iK'_{\alpha\alpha} K'_{\alpha\beta} + iK'_{\alpha\beta} K'_{\beta\beta}$$

$$- K'_{\alpha\beta} K'_{\beta\delta} K'_{\delta\beta} - K'_{\alpha\gamma} K'_{\gamma\alpha} K'_{\alpha\beta} + \ldots$$

$$\frac{T'_{\alpha\beta}}{2} = K'_{\alpha\beta} + iK'_{\alpha\beta}\left(K'_{\beta\beta} + i\,K'_{\beta\delta}\;K'_{\delta\beta} + \ldots\right)$$

$$+ i\left(K'_{\alpha\alpha} + iK'_{\alpha\gamma}\;K'_{\gamma\alpha} + \ldots\right)\;K'_{\alpha\beta}$$

$$= K'_{\alpha\beta} + iK'_{\alpha\beta}\;\frac{T'_{\beta\beta}}{2} + i\;\frac{T'_{\alpha\alpha}}{2}\;K'_{\alpha\beta}$$

$$T'_{\alpha\beta} = 2K'_{\alpha\beta} + iK'_{\alpha\beta}\;T'_{\beta\beta} + i\,T'_{\alpha\alpha}\;K'_{\alpha\beta}$$

$$= K'_{\alpha\beta} + iK'_{\alpha\beta}\;T'_{\beta\beta} + K'_{\alpha\beta} + i\,T'_{\alpha\alpha}\;K'_{\alpha\beta}$$

$$= K'_{\alpha\beta}\left(1 + i\,T'_{\beta\beta}\right) + \left(1 + i\,T'_{\alpha\alpha}\right)\;K'_{\alpha\beta}$$

$$= K'_{\alpha\beta}\;S'_{\beta\beta} + S'_{\alpha\alpha}\;K'_{\alpha\beta}\,.$$

Making the identification $K \simeq \frac{1}{2}\,T_{BORN}$ we obtain the traditional Watson formula [8]

$$T'_{\alpha\beta} = \tfrac{1}{2}\left((T_{BORN})'_{\alpha\beta}\;S'_{\beta\beta} + S'_{\alpha\alpha}\;(T_{BORN})'_{\alpha\beta}\right).$$

In this way the effects of unitarity are allowed for by assuming initial and final state interactions consisting of unitarized elastic scatterings, with no helicity changes. The absorption approximation involves truncation over only <u>one</u> set of intermediate states, and the elastic correction factors contain the combined effects of many complete sets of intermediate states.

Such an absorption calculation is in principle simple and elegant. The approach fails altogether for the Regge pole model for two reasons. Firstly that the Regge pole model is often used to calculate elastic scattering, and secondly that the real K-amplitude cannot be identified with the complex Regge pole amplitude.

Another form that is sometimes used is

$$T'_{\alpha\beta} = \sqrt{S}_{\alpha\alpha}\ T_{\alpha\beta}\ \sqrt{S}_{\beta\beta}$$

which is due to Sopkovich[6].

In practice we usually do not know anything about the elastic scattering in the final state, and so take $S_{\alpha\alpha} = S_{\beta\beta}$, so that both formulae reduce to

$$T'_{\alpha\beta} = T_{\alpha\beta}\ S_{\beta\beta} \quad .$$

As previously noted this is exact only for pair-wise equal mass scattering.

Now we have

$$T^{ABS} = \tfrac{1}{2}\ (T_{ex}\ S^{i}_{el} + S^{f}_{el}\ T_{ex}) \quad .$$

If we write

$$S_{el} = 1 + i\, T_{el} \ .$$

We have

$$T^{ABS} = T_{ex} + \tfrac{1}{2}\, i\, (T_{ex}\ T^{i}_{el} + T^{f}_{el}\ T_{ex}) \ .$$

We can think of this diagramatically as shown in Fig.9.

The first term is the single particle exchange while the other terms correspond to double particle exchange terms. In the absorption model the intermediate particles are put on the mass-shell. This only includes corrections due to elastic scattering in the initial and final states. It would seem reasonable to also include other intermediate states. This is, in addition to diagrams like

$$\overline{a|a|b} \quad \text{and} \quad \overline{a|b|b}$$

we should include terms like

$$\overline{a|c|b}$$

where $c \neq$ a or b.

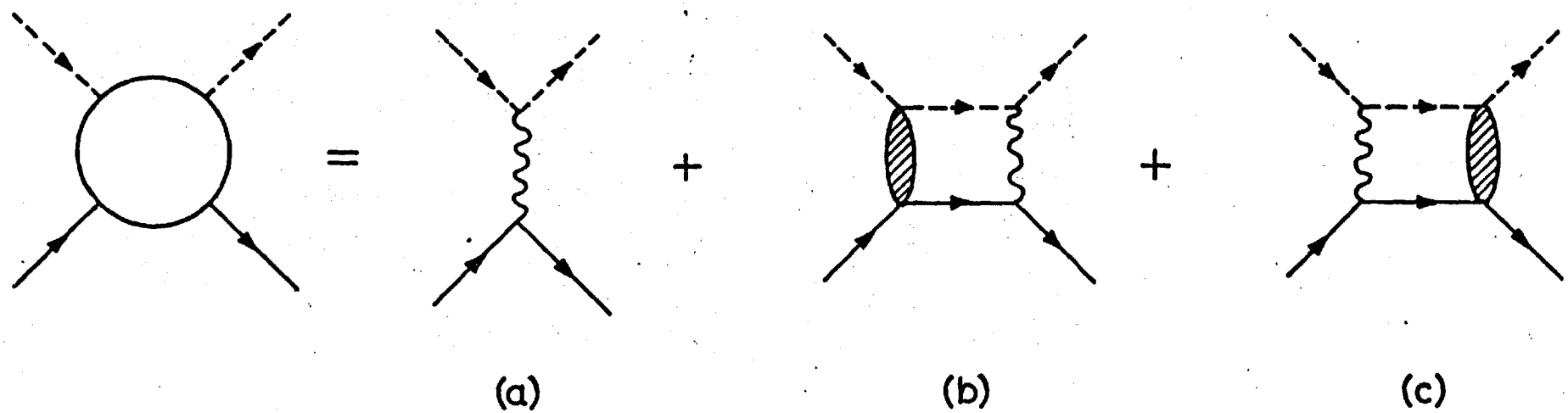

FIG. 9.

First-order absorptive corrections to the pole graph: ~~~ particle exchange, ---- on-shell meson, —— on-shell baryon, ◍ elastic rescattering.

2.5 Summary of the Model.

The OPE helicity amplitudes are calculated employing the U(6,6) couplings, and their partial wave projections found. These partial wave amplitudes are then multiplied by the absorption factor of the previous section, and the partial wave series resummed to give the modified amplitudes. These are used to calculate the differential cross-section, and the spin density matrix element in the case where one of the particles is a resonance.

This technique provides an essentially parameter-free model of nearly all two-body and quasi-two-body processes for which differential cross-sections exist, and the complete set of calculations has been performed by the Imperial College group[20,21,22,23].

The only arbitrariness in the model lies in -

a) The choice of masses to be used in the U(6,6) currents;

b) The choice of absorption parameters for final state elastic scattering, since this is usually inaccessible experimentally.

As pointed out previously the OPE graph for vector meson exchange has the wrong energy dependence, and the model is not expected to be successful for reactions dominated by such an

exchange, except over a very limited energy range. The main application of the model, with fixed pole exchange, has been in processes dominated by pseudoscalar exchange, but where the density matrix elements reveal an admixture of vector (or tensor) exchange. The hope is that the model will give a reasonable representation of the vector components over a reasonable range of intermediate energies.

CHAPTER III

FIXED POLE MODEL FOR $0^-\frac{1}{2}^+ \to 1^- 3/2^+$

3.1 Introduction.

In this section we present calculations of the $0^-\frac{1}{2}^+ \to 1^- 3/2^+$ processes for which data is presently available. U(6,6) symmetry is used to write down the peripheral matrix elements for pseudoscalar and vector exchange, and the absorption model is used to allow for the fact that there are many competing open channels available to the initial and final states.

In previous calculations on $0^-\frac{1}{2}^+ \to 1^- 3/2^+$ scattering processes with fixed pole exchange using the absorption model, only the contribution of the t-channel singularity nearest the physical region, the π pole, was considered. Generally this gave a good result for the reactions[21]

$$\pi^+ P \to \rho^0 \Delta^{++}$$

$$K^+ P \to K^{*0} \Delta^{++} \quad .$$

Data on $K^- n \to K^{*0} \Delta^-$ at high energy has only recently become available[24]. With elementary π and absorptive corrections there is a discrepancy between the experiment and theory of about a factor of two in normalization.

Here we consider the contributions of the t-channel singularities closest to the physical region, the π and the ρ poles, and, of course, the interference between the two. Rather than use an arbitrary mixture of π - and ρ-exchange matrix elements which would be varied at will to fit the experimental data, we use the U(6,6) symmetry scheme to fix uniquely the relative magnitude of each contribution. The absorption parameters used are given in Table 3.

3.2 Comparisons with the data.

In figure 10 we show the momentum transfer distribution resulting from an absorbed π exchange for the process $\pi^+P \to \rho^0\Delta^{++}$. [25,26] We see that the general structure of the theory seems to be correct, i.e. a sharp forward peak, due to the proximity of the pion pole followed by a broad relatively flat distribution. The normalization which is experimentally somewhat variable, is reproduced in the 6.95 and the 13.1 GeV/c theoretical distributions.

In figure 11 is shown the available experimental data [27,28] on the reaction $K^+P \to K^{*0}\Delta^{++}$ for $P_{Lab} \geq 3.0$ GeV/c along with the predicted theoretical distributions. We see that although absorbed π exchange alone adequately represents the data the addition of ρ exchange certainly results in a poorer fit. This fit gets worse with increasing energy, of course.

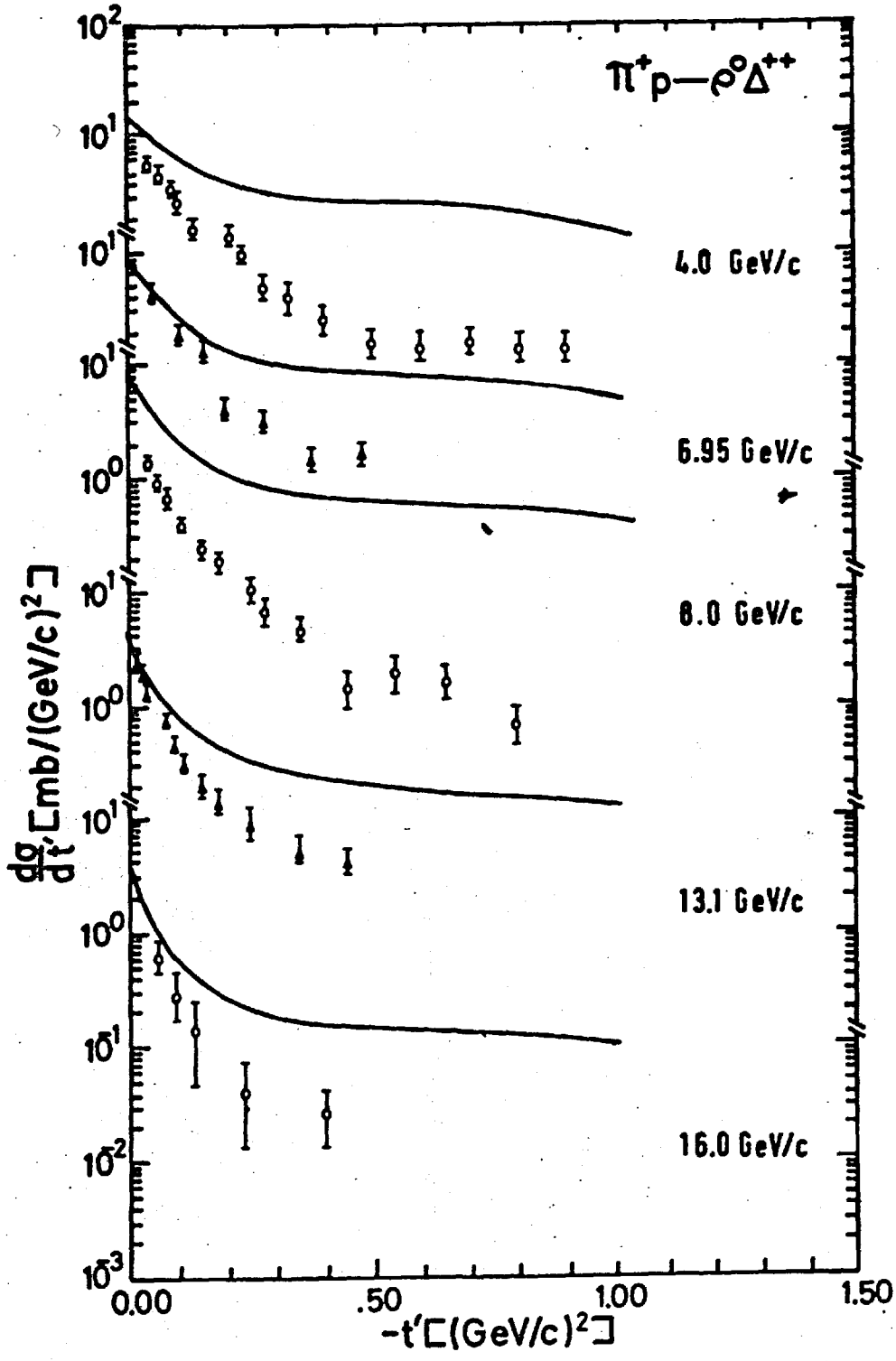
$\pi^+p \rightarrow \rho^0\Delta^{++}$
4.0 GeV/c
6.95 GeV/c
8.0 GeV/c
13.1 GeV/c
16.0 GeV/c
$\frac{d\sigma}{dt'}$[mb/(GeV/c)^2]
$-t'$[(GeV/c)^2]
0.00
.50
1.00
1.50

FIG. 10.

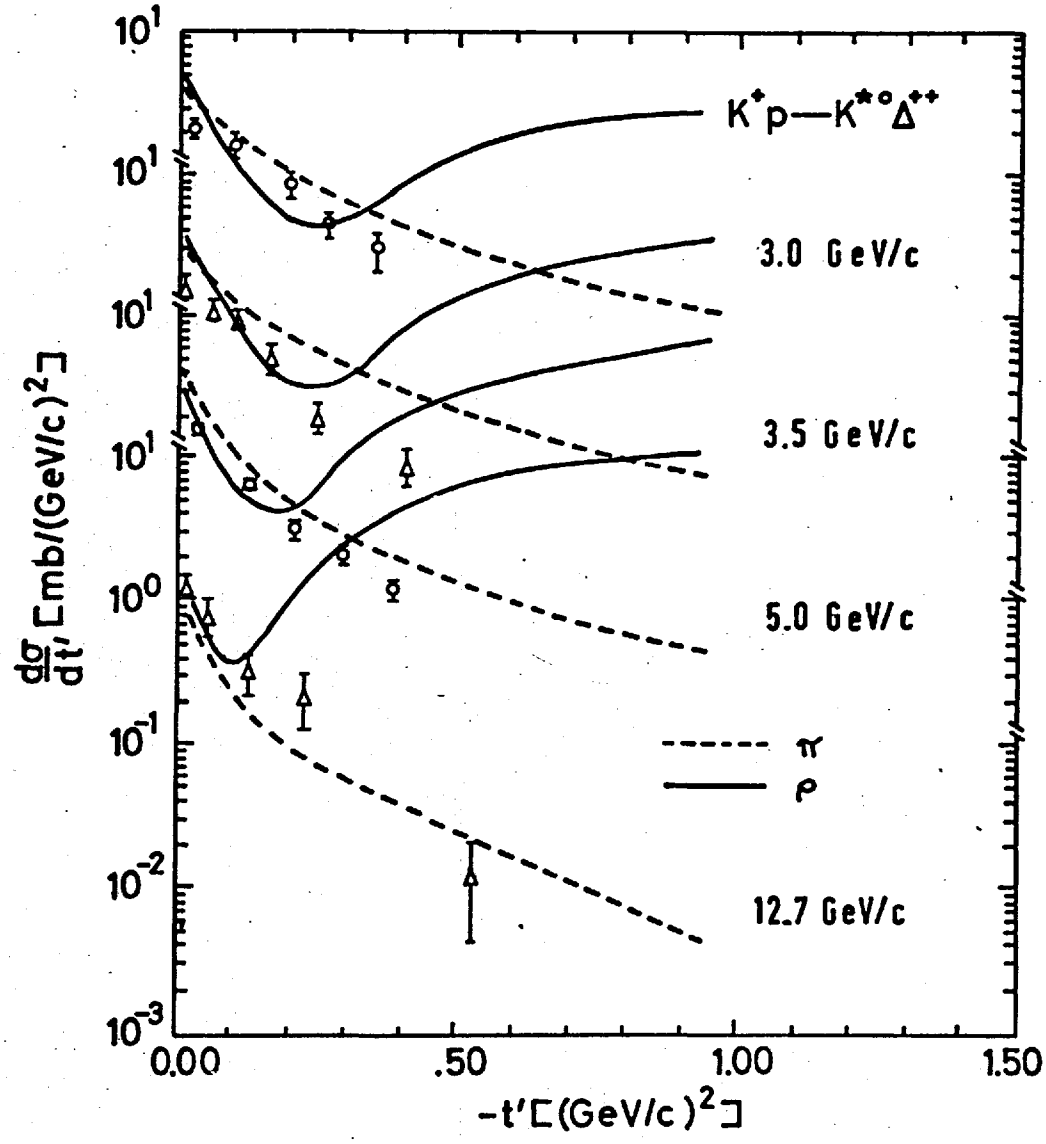
$K^+p \to K^{*\circ}\Delta^{++}$
3.0 GeV/c
3.5 GeV/c
5.0 GeV/c
12.7 GeV/c
π
ρ
$\frac{d\sigma}{dt'}$ [mb/(GeV/c)^2]
$-t'$ [(GeV/c)^2]
10^1
10^0
10^{-1}
10^{-2}
10^{-3}
0.00
.50
1.00
1.50

FIG. 11.

In figure 12 the data on the reaction $\pi^+P \to \omega^0\Delta^{++}$ (25,29) at 4 and 8 GeV/c is plotted. The theoretical curve is at 8 GeV/c. We see that the theory fails to reproduce the normalization, the s-dependence or the t-dependence of the experimental data. Since $\pi^+P \to \omega^0\Delta^{++}$ proceeds by ρ exchange the calculations of 4 GeV/c will produce an answer which is the same as that at 8 GeV/c. This shows most clearly the failings of the absorption model with fixed pole input.

The density matrices for the $K^*(890)$ decay in $K^+P \to K^{*0}\Delta^{++}$ (27) at 3.5 GeV/c are shown in fig. 13 . For elementary pion exchange without absorption we have

$$\rho_{00} = 1 \quad .$$

From Fig. 13 we see that

$$\rho_{00} \simeq .8 \qquad (\cos\theta \simeq +1) \, .$$

This density matrix element definitely indicates that pion exchange is the dominant mechanism by which the $K^*(890)$ is produced, at least in the forward direction.

We will discuss the density matrices further when we Reggeize our amplitudes. Thus to avoid needless repetition we will end our discussion here.

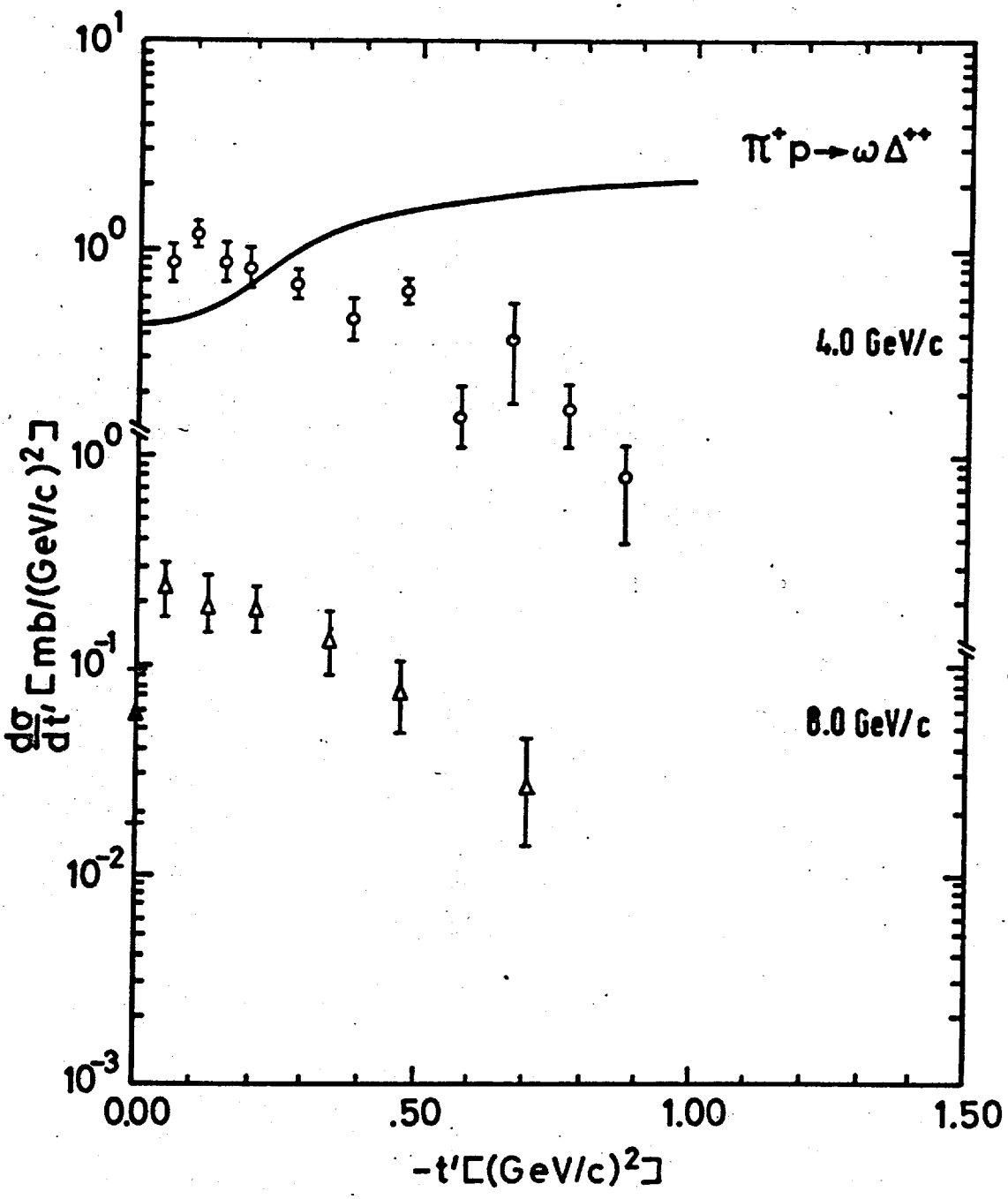
$\pi^+ p \to \omega \Delta^{++}$
4.0 GeV/c
8.0 GeV/c
$\frac{d\sigma}{dt'}$ [mb/(GeV/c)^2]
$-t'$[(GeV/c)^2]
10^1
10^0
10^0
10^{-1}
10^{-2}
10^{-3}
0.00
.50
1.00
1.50

FIG. 12.

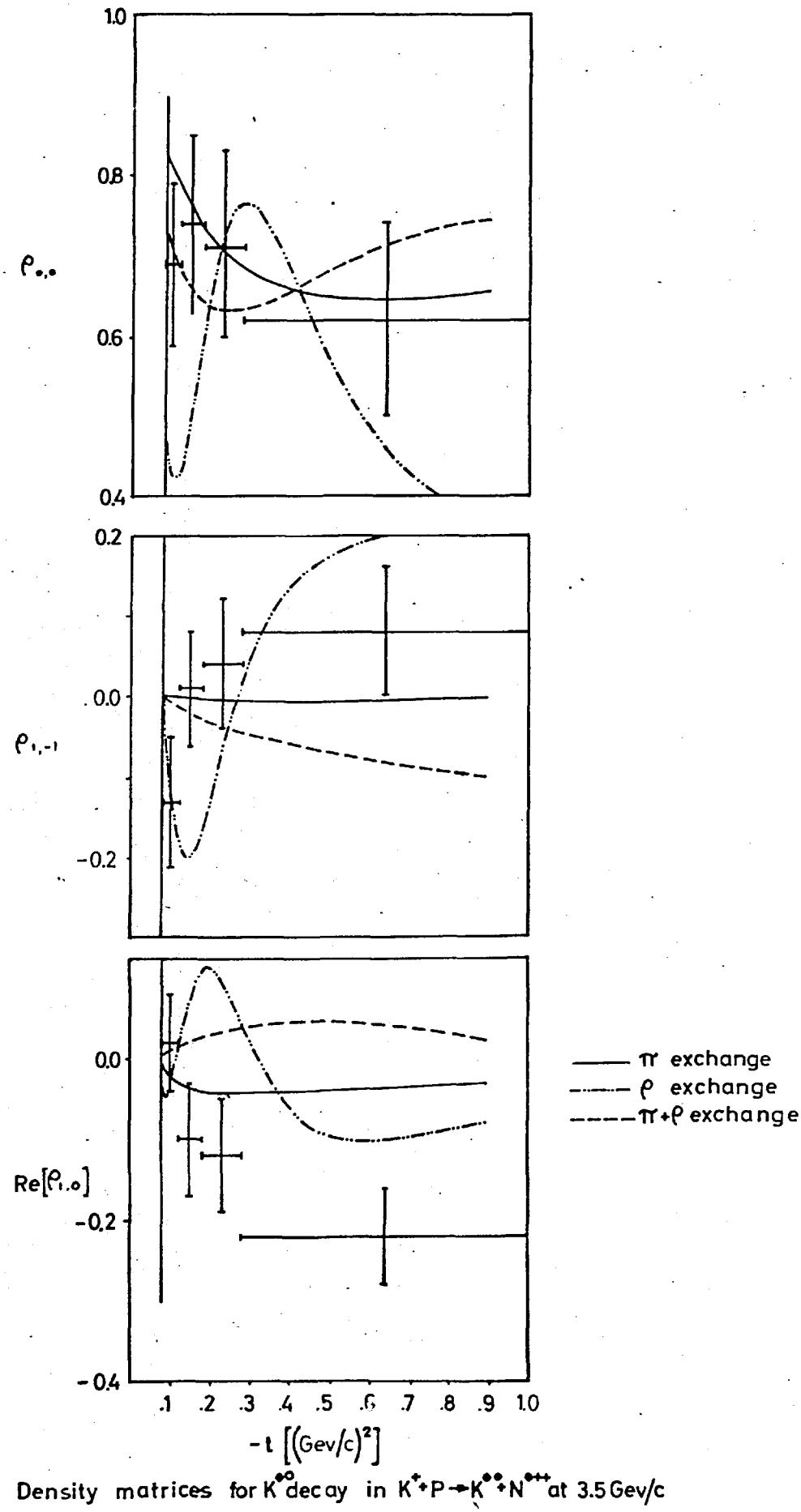

Density matrices for K^{*0} decay in $K^+P \to K^{*0}N^{*++}$ at 3.5 Gev/c

FIG. 13.

CHAPTER IV

REGGE POLES

4.1 Sommerfeld-Watson Transformation.

For the partial-wave expansion

$$A(s,z) = \sum_{\ell=0}^{\infty} (2\ell+1)\, A_\ell(s)\, P_\ell(z_s)$$

we can write equivalently

$$A(s,z) = -\frac{1}{2i} \oint_{C_0} d\ell\, \frac{(2\ell+1)\, A(s,\ell)\, P_\ell(-z_s)}{\sin\pi\ell}$$

where we integrate around the contour shown in Fig. 14 , picking up one term in the sum for each zero of $\sin\pi\ell$ enclosed. We have assumed that $A(s,\ell)$ is an analytic function of ℓ throughout the right-half ℓ-plane with only isolated singularities. The contour C_0 is chosen to include the positive integers and zero, but to avoid any singularities of $A(s,\ell)$. The integrand has a pole at each integer, n, when

$$\sin(\pi\ell) \xrightarrow[\ell \to n]{} (-1)^n (\ell - n)\, \pi$$

The residue of the pole is thus

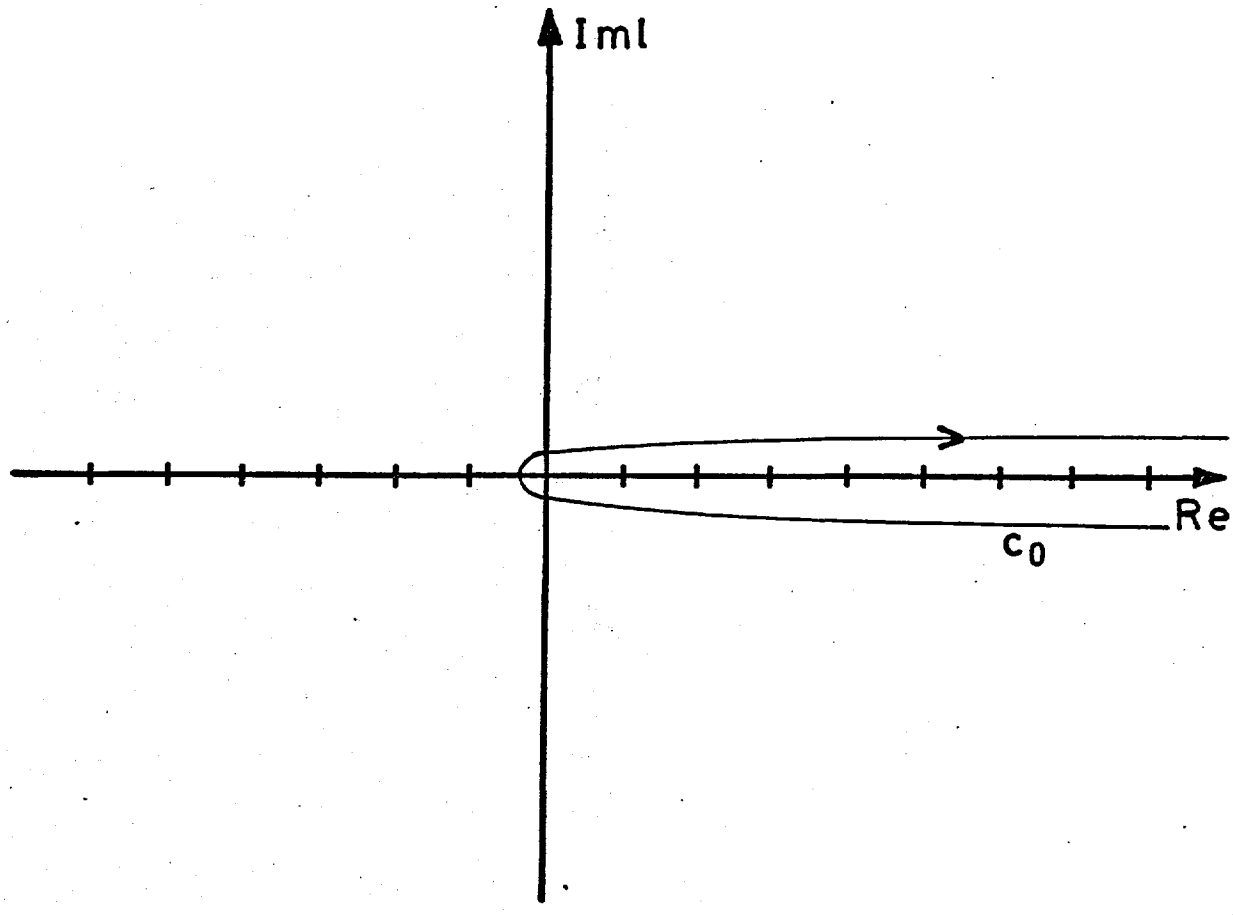

FIG. 14.

$$- \frac{1}{2i} (2\pi i) \left[\frac{(2n+1)\, A(s,n)\, P_n(-z_s)}{(-1)^n \pi} \right]$$

$$= - (2n+1)\, A(s,n)\, P_n (z_s)$$

where we have used the fact that

$$P_n (-z_s) = (-1)^n P_n (z_s)$$

So Cauchy's theorem gives (note that the clockwise path of integration gives a negative sign) our original partial-wave expansion as required.

Let us assume that the only singularities of $A(s,\ell)$ for $\mathrm{Re}\,\ell > -\frac{1}{2}$ are poles with $\mathrm{Im}\,\ell > 0$. So we now displace the contour C_0 to C_1 as shown in Fig.15 . If there are no singularities of $A(s,\ell)$ to the line L_1 then

$$\int_{C_0} = \int_{C_1}$$

It can be shown that the contribution from the semi-circle vanishes at infinity.

If we now displace the line parallel to the imaginary axis towards the imaginary axis, we shall encounter singularities of $A(s,\ell)$.

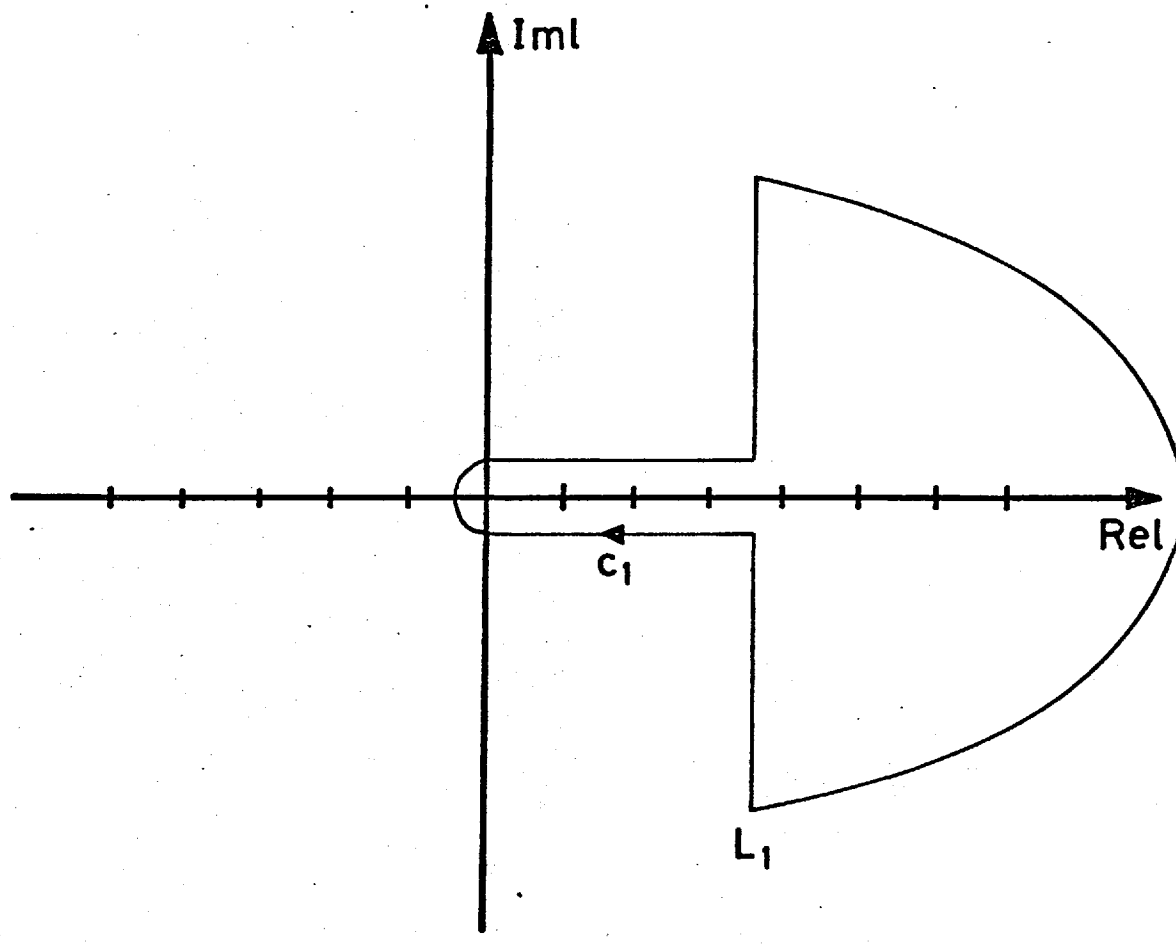

FIG. 15.

Suppose that the "leading singularity" encountered (i.e. the right-most in the complex ℓ-plane) is a pole at $\ell = \alpha_m(s)$, with residue $\beta_m(s)$, so that

$$A(s,\ell) \simeq \frac{\beta_m(s)}{\ell - \alpha_m(s)} \qquad \text{as} \qquad \ell \to \alpha_m(s)$$

Then in exposing this pole, as shown in Fig.16 , we get

$$A(s,t) = -\frac{1}{2i}\int_{C_2} (2\ell+1)\, A(s,\ell)\, \frac{P_\ell(-z_s)}{\sin \pi\ell}\, d\ell$$

$$- 2\pi i \left[\frac{1}{2i}\right] (2\alpha_m(s)+1)\, \beta_m(s)\, \frac{P_{\alpha_m(s)}(-z_s)}{\sin\pi\, \alpha_m(s)}$$

$$= -\frac{1}{2i}\int_{C_2} (2\ell+1)\, A(s,\ell)\, \frac{P_\ell(-z_s)}{\sin\pi\ell}\, d\ell$$

$$- \pi\,(2\alpha_m(s)+1)\, \beta_m(s)\, \frac{P_{\alpha_m(s)}(-z_s)}{\sin \pi\alpha_m(s)}$$

As $z \to \infty$ we have

$$P_\alpha(z) \xrightarrow[z\to\infty]{} Z^{|\alpha+\frac{1}{2}|-\frac{1}{2}} \qquad , \alpha \neq \text{negative integer}$$

So, since $\text{Re}\ \alpha_m(s) > L_2$ in Fig. 16 , the second term in the above will dominate asymptotically if $\text{Re}\ \alpha_m(s) > -\frac{1}{2}$ and we have

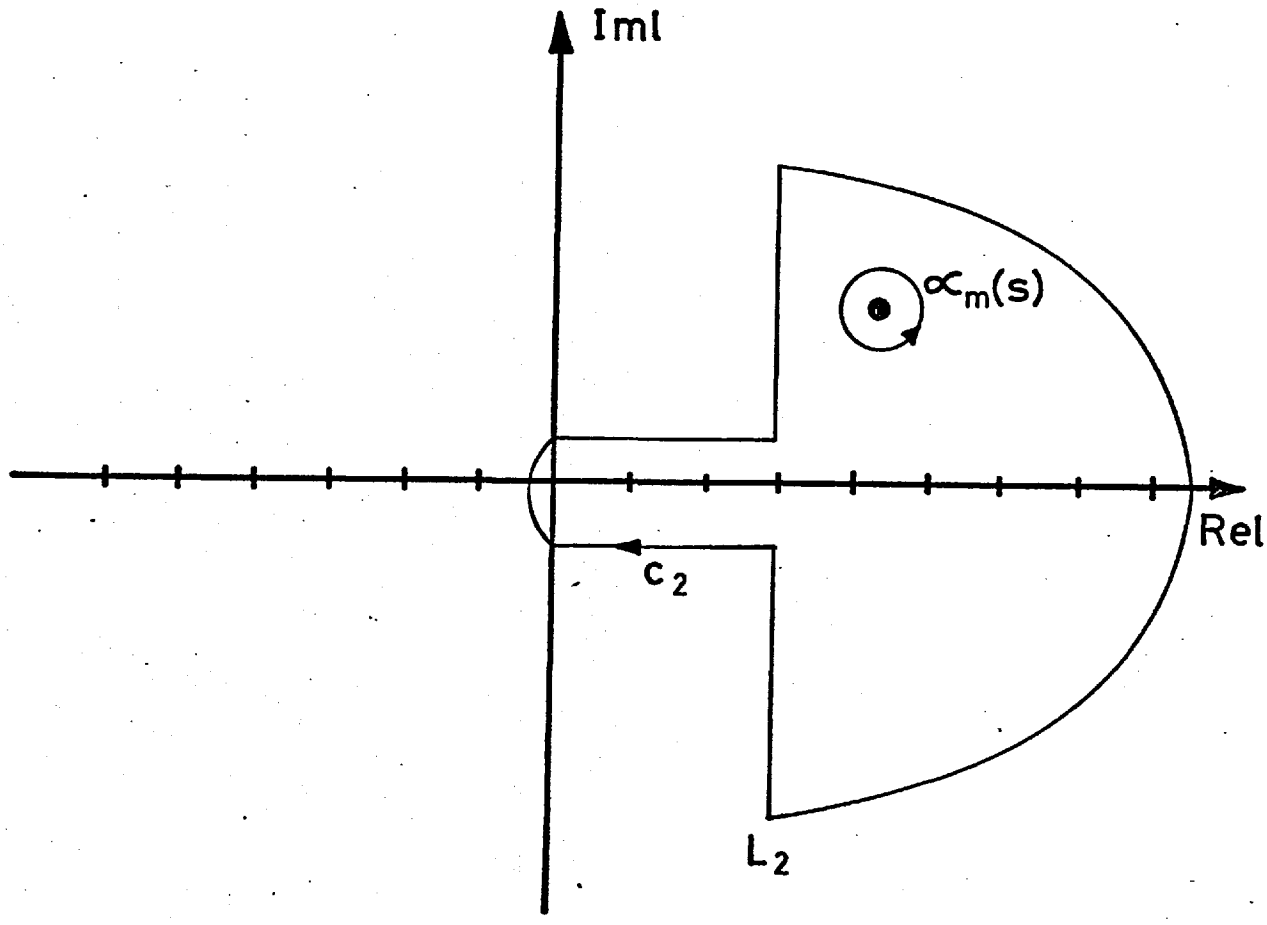

FIG. 16.

$$A(s,t) \underset{z_s \to \infty}{\sim} (Z_s)^{\mathrm{Re}(\alpha_m(s))}$$

If the singularity which we meet in deforming the contour is a branch point at $\alpha_c(s)$, we can draw a branch cut in the ℓ-plane running back towards negative Re ℓ as shown in Fig. 17 . The amplitude is then given by

$$A(s,t) = -\frac{1}{2i} \int_{B_i} (2\ell+1)\, A(s,\ell)\, \frac{P_\ell(-z_s)}{\sin \pi\ell}\, d\ell$$

and its asymptotic behaviour will be

$$A(s,t) \underset{z_s \to \infty}{\sim} (z_s)^{\mathrm{Re}\,(\alpha_c(s))}$$

apart from logarithmic factors.

As far as we know, the only singularities in the ℓ-plane are likely to be poles and branch points. We can minimize the contribution of the vertical path of integration by moving the contour back to Re$\ell = -\frac{1}{2}$ and obtain

$$A(s,t) = -\frac{1}{2i} \int_{-\frac{1}{2}-i\infty}^{-\frac{1}{2}+i\infty} (2\ell+1)\, A(s,\ell)\, \frac{P_\ell\,(-z_s)}{\sin\pi\ell}\, d\ell$$

$$- \sum_{i \text{ poles}} \pi\, (2\alpha_i(s)+1)\, \beta_i(s)\, \frac{P_{\alpha_i(s)}\,(-Z_s)}{\sin\pi\,\alpha_i(s)}$$

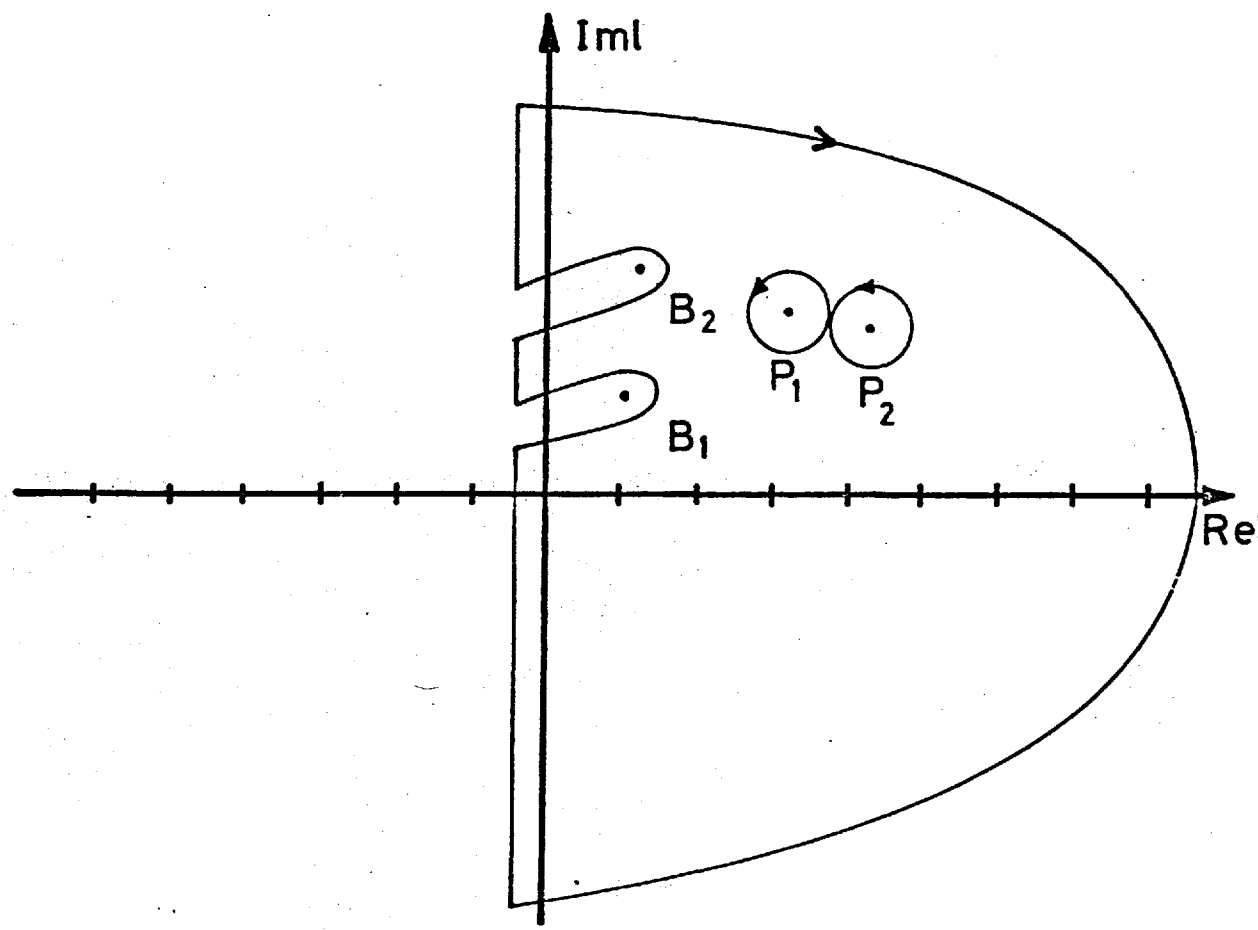

FIG. 17.

$$- \sum_{j \text{ cuts}} \frac{1}{2i} \int_{C_j} (2\ell+1)\, A(s;\ell)\, \frac{P_\ell(-Z_s)}{\sin \pi \ell}\, d\ell$$

The first term, the so called "background integral", vanishes as $z_s \to \infty$, leaving a sum of "Regge poles" and "Regge cuts". The function $\alpha_i(s)$ is referred to as a "Regge trajectory".

Froissart[30] showed by studying unitarity in the t channel that cross sections cannot increase indefinitely as a positive power of energy if the forces are of finite range, which is equivalent to requiring no zero-mass particles and is all right for the strong interactions. Thus σ_{TOT} and $d\sigma/dt$ are bounded and we may conclude

$$\alpha_i(s) \leq 1 \qquad \text{for} \qquad s \leq 0$$

Combining this with the requirement that all trajectories have positive slope shows why no trajectory lies above $\alpha_i(s = o) = 1$.

What is going on when the trajectory goes through J=0 at a negative square mass? The differential cross section goes to infinity unless the residue vanishes in such a way as to cancel the denominator as $\alpha_i(s) \to 0$, removing the pole at this one point. This must happen since unitarity does not allow the cross section to become infinite. Thus, as Gell-Mann first pointed out, the residue vanishes and no ghost state of imaginary mass appears.

Asymptotically a cut will give a contribution to a transition amplitude of the general form

$$A(s,t) = \int_{\text{(background)}}^{\alpha_c(t)} g(\ell,t) \left[\frac{s}{s_0} \right]^{\ell} d\ell$$

where $\alpha_c(t)$ is the branch point of the cut and $g(\ell,t)$ is obtained from the discontinuity of the partial-wave amplitude across the cut which has been chosen to lie to the left of the cut. The region of the cut away from $\alpha_c(t)$ does not effect the asymptotic behaviour so only the discontinuity close to the end points needs to be considered. If the discontinuity is regular at the branch point, we may expand $g(\ell,t)$ in a Taylor's series

$$g(\ell,t) = g(\alpha_c(t)) + (\ell - \alpha_c(t)) \left[\frac{\partial g}{\partial \ell} \right]_{\ell = \alpha_c(t)} + \ldots$$

$$= \beta_0(t) + (\ell - \alpha_c(t)) \quad \beta_1(t) \quad + \ldots$$

We get

$$A(s,t) = \int_{\text{(background)}}^{\alpha_c(t)} g(\ell,t) \left[\frac{s}{s_0} \right]^{\ell} d\ell$$

$$= \int_{-\infty}^{\alpha_c(t)} \{\beta_0(t) + (\ell - \alpha_c(t)) \ \beta_1(t) + \ldots \} \quad e^{\ell \ln \left[\frac{s}{s_0} \right]} d\ell$$

$$A(s,t) = \beta_0(t) \int_{-\infty}^{\alpha_c(t)} e^{\ell \ln\left(\frac{s}{s_0}\right)} d\ell + \beta_1(t) \int_{-\infty}^{\alpha_c(t)} (\ell - \alpha_c(t)) \, e^{\ell \ln\left(\frac{s}{s_0}\right)} d\ell + \ldots$$

$$= \beta_0(t) \frac{e^{\alpha_c(t) \ln\left(\frac{s}{s_0}\right)}}{\ln\left(\frac{s}{s_0}\right)} + \beta_1(t) \frac{e^{\alpha_c(t) \ln\left(\frac{s}{s_0}\right)}}{\left(\ln \frac{s}{s_0}\right)^2} \left(\alpha_c(t) \ln\left(\frac{s}{s_0}\right) - 1\right)$$

$$- \alpha_c(t) \frac{e^{\alpha_c \ln\left(\frac{s}{s_0}\right)}}{\ln\left(\frac{s}{s_0}\right)} + \ldots$$

$$= \beta_0(t) \frac{\left(\frac{s}{s_0}\right)^{\alpha_c(t)}}{\ln\left(\frac{s}{s_0}\right)} + \beta_1(t)\,(-1) \frac{\left(\frac{s}{s_0}\right)^{\alpha_c(t)}}{\left(\ln\left(\frac{s}{s_0}\right)\right)^2} + \ldots$$

$$= \beta_0'(t) \frac{s^{\alpha_c(t)}}{\ln s} + \beta_1'(t) \frac{s^{\alpha_c(t)}}{(\ln s)^2} + \ldots$$

In general, if the discontinuity behaves as

$$\left[\ell - \alpha_c(t) \right]^n$$

at the branch point, the asymptotic contribution of the cut is

$$\frac{\left(\frac{s}{s_0} \right)^{\alpha_c(t)}}{\left[\ln \left(\frac{s}{s_0} \right) - i \frac{\pi}{2} \right]^{n+1}}$$

where the phase in the denominator comes from keeping track of the phase of the signature factor. This only differs from a pole by the logarithmic factor, but, of course, different models for $g(\ell,t)$ can give different sorts of behaviour.

In the above series the first term represents a constant discontinuity while the other terms represent discontinuities that vanish at the branch point.

It was hoped for a long time that the only singularities in the complex J-plane which would need to be considered would be simple poles. A model based entirely on poles has been very successful in explaining many of the features of high-energy scattering data[31]; in particular, the simple power law behaviour of the differential cross sections. However, there are a number of facts that cannot be explained in terms of a model based only on poles. These can be briefly summarized as: (i) Polarization Phenomena, (ii) Pion Peaks and (iii) the Cross-Over Mechanisms. (iv) High-Energy Total cross sections and (v) Q=2 exchanges.

4.2. Polarization Phenomena.

In reactions where only one Regge Pole can be exchanged, the polarization is predicted to be identically zero. For example, in the charge-exchange reaction

$$\pi^- P \rightarrow \pi^0 n$$

there is only one known Regge pole which can be exchanged, namely the ρ, which is a $J^P = 1^-$ particle. Now the polarization depends on the term

$$P(t) \sim \mathrm{Im}\,(\phi_{++}\ \phi^*_{+-})$$

where ϕ_{++} and ϕ_{+-} are the s-channel helicity non-flip and helicity flip amplitudes. Since only one Regge pole can be exchanged, both ϕ_{++} and ϕ_{+-} have the same phase, given by the phase factor

$$1 - e^{-i\pi\alpha_\rho(t)}$$

so that the polarization is zero. However, experimentally the polarization is about 25%[32].

We can explain this in terms of a pure Regge pole model by introducing another trajectory, which we call the ρ'[33]. We can then obtain polarization by interference between the two poles.

In the case of the reaction

$$\pi^- P \to \eta n$$

which goes by A_2 exchange only, we could appeal to a second A_2 trajectory, since the A_2 resonance is known to be split[34].

But there is no known particle corresponding to the ρ'.[35] Analysis suggests that the ρ' would need an intercept

$$\alpha_{\rho'}(0) \simeq 0$$

but the nearest candidate for this 1^- particle has a mass of 1.55 GeV, which, if we suppose a linear trajectory of slope about 1, suggests an intercept of ~ -1.

A far more likely explanation is the existence of a Regge cut resembling a nearby secondary pole.

4.3 Pion Peaks.

For reactions where the pion can be exchanged, for example, the charge-exchange reaction

$$pn \to np$$

the experimental differential cross section shows a very sharp forward peak of width

$$\Delta t \simeq m_\pi^2 = .02$$

and an s-dependence of s^{-2}. Since

$$\frac{d\sigma}{dt} \sim s^{2\alpha - 2}$$

and $\alpha_\pi(0) \simeq 0$ this strongly suggests that π exchange is the dominant mechanism.

However, normal π exchange is <u>evasive</u>, that is, it vanishes at $t=0$, giving a forward dip rather than a forward peak.

In the reaction $pn \to np$, the π contributes to two helicity amplitudes, which are usually known as[36]

$$\phi_2 = \phi_{++,--}$$

$$\phi_4 = \phi_{+-,-+}$$

Because the π is a 0^- particle, parity considerations mean that

$$\phi_2^\pi = \phi_4^\pi \qquad\qquad 0^-$$

Now ϕ_4 corresponds to a net helicity flip of 2, and so, from angular momentum conservation, we must have

$$\phi_4^\pi \to 0 \qquad \text{as} \qquad t \to 0$$

and hence $\phi_2^\pi \to 0$

and the π contribution vanishes in the forward direction.

Now ϕ_2 corresponds to zero net helicity flip, so it need not vanish at $t=0$. The only way out in a pure Regge pole framework is to invoke a parity doublet to the π, a 0^+ particle, known as the pion conspirator. We then have

$$\phi_2^C = -\phi_4^C \quad . \qquad 0^+$$

Hence $$\phi_2 = \phi_2^\pi + \phi_2^C$$

and $$\phi_4 = \phi_4^\pi + \phi_4^C$$

$$= \phi_2^\pi - \phi_2^C \quad .$$

If we make $\phi_2^\pi = \phi_2^C$ at $t = 0$ by making the trajectories cross, we then have

$$\phi_2 = 2\phi_2^\pi$$

and $$\phi_4 = 0 \quad .$$

This satisfies angular momentum conservation without having $\phi_2 \to 0$ as $t \to 0$, so we can get a pion peak.

There are two difficulties with this conspiracy solution. Firstly, there is no evidence for the existence of a particle lying on this trajectory, and secondly, if this approach is carried through

all pion exchange reactions, by using factorization we predict a forward dip for

$$\pi N \rightarrow \rho\Delta$$

whereas a forward peak is seen experimentally[37].

Much fancier schemes have been proposed with, for example, the A_1 playing a major role instead, but all these solutions ultimately founder on factorization difficulties.

Introducing a Regge cut is an obvious solution. It can conspire with the evasive pion to give non-vanishing terms at t=0 and hence a sharp forward peak. We will return to this point later.

4.4. Cross-Over Mechanism.

High energy PP and $P\bar{P}$ elastic scattering are supposed to be dominated by the P, P' and the ω Regge poles. The A_1, A_2, ρ, π and B are also present but give small contributions, since they control $pn \rightarrow np$ and $p\bar{p} \rightarrow n\bar{n}$ charge exchange, which are small in comparison.

We can write the amplitudes symbolically as

$$A(PP) = P + P' - \omega$$
$$A(P\bar{P}) = P + P' + \omega$$

Now experimentally $d\sigma/dt$ for $P\bar{P}$ is larger at $t=0$ but more steeply t-dependent than $d\sigma/dt$ for PP, so that they intersect at $t \simeq t_0 \simeq -.1$. In terms of pure Regge poles this cross-over requires the ω residue to change sign at $t = t_0$.

Factorizing, the residue is a square

$$\gamma = \gamma_1^2$$

so γ_1 must contain the factor

$$\gamma_1 \sim (t - t_0)^{\frac{1}{2}}$$

Now, other NN scattering amplitudes have residues factorizing like

$$\gamma_1 \gamma_2, \quad \gamma_2^2$$

If all these residues are real and free from singularities at $t = t_0$, as is normally expected, then γ_2 must contain the factor $\gamma_2 \sim (t - t_0)^{\frac{1}{2}}$. Similarly by considering chains of inelastic processes with and without a nucleon vertex, with residues like $\gamma_i\gamma_j$, γ_j^2, $\gamma_j \gamma_k$, γ_k^2 and so on, we see that all ω residue functions must have at least this factor of $(t - t_0)^{\frac{1}{2}}$, so that all ω residue functions vanish at t_0 giving a universal zero.

This agrees nicely with the observed cross-over in $K^{\pm}P$ elastic scattering, which is also dominated by $P + P' \pm \omega$, but it does not show up universally. For example $\gamma P \to \pi^0 P$ is supposed to be

dominated by ω exchange, but it does not show a minimum at t_0.

One solution is to have another ω -like term, ω'. The cross-over is then explained by having the $\omega + \omega'$ amplitude changing sign at t_0, without having to have a zero in the residue. However, there is no plausible candidate for the ω', so possibly the ω' term is a Regge cut.

4.5. High-Energy Total Cross Section.

The new Serpukov data[38] on high-energy total cross sections for πN and KN are very much flatter than would be expected by extrapolating pure Regge pole fits.

Possibly these results can be understood by appealing to cut contributions[39].

4.6. Q = 2 Exchanges.

Certain reactions cannot be mediated by the exchange of any single particle contained in the known U(3) singlet, octet, or deciments. However, the successive exchange of two single particles could take place. Examples of two such reactions on which data now exists are :

$$pn \to \Delta^- \Delta^{++} \quad (40)$$

and

$$p\bar{p} \to \Sigma^- \bar{\Sigma}^- \quad (41)$$

4.7. Regge Cuts and Absorptive Corrections.

The existence of cuts in the complex angular momentum plane was first proposed by Amati, Fubini and Stangehellini[42] from a study of perturbation theory. Mandelstam[43] later showed that the two-Reggeon cut in the AFS diagrams were cancelled by other contributions, but he showed how to generate cut diagrams which really have a cut contribution.

The essential difference between the AFS and Mandelstam diagrams is that, whereas the AFS diagram does not have a third double spectral function ρ_{st}, the Mandelstam diagrams do.

No one really knows how to calculate the cuts, but we do know some general properties, which we will now mention[44].

(i) The discontinuity across the cut near $j = \alpha_n^c$ is given by

$$\text{disc} \sim \left(\alpha_n^c(t) - j \right)^{n-2}$$

for the n-Reggeon exchange. Then the cut contribution to the amplitude behaves like

$$f^{\text{cut}} \sim \frac{s^{\alpha_c(t)}}{\ln s^{n-1}}$$

It would be nice if we could detect the presence of Regge cuts directly from experiment by measuring this extra logarithmic

s-dependence of the cut, but in practice this is not possible because the logarithmic dependence is too slow.

(ii) If n Regge poles $\alpha_i(t)$ are exchanged, the leading cut has a branch point given by

$$\alpha_n^c(t) = \text{Max} \left(\sum_{i=1}^{n} \alpha_i(t_i) \right) - n + 1$$

where the quantities $\sqrt{|t|}$ and $\sqrt{|t_i|}$ have to form a closed polygon.

For two linear trajectories

$$\alpha_i(t) = \alpha_i(0) + \alpha_i' t$$

the two Reggeon branch point is also linear and is given by

$$\alpha_{12}(t) = \alpha_1(0) + \alpha_2(0) - 1 + \frac{\alpha_1' \alpha_2'}{\alpha_1' + \alpha_2'} t$$

The cut not only has a slope smaller than either slope (if $\alpha_i' > 0$) but also generally has lower intercept at $t = 0$. So the pole will always dominate for a range of t near zero, but the cuts will be important for sufficiently large $|t|$. If all the Reggeons except one are pomerons, with $\alpha_p(0) = 1$, the branch points of all the cuts coincide at $t=0$ with α_1 and lie above it for $t < 0$. So we expect pomeron-induced cut corrections to dominate asymptotically over poles

for $t < 0$. At $t = 0$ they are unfavoured logarithmically.

(iii) A Regge pole belongs to a unique spin-parity class whereas a two-Reggeon cut does not. It can have contributions to both parities, and so can conspire with itself.

(iv) Cut contributions are non-factorizable so this eliminates the problems arising from factorizing residues and relating different processes.

One of the difficulties with Regge cuts is the lack of knowledge of the discontinuity function. At present there is no really satisfactory way to estimate the cut discontinuities, the standard approach is to use the ideas of the absorption model of Jackson[7]. (A popular approach is to identify the Regge pole term as the first term in some series. The higher terms are then given by interactions of the first term, generating cuts. One of these approaches is the absorption model).

The traditional Watson formula[8] is the basic formula of the absorption model and has been used with considerable success for processes dominated by pion exchange[20,21,22]. It also serves as the starting point for the generation of Regge cut amplitudes.

The traditional Watson formula, or closely related expressions, forms the basis for numerous calculations of peripheral processes with "absorbed" Regge poles[45]. A number of these papers address themselves to the polarization seen in πN charge exchange, as well as

the shape of the differential cross section. There are two viewpoints here. One is that the basic Regge pole amplitude which is to be inserted into the Watson formula should be a traditional amplitude with appropriate factors to cause it to vanish at "nonsense" J values ($J < |J_z|$). In the Watson formula we have terms like

$$R^{\emptyset} P$$

If R which is put into the convolution changes sign in the region of integration, there will be a cancellation in the integral and the resulting cut amplitude will tend to be small. Thus the absorptive correction will cause only modest changes from the pure pole term. Dips will still be mainly a consequence of the structure of the pole amplitude itself. The idea that the pole amplitudes possess the sense-nonsense factors is partly supported by the successes of exchange degeneracy in correlating the presence or absence of direct channel resonances with the Regge poles in the crossed channels.

An alternative view, put forward by Henyey et. al.[46], is that in the presence of absorptive corrections all prior notions about sense-nonsense factors should be discarded. This idea rests upon the work of Jones and Teplitz [47] and Mandelstam and Wang[48] who showed that the usual arguments for the presence of sense-nonsense factors fail because the residues become singular at wrong-signature nonsense points when the third double spectral function is present. The mechanism for the dip in the differential cross section is then the distructive interference berween the pole and the cut amplitudes[46].

One important point should be made about t = 0. There are a number of processes ($pn \to np$, $\gamma p \to \pi^+ n$, $\pi^+ p \to \rho^0 \Delta^{++}$) that appear to be dominated by the exchange of a single Regge pole (in the examples listed, the pion). In some of these processes, the amplitude of the single Regge pole must vanish at t = 0 for kinematic reasons[36]. The differential cross section is then expected to vanish in the forward direction. The observations show, on the contrary, sharp forward peaks. Such peaks find a natural explanation in terms of absorptive corrections. The cut amplitude, being a convolution, is smoothly varying and non-zero at t = 0. The pole amplitude increases away from t = 0, causing distructive interference and a sharply falling cross section. This mechanism explains all the sharp forward peaks and avoids the difficulties of conspiracies.

At the high energies we are considering, we are approaching the classical limit and thus the low energy analysis of the scattering in terms of angular momentum may be replaced by a description in terms of the impact parameter. The scattering amplitude for the transition $i \to f$ in terms of the angular momentum, assuming no spin, is

$$\frac{T_{fi}(\cos\theta)}{8\pi\sqrt{s}} = i \sum_{\ell=0}^{\infty} (2\ell+1) \frac{(1 - e^{i\chi})}{2} fi \quad P_\ell(\cos\theta)$$

where $\chi(\ell)$ is the "eikonal matrix". Using the orthogonality property of the Legendre polynomials,

$$\int_{-1}^{1} P_\ell(\cos\theta)\, P_{\ell'}(\cos\theta)\, d(\cos\theta) = \frac{2\delta_{\ell\ell'}}{2\ell+1}$$

this gives

$$(1 - e^{i\chi})_{fi} = -i\, P \int_{-1}^{1} \frac{T_{fi}(\cos\theta)}{8\pi\sqrt{s}}\, P_\ell(\cos\theta)\, d(\cos\theta)$$

Taking $(1 - e^{i\chi})_{fi} \simeq -i\chi_{fi}$ (49) This gives

$$\chi_{fi}(\ell) = P \int_{-1}^{1} \frac{T_{fi}(\cos\theta)}{8\pi\sqrt{s}}\, P_\ell(\cos\theta)\, d(\cos\theta)$$

The term $T_{fi}(\cos\theta)$ is the "Born amplitude" of the model and is identified with an amplitude for the transition $i \to f$ parameterized in a simple Regge pole exchange model, i.e.

$$T_{fi}(\cos\theta) = \sum_{\substack{\text{Regge} \\ \text{poles}}} .$$

The impact parameter representation has been introduced in Chapter II.

Let us assume

$$T_{fi}(\cos\theta) = \left(\frac{s}{s_0} \right)^{\alpha(t)}$$

which is the typical Regge pole form without signature. Then

$$\chi_{fi}(\ell) = P \int_{-1}^{1} \frac{T_{fi}(\cos\theta)}{8\pi\sqrt{s}} \; P_{\ell}(\cos\theta)\, d\,(\cos\theta)$$

which in the impact parameter representation becomes

$$\chi^{R}_{fi}(b) = P \int_{0}^{\infty} \frac{1}{p^2} \sqrt{|t|} \; d\,(\sqrt{|t|}\,)\, J_0(b\sqrt{|t|}) \; \frac{1}{8\pi\sqrt{s}} \left(\frac{s}{s_0} \right)^{\alpha(t)}$$

Taking $\alpha(t) = \alpha_0 + \alpha' t$

$$\chi^{R}_{fi}(b) = \frac{1}{8\pi P\sqrt{s}} \int_{0}^{\infty} \sqrt{|t|} \; d(\sqrt{|t|}\,)\, J_0\,(b\sqrt{|t|}\,)\; e^{\ln\left(\frac{s}{s_0} \right)^{\alpha(t)}}$$

$$= \frac{1}{8\pi P\sqrt{s}} \int_{0}^{\infty} \sqrt{|t|} \; d(\sqrt{|t|}\,)\; J_0\,(b\sqrt{|t|}\,)\; e^{\alpha(t)\ \ln\left(\frac{s}{s_0} \right)}$$

$$= \frac{1}{8\pi P\sqrt{s}} \int_{0}^{\infty} \sqrt{|t|} \; d(\sqrt{|t|}\,)\; J_0\,(b\sqrt{|t|}\,)\; e^{\alpha_0 \ln\left(\frac{s}{s_0} \right)} \; e^{-\alpha' \ln\left(\frac{s}{s_0} \right) |t|}$$

The calculation of the Regge cut in the impact parameter representation is based entirely on the application of the Fourier-Bessel transform.

$$\int_0^\infty x^{\nu+1}\, e^{-\alpha x^2}\, J_\nu(\beta x)\, dx = \frac{\beta^\nu}{(2\alpha)^{\nu+1}}\, e^{-\frac{\beta^2}{4\alpha}}$$

$$(\mathrm{Re}\,\alpha > 0\ ;\ \mathrm{Re}\,\nu > -1)$$

In our case we obtain with

$$\nu = 0;\quad \beta = b;\quad \alpha = \alpha' \ln\left(\frac{s}{s_0}\right)$$

$$\chi_{fi}^{R}(b) = \frac{e^{\alpha_0 \ln\left(\frac{s}{s_0}\right)}}{8\pi P\sqrt{s}} \cdot \frac{1}{\left(2\alpha' \ln\left(\frac{s}{s_0}\right)\right)}\, e^{-\frac{b^2}{4\alpha' \ln\left(\frac{s}{s_0}\right)}}$$

$$\chi_{fi}^{R}(b) = \frac{1}{8\pi P\sqrt{s}} \left(\frac{s}{s_0}\right)^{\alpha_0} \cdot \frac{1}{\left(2\alpha' \ln\left(\frac{s}{s_0}\right)\right)}\, e^{-\frac{b^2}{4\alpha' \ln\left(\frac{s}{s_0}\right)}}$$

Thus, for the exchange of n Regge poles described by the trajectory $\alpha(t)$ we get

$$R_1 \otimes R_2 \otimes \ldots R_n = \sum_{\ell=0}^{\infty} (2\ell+1)\, \frac{1}{2iP}\, P_\ell(\cos\theta) \prod_{i=1}^{n} \left(i\, \chi^R\right)_{fi}$$

$$= \int_0^\infty P^2\, db(2Pb)\ \frac{1}{2iP}\ J_0(b\sqrt{|t|})\left[\frac{i}{8\pi P\sqrt{s}}\left(\frac{s}{s_0}\right)^{\alpha_0}\frac{1}{2\alpha' \ln\left(\frac{s}{s_0}\right)}\ e^{-\frac{b^2}{4\alpha' \ln\left(\frac{s}{s_0}\right)}}\right]$$

$$= \frac{i^n}{(8\pi P\sqrt{s})^n}\ \frac{1}{2i}\left(\frac{s}{s_0}\right)^{n\alpha_0}\frac{(2P^2)}{\left(2\alpha' \ln\left(\frac{s}{s_0}\right)^n\right)}\int_0^\infty bdb\, J_0(b\sqrt{|t|})\ e^{-\frac{nb^2}{4\alpha' \ln\left(\frac{s}{s_0}\right)}}$$

With $\nu = 0$; $\beta = \sqrt{|t|}$; $\alpha = \dfrac{n}{4\alpha' \ln\left(\frac{s}{s_0}\right)}$ we have

$R_1 \otimes R_2 \otimes \ldots R_n$

$$= \frac{i^{n-1}P^2}{(8\pi P\sqrt{s})^n}\left(\frac{s}{s_0}\right)^{n\alpha_0}\frac{1}{\left(2\alpha' \ln\left(\frac{s}{s_0}\right)^n\right)}\left(\frac{1}{\frac{2n}{4\alpha' \ln\left(\frac{s}{s_0}\right)}}\right)e^{-\frac{4\alpha' \ln\left(\frac{s}{s_0}\right)|t|}{4n}}$$

$$= \frac{i^{n-1}P^2}{(8\pi P\sqrt{s})^n}\left(\frac{s}{s_0}\right)^{n\alpha_0}\cdot\frac{1}{\left\{2\alpha' \ln\left(\frac{s}{s_0}\right)\right\}^{n-1}\ n}\ e^{-\frac{4\alpha'|t| \ln\left(\frac{s}{s_0}\right)}{4n}}$$

$R_1 \otimes R_2 \otimes \ldots R_n$

$$= \frac{i^{n-1}P^2}{(8\pi P\sqrt{s})^n}\left(\frac{s}{s_0}\right)^{n\alpha_0}\frac{1}{n\left\{2\alpha' \ln\left(\frac{s}{s_0}\right)\right\}^{n-1}}\ e^{\ln\left(\frac{s}{s_0}\right)^{-\frac{\alpha'}{n}|t|}}$$

$$= \frac{i^{n-1} P^2}{(8\pi P\sqrt{s})^n} \left(\frac{s}{s_0}\right)^{n\alpha_0} \frac{1}{n\left(2\alpha' \ln\left(\frac{s}{s_0}\right)\right)^{n-1}} \left(\frac{s}{s_0}\right)^{-\frac{\alpha'}{n}|t|}$$

$$= \frac{i^{n-1} P^2}{(8\pi P\sqrt{s})^n} \frac{1}{n\left(2\alpha' \ln\left(\frac{s}{s_0}\right)^{n-1}\right)} \left(\frac{s}{s_0}\right)^{n\alpha_0 - \frac{\alpha'}{n}|t|}$$

So we have the result

$$R_1 \quad \theta \quad R_2 \quad \theta \quad \ldots \quad R_n$$

$$= \frac{i^{n-1} P^2}{(8\pi P\sqrt{s})^n} \frac{1}{n\left(2\alpha' \ln\left(\frac{s}{s_0}\right)^{n-1}\right)} \left(\frac{s}{s_0}\right)^{n\alpha_0 - \frac{\alpha'}{n}|t|}$$

Taking the high-energy limit, i.e. $s \to \infty$ and $P \to \sqrt{s}$, we have

$$R_1 \quad \theta \quad R_2 \quad \theta \ldots R_n \to \frac{(s)}{(s)^n} \left(\frac{s}{s_0}\right)^{n\alpha_0 - \frac{\alpha'}{n}|t|} \frac{1}{\left(\ln\left(\frac{s}{s_0}\right)^{n-1}\right)}$$

$$R_1 \; 0 \; R_2 \; 0 \ldots R_n \to \left(\frac{s}{s_o}\right)^{-n+1} \left(\frac{s}{s_o}\right)^{n\alpha_o - \frac{\alpha'}{n}|t|} \frac{1}{\left(\ln\left(\frac{s}{s_o}\right)^{n-1}\right)}$$

$$R_1 \; 0 \; R_2 \; 0 \ldots R_n \to \frac{\left(\frac{s}{s_o}\right)^{n\alpha_o - n + 1 - \frac{\alpha'}{n}|t|}}{\left(\ln\left(\frac{s}{s_o}\right)\right)^{n-1}}$$

Saving only factors in s we have

$$R_1 \; 0 \; R_2 \; 0 \ldots R_n \xrightarrow[s \to \infty]{} \frac{s^{\alpha_c(t)}}{\left(\ln s\right)^{n-1}}$$

where $\alpha_c(t) = n\alpha_o - n + 1 + \frac{\alpha'}{n} t$

Thus we see that absorptive corrections to Reggeized pole graphs gives rise to cut contributions to the transition amplitude.

CHAPTER V

REGGE POLE MODEL FOR $0^-\frac{1}{2}^+ \to 1^-3/2^+$.

5.1 Introduction.

To Reggeize the amplitudes we make the replacement

$$\frac{1}{t-M^2} \to \frac{d\alpha}{dt}\bigg|_{t=M^2} \frac{\pi}{\sin\pi(\alpha-J)} \frac{1+\tau e^{-i\pi\alpha}}{2} \left(\frac{s+\frac{1}{2}t - \frac{1}{2}\sum_{i=1}^{4} m_i^2}{s_0} \right)^{\alpha-J},$$

where $\alpha = J$ at the pole $t = M^2$ and τ is the signature. The scale factor s_0 is taken to have the value $1\ (\text{GeV})^2$ since any other choice is equivalent to the introduction of an exponential factor into the residue. The coupling constants g and h retain the values at the poles. By expanding in a Taylor series about $t = M^2$

$$\sin\pi(\alpha-J) \simeq \sin\pi(\alpha-J)\Big|_{t=M^2} + \frac{d}{dt}\sin\pi(\alpha-J)\Big|_{t=M^2} (t-M^2)$$

$$\simeq \pi \frac{d\alpha}{dt}\bigg|_{t=M^2} (t-M^2),$$

and noting that the signature and $s^{\alpha-J}$ factors are unity at $t = M^2$, we see that this relation is exact at the pole $t = M^2$.

The Gell-Mann ghost eliminating mechanism[36] is then introduced by making the replacement

$$\frac{\pi}{\sin \pi\alpha} = \Gamma(\alpha)\,\Gamma(1-\alpha)$$

and dividing by $\Gamma(\alpha)$ for natural-parity exchange, and making the replacement

$$\frac{\pi}{\sin \pi\alpha} = -\Gamma(-\alpha)\,\Gamma(1+\alpha)$$

and dividing by $\Gamma(1+\alpha)$ for unnatural-parity exchange in all amplitudes. Here natural parity is defined by $(-1)^J=P$ and unnatural parity by $-(-1)^J=P$ where P is the intrinsic parity. This mechanism retains the same ratio between the helicity amplitudes when they are extrapolated from the pole.

We also wish to consider the exchange of the A_2 meson ($J^P = 2^+$), which does not belong to the ($\underline{35}$, $\ell = 0$). By employing the representation of U(6,6) which contains the A_2, namely, the $\underline{4212}$, we have forced upon us exotics, for which no experimental evidence has been found. Therefore, to obtain mesons not belonging to the ($\underline{35}$, $\ell = 0$) we angular-momentum excitate this lowest representation of U(6,6) to obtain U(6,6) $\otimes$ O(3,1). This has the effect of only changing the spin and parity of the particles. Using a spin-2 field-theoretic propagator then gives amplitudes which are similar to those for 1^- exchange but containing one more power of s and some extra terms which are non-leading in s. If we ignore these extra terms, we may obtain the Reggeized 2^+-exchange amplitudes simply by changing the signature and Clebsch-Gordan coefficients. This is the

procedure we adopt since we wish to obtain the coupling strength from the additional assumption of strong exchange degeneracy. The 1^+-exchange amplitudes are obtained from the 0^--exchange amplitudes in a similar manner. Since previous authors have shown the applicability of ρ - A_2 exchange degeneracy and SU(3) symmetry to $0^-\frac{1}{2}^+ \to 0^-\ \frac{1}{2}^+$ charge-exchange reactions[3], we consider this a reasonable prescription.

Explicit expressions for the s-channel helicity amplitudes are given in Appendix E.

The Regge trajectories required were obtained from the Chew-Frautschi plot shown in fig. 18 by assuming

$$\rho\ (765)\ -\ A_2(1300)$$

$$\pi\ (140)\ -\ B\ (1235)$$

exchange degeneracy. The result is given in Table 2.

For processes of the type $0^-\frac{1}{2}^+ \to 1^-\ 3/2^+$ data is available for the following reactions

$$\pi^+ p \to \rho^0 \Delta^{++} \quad (25,26,50)$$
$$K^+ p \to K^{*0} \Delta^{++} \quad (27)$$
$$K^- n \to \bar{K}^{*0} \Delta^- \quad (24)$$
$$\pi^+ p \to \omega \Delta^{++} \quad (25,29,50)$$

The ρ - and K^* - production data are characterized by the presence of a forward peak, presumably due to π exchange.

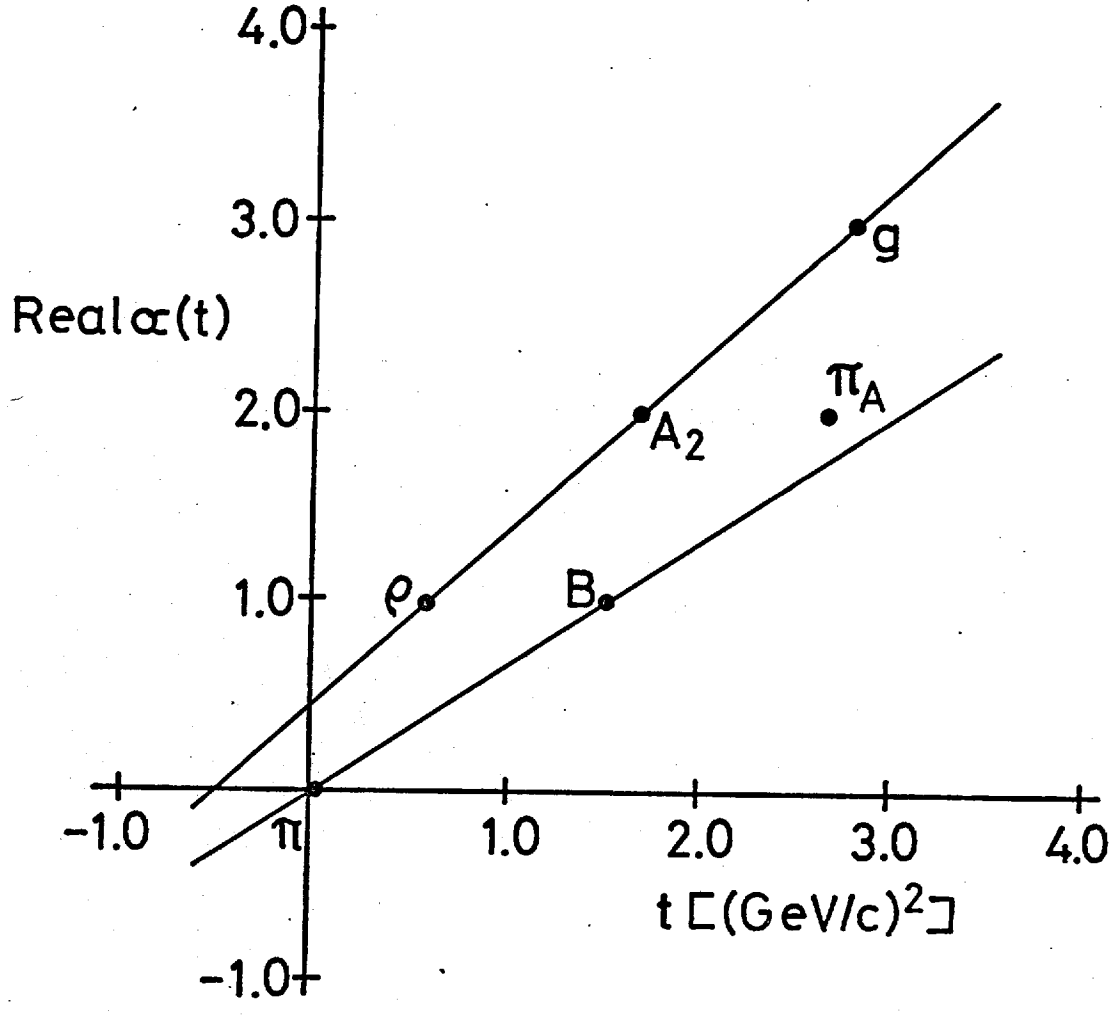

FIG. 18.

5.2 $\pi^+ p \to \rho^0 \Delta^{++}$

Our results for the differential cross section for $\pi^+ p \to \rho^0 \Delta^{++}$, which proceeds by the exchange of π and A_2, are shown in Fig. 19 . The essential features of the theoretical curves are a sharp forward peak due to π exchange and a relatively flat wide-angle distribution due to $\pi + A_2$ exchange. This behaviour is exhibited by the data, most markedly at 13.1 GeV/c. In general the theory agrees with the experimental data in respect of the forward peak and reproduces the s dependence of the data. For larger momentum transfers the theoretical distributions are consistently too high.

The density matrix elements for this reaction are shown in Fig.20 Before absorption unnatural-parity exchange ($\pi$and B) gives

$$\rho_{oo} = 1 \quad , \quad \rho_{1,-1} = 0 \quad , \quad \mathrm{Re}\,\rho_{10} = 0,$$

while natural-parity exchange ($\rho$and A_2) gives

$$\rho_{oo} = 0, \quad \rho_{1,-1} = \tfrac{1}{2}, \quad \mathrm{Re}\,\rho_{10} = 0,$$

for the density matrix elements of the meson resonance. For the Δ resonance unnatural-parity exchange gives

$$\rho_{3\,3} = 0, \quad \mathrm{Re}\rho_{3,-1} = 0, \quad \mathrm{Re}\rho_{3\,1} = 0,$$

while natural-parity exchange gives

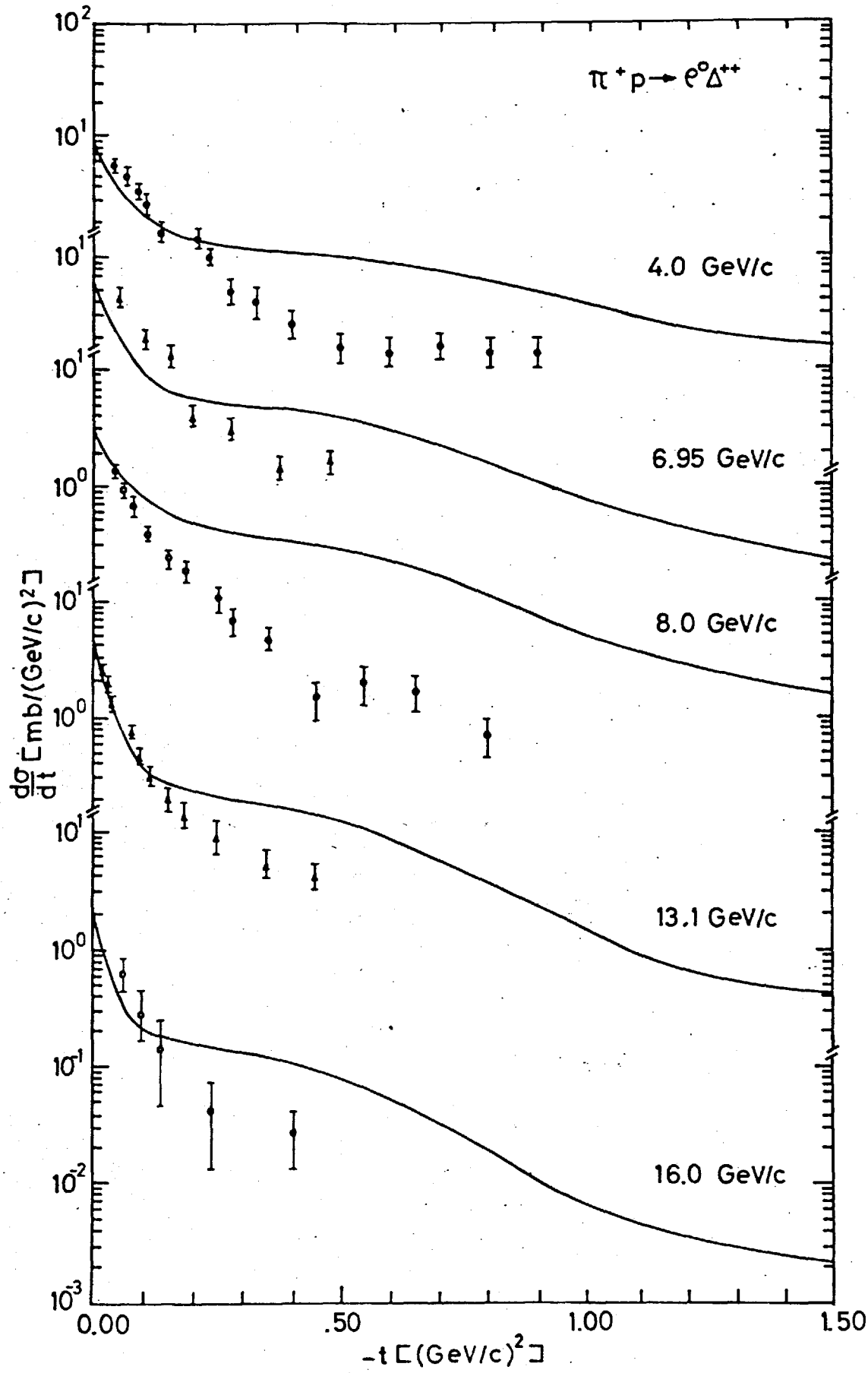
$\pi^+ p \rightarrow \rho^0 \Delta^{++}$
4.0 GeV/c
6.95 GeV/c
8.0 GeV/c
13.1 GeV/c
16.0 GeV/c
$\frac{d\sigma}{dt}$ [mb/(GeV/c)^2]
$-t$ [(GeV/c)^2]
10^2
10^1
10^0
10^{-1}
10^{-2}
10^{-3}
0.00
.50
1.00
1.50

FIG. 19.

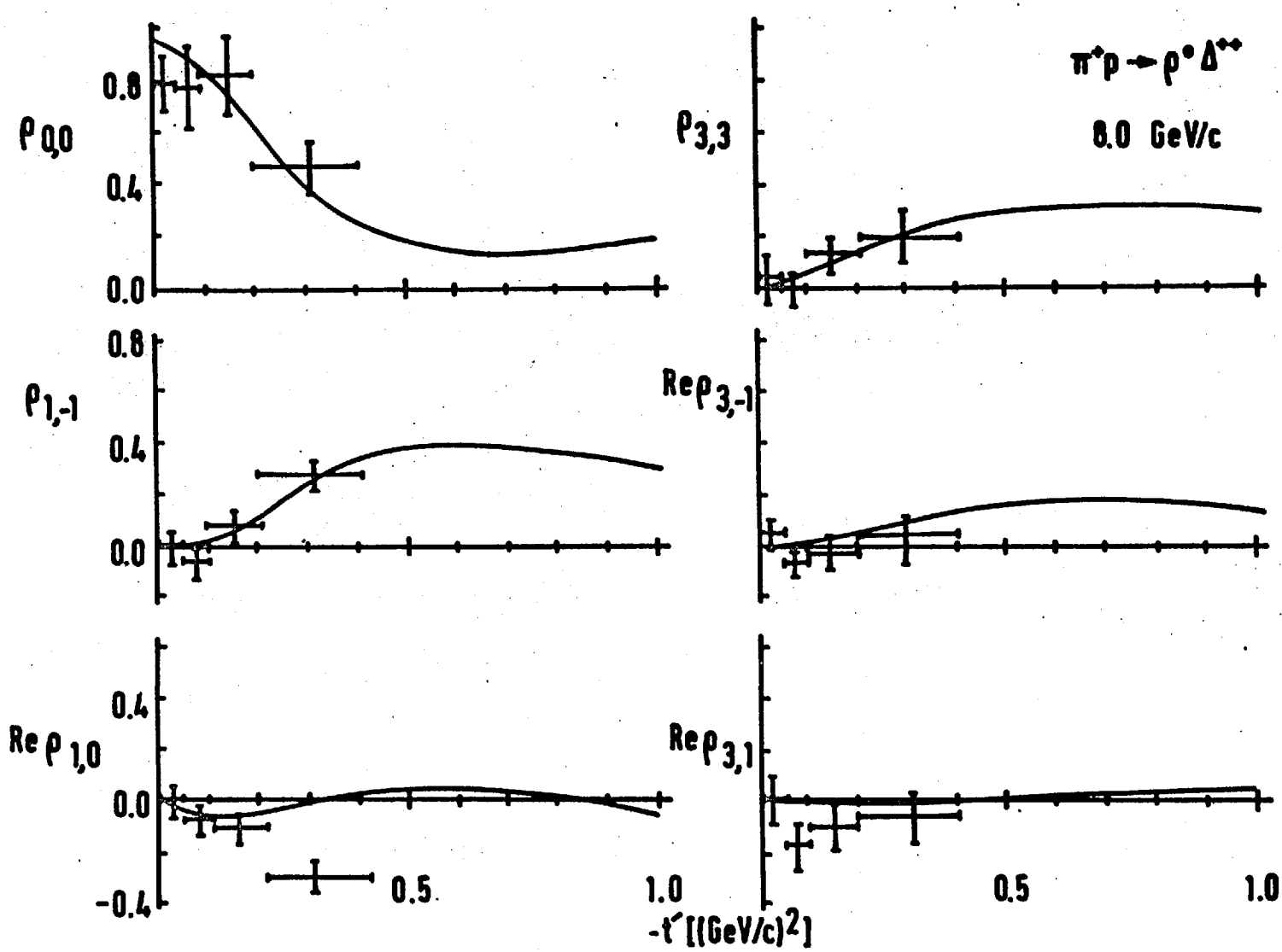
$\pi^+p \to \rho^0\Delta^{++}$
8.0 GeV/c
$\rho_{0,0}$
$\rho_{3,3}$
$\rho_{1,-1}$
$Re\,\rho_{3,-1}$
$Re\,\rho_{1,0}$
$Re\,\rho_{3,1}$
0.8
0.4
0.0
-0.4
0.5
1.0
$-t' [(GeV/c)^2]$

FIG. 20.

$$\rho_{3\,3} = 3/8 \quad , \qquad \text{Re}\,\rho_{3,-1} = \sqrt{3/8} \quad , \quad \text{Re}\,\rho_{3\,1} = 0.$$

The absorption does not have much effect on these values. The large value of ρ_{00} and the small values of $\rho_{1,-1}$, $\rho_{3\,3}$ and $\text{Re}\,\rho_{3,-1}$ indicate strong unnatural-parity exchange dominance, particularly for small t. This is given by the model, π exchange being the dominant mechanism.

5.3 $K^+p \to K^{*o}\Delta^{++}$

In fig.21 we compare with the data our results for the differential cross section for the reaction $K^+p \to K^{*o}\Delta^{++}$, which permits π , ρ, B and A_2 exchanges. The data for this reaction is poorer than for $\pi^+p \to \rho^o\Delta^{++}$, thus making it difficult to discern details in the momentum transfer distributions. Our theoretical predictions show a pion forward peak which, as in the previous reaction, becomes sharper with increasing energy as $t_{min} \to 0$, followed by a relatively flat distribution. The s dependence of the data is well reproduced at 3.0, 3.5 and 5.0 GeV/c but is poorer at 12.7 GeV/c.

The density matrix elements for this reaction, shown in fig. 22 have the same general experimental features as in the previous reaction and appear to be well represented by our model.

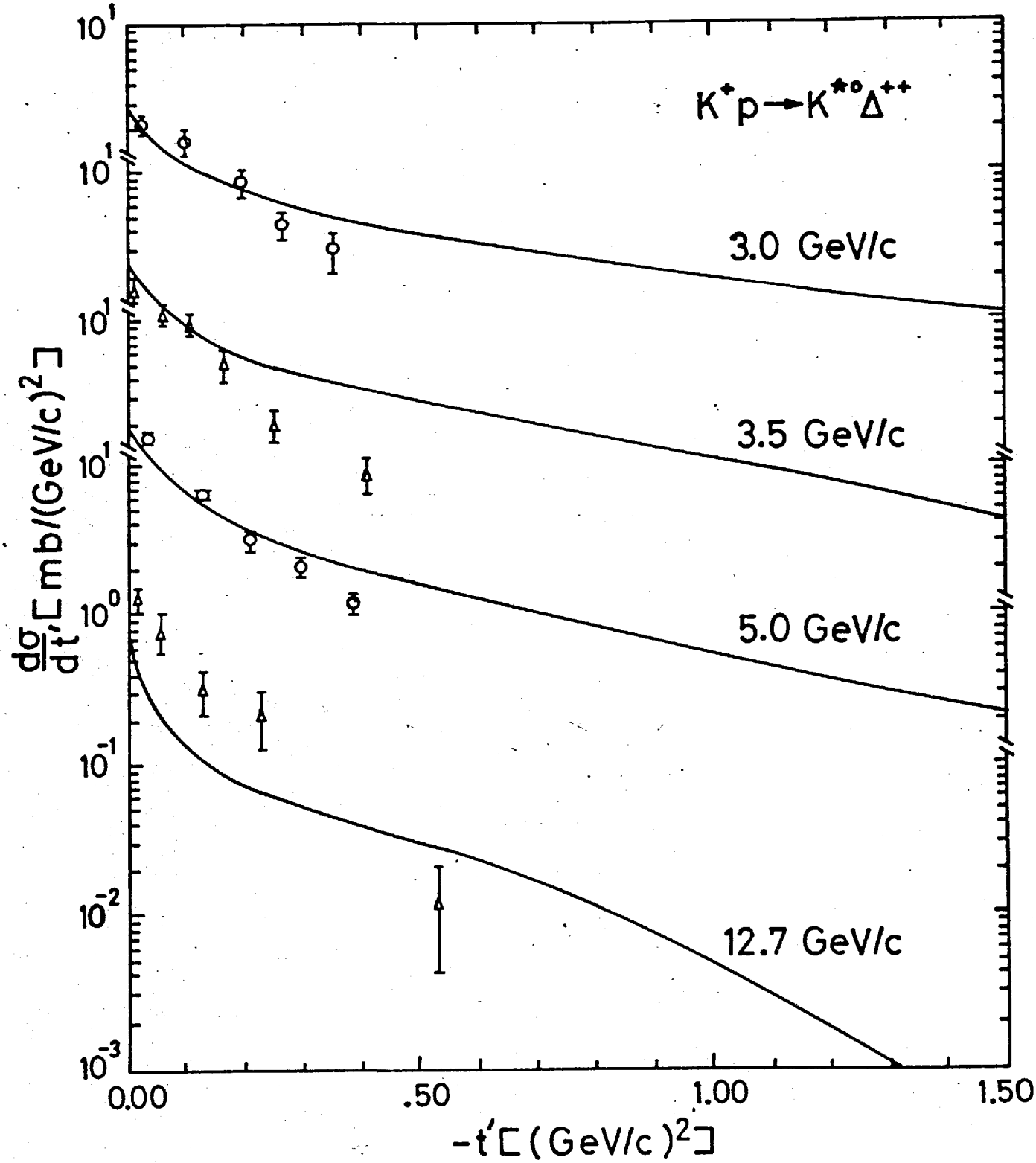
$K^+p \to K^{*0}\Delta^{++}$
3.0 GeV/c
3.5 GeV/c
5.0 GeV/c
12.7 GeV/c
$\frac{d\sigma}{dt'}$ [mb/(GeV/c)^2]
$-t'$ [(GeV/c)^2]
10^1
10^0
10^{-1}
10^{-2}
10^{-3}
0.00
.50
1.00
1.50

FIG. 21.

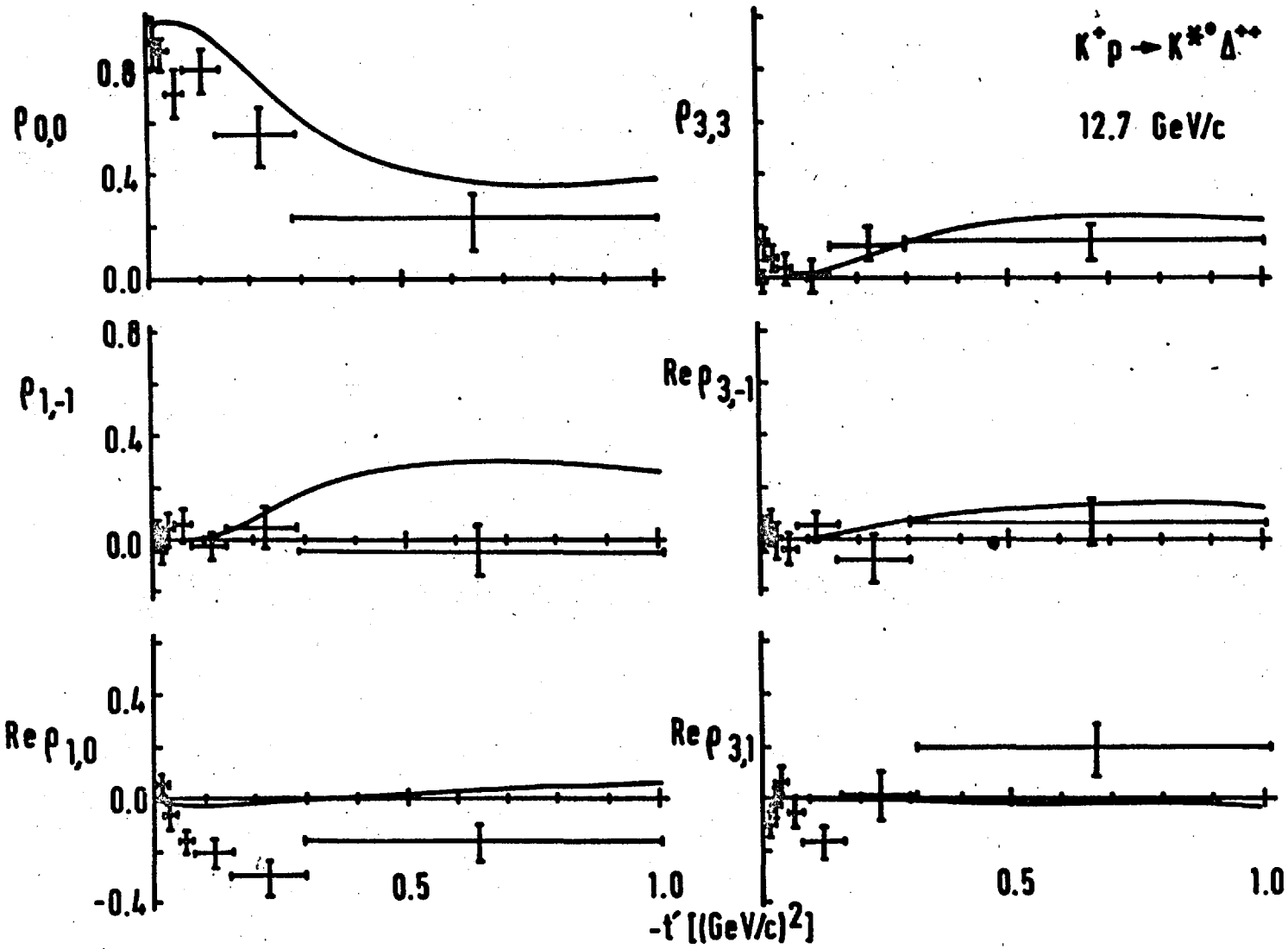
$K^+p \to K^{*0}\Delta^{++}$
12.7 GeV/c
$\rho_{0,0}$
$\rho_{3,3}$
$\rho_{1,-1}$
$Re\,\rho_{3,-1}$
$Re\,\rho_{1,0}$
$Re\,\rho_{3,1}$
0.8
0.4
0.0
-0.4
0.5
1.0
$-t' [(GeV/c)^2]$

FIG. 22

5.4. $K^- n \to \overline{K^{*o}} \Delta^-$

The reaction $K^- n \to \overline{K^{*o}} \Delta^-$ is similar to $K^+ p \to K^{*o} \Delta^{++}$ except that the ρ - and B-exchange contributions change sign. In particular, for the pole graphs

$$\frac{d\sigma}{dt}\left(K^- n \xrightarrow{\pi} \overline{K^{*o}} \Delta^-\right) = \frac{d\sigma}{dt}\left(K^+ p \xrightarrow{\pi} K^{*o} \Delta^{++}\right).$$

A comparison of the data at 5.5 and 5.0 GeV/c, respectively, for these two reactions suggests that this prediction is broken by about 50%, indicating the importance of including contributions from the ρ and A_2 exchanges and dis-similar absorption corrections. The theoretical distributions and the available data for $K^{*o} \Delta^-$ production are shown in fig. 23. The normalization is too large but the t dependence appears to be correct, although the data is not good enough to observe detailed structure, in particular, the expected sharp forward pion peak. No data is available for the density matrix elements.

5.5 $\pi^+ p \to \omega \Delta^{++}$

In fig.24 we show the contributions of ρ, B and ρ + B exchange to the differential cross section for $\pi^+ p \to \omega \Delta^{++}$. The ρ exchange shows a large dip at $t = -.5$. As in the reaction $\pi^+ n \to \omega\, p$, the constructive interference between the ρ and B exchanges helps to fill in this dip but the coupling of the B given by strong exchange degeneracy is not sufficiently large to completely eliminate this structure.

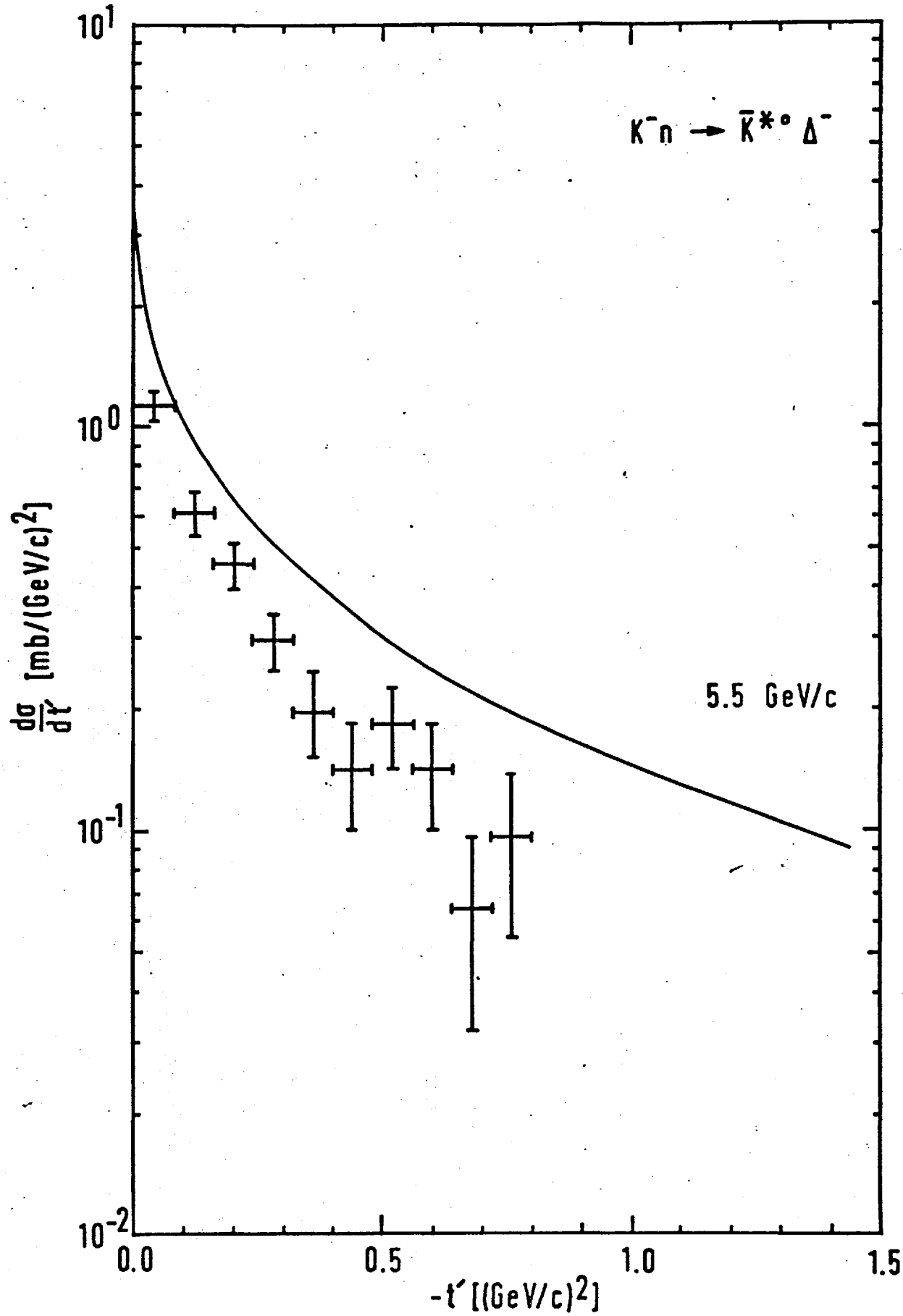
10^1
10^0
10^{-1}
10^{-2}
$K^-n \rightarrow \bar{K}^{*\circ}\Delta^-$
5.5 GeV/c
$\frac{d\sigma}{dt'}$ [mb/(GeV/c)^2]
0.0
0.5
1.0
1.5
$-t'$ [(GeV/c)^2]

FIG. 23.

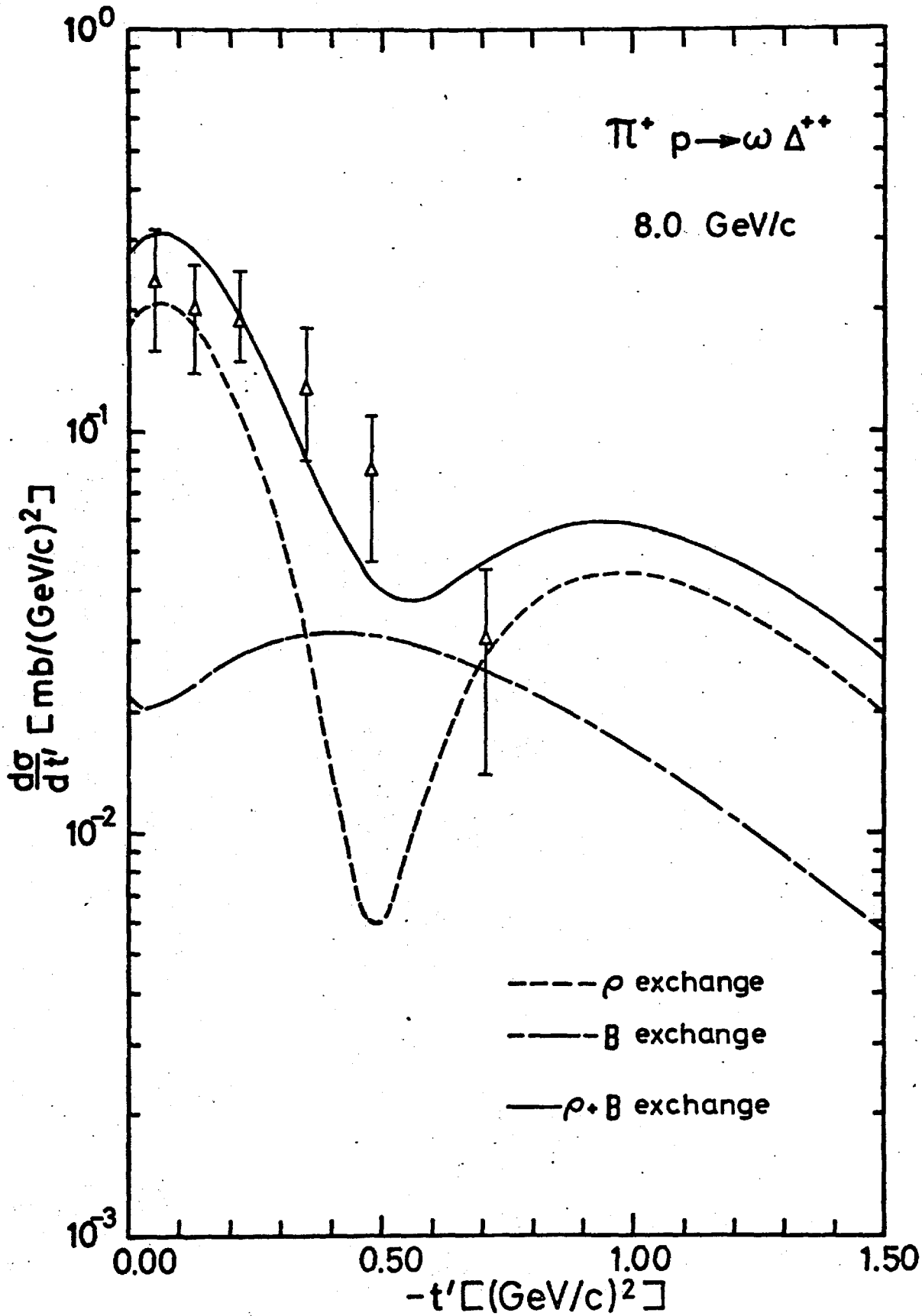
10^0
10^{-1}
10^{-2}
10^{-3}
$\pi^+ p \rightarrow \omega \Delta^{++}$
8.0 GeV/c
$\frac{d\sigma}{dt'}$ [mb/(GeV/c)^2]
ρ exchange
B exchange
ρ + B exchange
0.00
0.50
1.00
1.50
$-t'$[(GeV/c)^2]

FIG. 24.

The available high-energy data for this reaction and the theoretical predictions for the momentum transfer distributions are shown in fig. 25 . The s dependence of the theory is quite satisfactory.

The contributions to the density matrix elements for this reaction from ρ,B and ρ + B exchanges are shown in fig. 26 . As in $\pi^+ n \rightarrow \omega p$[61] the addition of B meson exchange improves the results obtained from pure ρ exchange to give reasonable agreement with the data.

5.6 Discussion and Conclusions.

In summary we make the following observations.

For the processes we have analysed the angular dependence of the differential cross sections predicted by the model agrees with the essential features of the experimental data, in particular, forward peaks, turnovers and dips, in all cases where the data is sufficiently good to enable such comparisons to be made. This is also true of the density matrix elements. Although the dips in the differential cross sections arise originally from the nonsense zeros introduced in the Reggeization procedure, this feature is largely due to the influence of the symmetry scheme, which determines the ratios of the helicity amplitudes and the relative strengths of the couplings at the vertices.

The energy dependence of the model derives mainly from the replacement of s^J by s^α in the Reggeization of the amplitudes, although

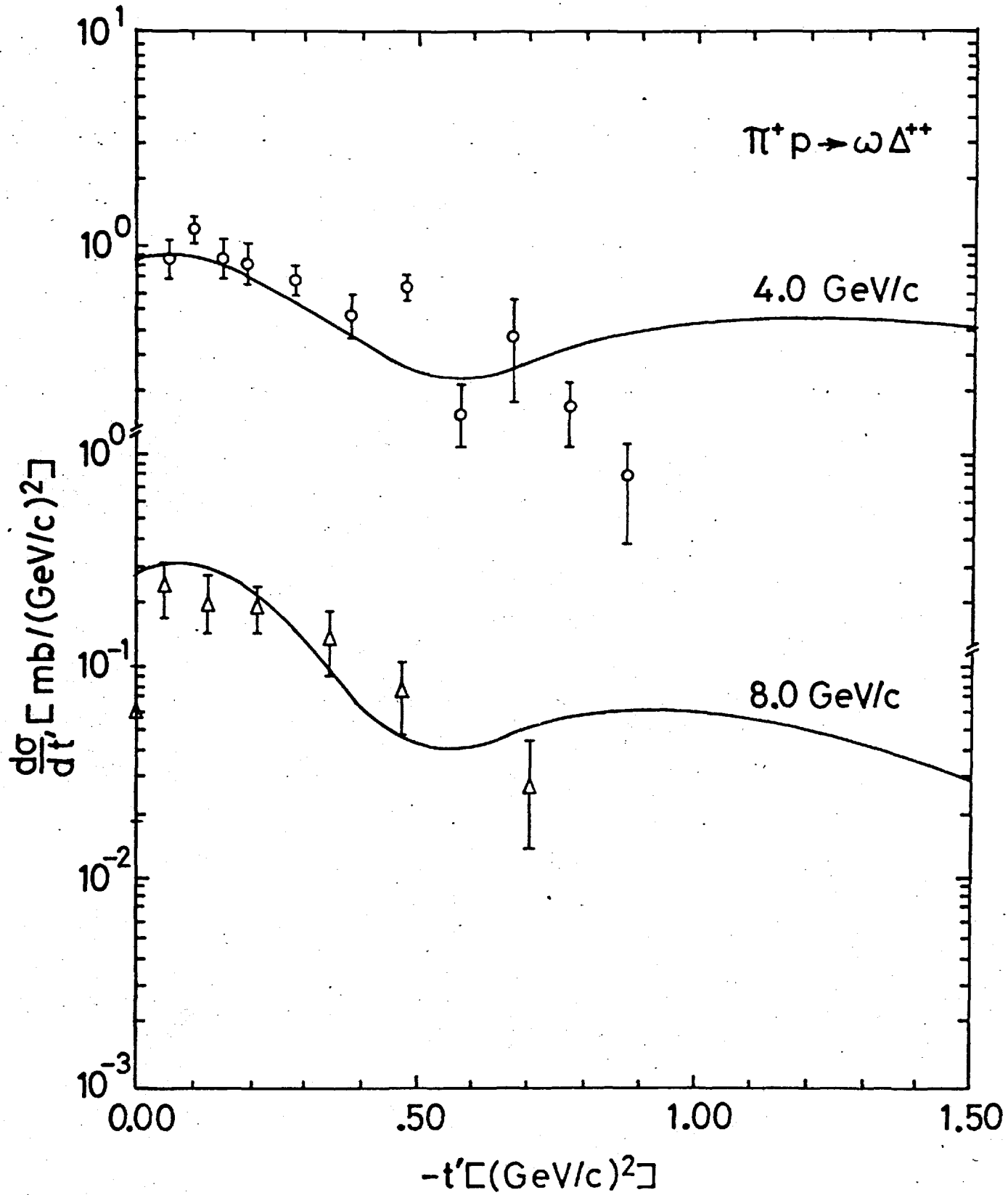
$\pi^+ p \to \omega \Delta^{++}$
4.0 GeV/c
8.0 GeV/c
$\frac{d\sigma}{dt'}$ [mb/(GeV/c)^2]
$-t'$ [(GeV/c)^2]
10^1
10^0
10^0
10^{-1}
10^{-2}
10^{-3}
0.00
.50
1.00
1.50

FIG. 25.

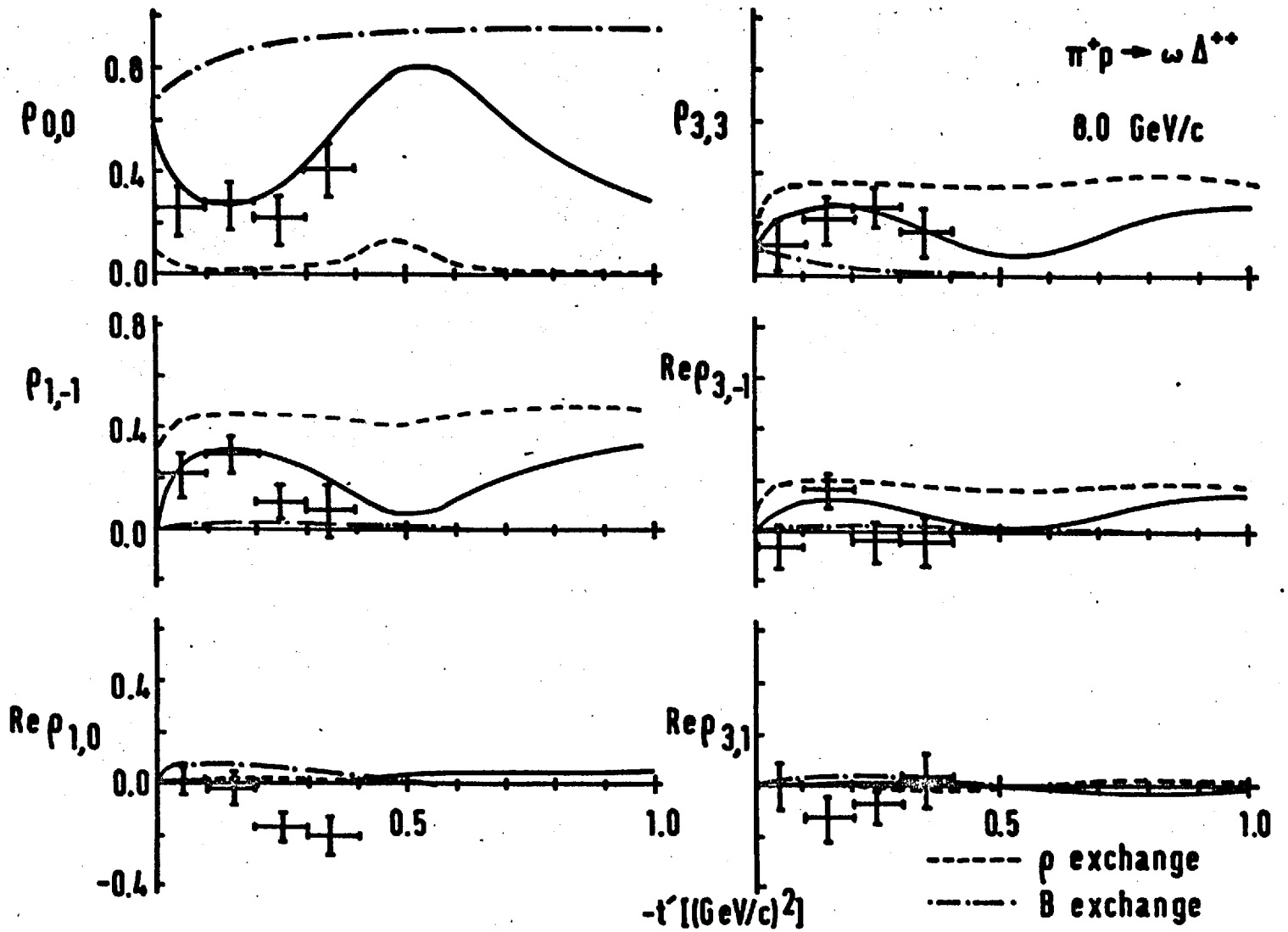
$\rho_{0,0}$
$\rho_{3,3}$
$\pi^+p \to \omega\Delta^{++}$
8.0 GeV/c
$\rho_{1,-1}$
$Re\rho_{3,-1}$
$Re\rho_{1,0}$
$Re\rho_{3,1}$
0.8
0.4
0.0
-0.4
0.5
1.0
$-t'$ [(GeV/c)^2]
ρ exchange
B exchange
ρ+B exchange

FIG. 26.

there is an addition slow s dependence in the absorption parameters. This is in general agreement with experiment.

One not entirely unexpected shortcoming of the model we have found is in the prediction of absolute normalizations, which do not always coincide with the data. This may not be unconnected with the difficulty of obtaining absolute normalizations experimentally. It should be remembered that the quoted normalization errors on experimental data are often in the region of 20 - 30% and frequently higher. When data is available for a particular reaction from different experimental groups, agreement may be reasonably good for one set of data but poor for another. Although such a procedure is justified, we have not smoothed the data within the stated normalization errors in order to improve the appearance of our results. We should also remark that this difficulty of relative normalization errors makes the extraction of meaningful parameters from data extremely difficult.

It should be emphasised that in this model we are in a theoretical strait-jacket, in that the symmetry scheme and strong exchange degeneracy fix completely the pole graphs. Since SU(3) is well known to be broken, we certainly do not expect U(6,6) to give perfect agreement with experiment. However, rather than at this point introduce a few arbitrary parameters and perform curve fitting procedures to bring about detailed agreement between theory and experiment, we feel that effort could more profitably be directed towards investigating a better consistent and physically plausible scheme for mass-splitting in $U(6,6) \otimes O(3,1)$ and a method of breaking strong exchange degeneracy.

Discrepancies between the predictions of our model and the experimental data, particularly the steepness of the t dependence, could be reduced by allowing the final-state absorption to be different from the initial-state absorption. However, the coefficients cannot be determined experimentally and we feel that little real insight is to be gained by making these arbitrary parameters to be fitted to the data. [51]

It must also be borne in mind that while the general concept of the absorption model is probably correct, the exact procedure for including such corrections is not at all clear at present, and that although our Reggeization procedure seems very natural, other reasonable schemes could be devised.

This model has also been applied to baryon-baryon scattering processes. Extremely satisfactory agreement with the experimental data on the differential cross sections and density matrix elements has been obtained for the reactions

$$pp \rightarrow n\Delta^{++}$$
$$pp \rightarrow p\,\Delta^{+}$$

and for the reaction

$$pp \rightarrow \Delta^{++}\Delta^{0}$$

over a wide range of energies[52]. We feel that useful tests of this model would be its application to the reactions

$$pn \rightarrow np$$

$$\bar{p}p \rightarrow \bar{n}n \quad ,$$

backward scattering[53] and photoproduction. These are currently being considered.

Encouraging results have been obtained by applying the Veneziano model to 3-particle production processes both in the spinless approximation[54] and taking some account of spin[55]. U(6,6) has been included in such B_5 calculations to produce a Veneziano model with spin with favourable results for the reactions

$$K^- p \rightarrow \pi^- \pi^+ \Lambda$$

$$K^- p \rightarrow \bar{K}^0 \pi^- p. \quad [56]$$

More sophisticated models are currently being developed[57]. Since most of the assumptions of the present paper are consistent with the Veneziano model, a Venezianoized U(6,6) absorptive peripheral model has been developed with a preliminary application to KN and $\bar{K}N$ charge-exchange reactions[58]. The model is presently being applied to $K^*(890)$ and $\Delta(1236)$ production[59].

For the numerical work we used an exact partial-wave series[60] as discussed in Appendix F rather than suffer the laboriousness and

inaccuracies of the impact-parameter representation. We employed a 48-point Gaussian quadrature to calculate explicitly 30 partial waves. Previous experience has shown this to be extremely accurate. To perform the partial-wave expansion, to modify the partial waves and re-sum the series to obtain the results for all the reactions presented in this thesis took approximately 60 seconds on a CDC 6600. Along with Lovelace, we find it easier to be exact.[61]

Reaction	Exchange	Baryon Vertex	Meson Vertex	
		G	D	F
$\pi^+ p \to \rho^0 \Delta^{++}$	π, A_2	$-\sqrt{2}$		-2
$K^+ p \to K^{*0} \Delta^{++}$	π, A_2	$-\sqrt{2}$		$\sqrt{2}$
	ρ, B	$-\sqrt{2}$	$\sqrt{2}$	
$K^- n \to \bar{K}^{*0} \Delta^-$	π, A_2	$\sqrt{2}$		$-\sqrt{2}$
	ρ, B	$\sqrt{2}$	$\sqrt{2}$	
$\pi^+ p \to \omega \Delta^{++}$	ρ, B	$-\sqrt{2}$	2	

TABLE 1

Clebsch-Gordan coefficients for $0^- \frac{1}{2}^+ \to 1^- \ 3/2^+$

Trajectory	α_0	$\alpha'\{(GeV/c)^{-2}\}$
π , B	- .013	.665
ρ , A_2	.470	.905

TABLE 2.

Regge trajectories.

Channel	p_{lab} (GeV/c)	C	(R^{-1})(GeV/c)
π^+p	3.54	.90	.27
	4.0	.87	.27
	6.95	.79	.27
	8.0	.78	.27
	13.1	.74	.27
	16.0	.73	.27
K^-p	5.5	.73	.26
K^+p	3.0	.91	.36
	3.5	.85	.34
	5.0	.71	.32
	12.7	.51	.27

TABLE 3

Absorption coefficients.

λ_3 λ_4 \ λ_1 λ_2	$0 \quad +\frac{1}{2}$	$0 \quad -\frac{1}{2}$
$+1 \quad +3/2$	ϕ_1	$-\phi_{12}$
$0 \quad +3/2$	ϕ_2	ϕ_{11}
$-1 \quad +3/2$	ϕ_3	$-\phi_{10}$
$+1 \quad +\frac{1}{2}$	ϕ_4	ϕ_9
$0 \quad +\frac{1}{2}$	ϕ_5	$-\phi_8$
$-1 \quad +\frac{1}{2}$	ϕ_6	ϕ_7
$+1 \quad -\frac{1}{2}$	ϕ_7	$-\phi_6$
$0 \quad -\frac{1}{2}$	ϕ_8	ϕ_5
$-1 \quad -\frac{1}{2}$	ϕ_9	$-\phi_4$
$+1 \quad -3/2$	ϕ_{10}	ϕ_3
$0 \quad -3/2$	ϕ_{11}	$-\phi_2$
$-1 \quad -3/2$	ϕ_{12}	ϕ_1

TABLE 4

Helicity dependence of amplitudes for $0^-\frac{1}{2}^+ \to 1^-\,3/2^+$

APPENDIX A

DEFINITIONS, NOMENCLATURE & NORMALIZATIONS.

The two-particle helicity states $|P\theta\phi;\lambda_1\lambda_2>$ are used to describe a system of two particles in the center of mass frame. $\underline{P_1}$ is the three-momentum of particle 1 which in polar coordinates is denoted by $\underline{P_1}=(|P_1|,\theta,\phi)$; λ_1 is its spin projection along its direction of motion (i.e. its helicity). Particle 2 moves in the opposite direction and has helicity λ_2. The two particle state is constructed out of two single-particle states with covariant normalization

$$< \underline{P}'|\underline{P} > \;=\; 2E_{\underline{p}}\,(2\pi)^3\,\delta^3\,(\underline{P}' - \underline{P}) \quad .$$

The S and T matrices are related by

$$S \;=\; 1 + iT \quad .$$

When taking matrix elements we get

$$< f|S|i> = < f|i> \;+\; i\,(2\pi)^4\,\delta^4\,(P_i - P_f) < f\,|T|\,i >$$

where the δ-function is inserted to ensure overall energy-momentum conservation. Here i and f denote initial and final states respectively.

The incoming meson and baryon and outgoing meson and baryon are denoted by "1", "2", "3" and "4" respectively. We take m_i, E_i, P_i and λ_i to be the mass, energy, four-momentum and helicity of particle "i" respectively. The magnitudes of the centre-of-mass three-momentum in the initial and final states are taken as K and q respectively. The square of the centre of mass energy is denoted by s. As we are considering the scattering of unpolarized particles the scattering has azimuthal symmetry, and we therefore consider scattering in the xz plane. The incident meson travels along the positive z axis, and the scattered meson at an angle θ to this axis.

Thus the covariantly normalized centre-of-mass scattering amplitude is

$$T_{\lambda_3\lambda_4\lambda_1\lambda_2}(S,\cos\theta) = \langle q\theta\emptyset;\lambda_3\lambda_4|T|K\ 0\ 0;\lambda_1\lambda_2\rangle \quad .$$

The differential cross section is then

$$\frac{d\sigma}{d\Omega} = \frac{1}{64\pi^2 s}\ \frac{q}{K}\ \frac{1}{(2s_1+1)(2s_2+1)}\ \sum_{(\lambda)} |\langle\lambda_3\lambda_4|T|\lambda_1\lambda_2\rangle|^2$$

$$\frac{d\sigma}{dt} = \frac{\pi}{qK}\ \frac{d\sigma}{d\Omega} \quad .$$

The various helicity amplitudes are related in pairs by the conservation of parity

$$< -\lambda_3\ -\lambda_4|\ T|\ -\lambda_1\ -\lambda_2> \ = \ \eta_p < \lambda_3\ \lambda_4|T|\lambda_1\lambda_2>$$

$$\eta_p = \frac{\eta_1\,\eta_2}{\eta_3\eta_4}\,(-1)^{s_1+s_2-s_3-s_4}\,(-1)^{\lambda_3\ -\lambda_4\ -\ \lambda_1\ +\lambda_2}$$

where η_i's are the intrinsic parities of the particles.

The partial wave decomposition of the scattering amplitude is

$$T_{\lambda_3\lambda_4,\lambda_1\lambda_2}\ (\cos\theta) \ = \ \sum_J\ (2J+1)\ T^J_{\lambda_3\lambda_4\ ,\lambda_1\lambda_2}\ d^J_{\lambda\mu}(\theta)$$

with

$$T^J_{\lambda_3\lambda_4,\lambda_1\lambda_2} \ = \ \frac{1}{2}\ \int_{-1}^{1}\ T_{\lambda_3\lambda_4,\lambda_1\lambda_2}\ (\cos\theta)\ d^J_{\lambda\mu}(\theta)\ d\cos\theta$$

where $\lambda = \lambda_1 - \lambda_2$ and $\mu = \lambda_3 - \lambda_4$.

If we define angular momentum helicity states $|JM;\lambda_1\lambda_2>$ with the normalization

$$< J'M';\ \lambda_1'\lambda_2'|\ JM;\lambda_1\lambda_2> \ = \delta_{JJ'}\ \ \delta_{MM'}\ \delta_{\lambda_1\lambda_1'}\ \ \ \ \delta_{\lambda_2\lambda_2'}$$

we obtain a different normalization for the partial wave amplitude

$$<J'M';\lambda_3\lambda_4|T|JM;\lambda_1\lambda_2> \ = \ \delta_{JJ'}\ \ \delta_{MM'}\ \ t^J_{\lambda_3\lambda_4;\lambda_1\lambda_2}\ .$$

The relation between the two normalization is

$$t^J = \frac{2\,(Kq)^{\frac{1}{2}}}{8\pi\ \sqrt{s}}\ T^J \quad .$$

The usual partial-wave S-matrix element is then

$$S^J_{\lambda_3\lambda_4,\lambda_1\lambda_2} = \delta_{\lambda_3\lambda_1}\ \delta_{\lambda_4\lambda_2} + i\ t^J_{\lambda_3\lambda_4,\lambda_1\lambda_2} \quad .$$

APPENDIX B

PARTIAL-WAVE EXPANSIONS.

We are interested in obtaining the helicity states for processes of the type

$$0^- + \tfrac{1}{2}^+ \to 1^- + \tfrac{3}{2}^+ \quad .$$

The production amplitudes in the helicity representation are denoted by

$$< \lambda_3\lambda_4|\Phi|\ \lambda_1\lambda_2 > \quad .$$

By parity invariance we have

$$< \lambda_3\lambda_4\ |\Phi|\lambda_1\lambda_2> = \frac{\eta_3\eta_4}{\eta_1\eta_2}\,(-1)^{s_3+s_4-s_1-s_2}\,(-1)^{\lambda-\mu} <-\lambda_3-\lambda_4|\ \Phi\ |-\lambda_1-\lambda_2>$$

where s_i are the spins of the particles and η_i are their intrinsic parities. Here $\mu = \lambda_3 - \lambda_4$ and $\lambda = \lambda_1 - \lambda_2$.

Our general partial-wave expansion in the helicity representation is

$$< \lambda_3\lambda_4|\Phi|\ \lambda_1\lambda_2> = \sum_j (2j+1)<\lambda_3\lambda_4|T^j(E)|\lambda_1\lambda_2>\ d^j_{\lambda\mu}(\theta) \quad .$$

Our partial-wave expansions are :

$$\phi_1 = \sum_{\ell=0} (2j+1)\, T_1^j(E)\, d^j_{-\frac{1}{2}-\frac{1}{2}}(\theta)$$

$$\phi_2 = \sum_{\ell=1} (2j+1)\, T_2^j(E)\, d^j_{-\frac{1}{2}-\frac{3}{2}}(\theta)$$

$$\phi_3 = \sum_{\ell=2} (2j+1)\, T_3^j(E)\, d^j_{\frac{1}{2}\frac{5}{2}}(\theta)$$

$$\phi_4 = \sum_{\ell=0} (2j+1)\, T_4^j(E)\, d^j_{-\frac{1}{2}\frac{1}{2}}(\theta)$$

$$\phi_5 = \sum_{\ell=0} (2j+1)\, T_5^j(E)\, d^j_{-\frac{1}{2}-\frac{1}{2}}(\theta)$$

$$\phi_6 = \sum_{\ell=1} (2j+1)\, T_6^j(E)\, d^j_{\frac{1}{2}\frac{3}{2}}(\theta)$$

$$\phi_7 = \sum_{\ell=1} (2j+1)\, T_7^j(E)\, d^j_{-\frac{1}{2}\frac{3}{2}}(\theta)$$

$$\phi_8 = \sum_{\ell=0} (2j+1)\, T_8^j(E)\, d^j_{\frac{1}{2}-\frac{1}{2}}(\theta)$$

$$\phi_9 = \sum_{\ell=0} (2j+1)\, T_9^j(E)\, d^j_{\frac{1}{2}\frac{1}{2}}(\theta)$$

$$\phi_{10} = \sum_{\ell=2} (2j+1)\, T_{10}^j(E)\, d^j_{-\frac{1}{2}\frac{5}{2}}(\theta)$$

$$\phi_{11} = \sum_{\ell=1} (2j+1)\, T_{11}^j(E)\, d^j_{\frac{1}{2}-\frac{3}{2}}(\theta)$$

$$\phi_{12} = \sum_{\ell=0} (2j+1)\, T_{12}^j(E)\, d^j_{\frac{1}{2}-\frac{1}{2}}(\theta) .$$

APPENDIX C

DENSITY MATRICES.

In a 2-body reaction where either of the final particles is a resonance, information concerning the production process may be obtained from the spin density matrix elements of the resonance.

Taking particle 3 to be the resonance, in the c.m. frame the density matrix elements are given by

$$\rho_{\lambda_3'\lambda_3} = \frac{\sum_{\lambda_1\lambda_2\lambda_4} \langle \lambda_3'\lambda_4 | \phi' | \lambda_1\lambda_2 \rangle \langle \lambda_3\lambda_4 | \phi' | \lambda_1\lambda_2 \rangle^*}{\sum_i |\phi_i'|^2} .$$

Experimental results are usually quoted in the Jackson frame i.e. the rest frame of the decaying resonance, particle 3, in which the z axis is taken parallel to the momentum of the incident particle, particle 1, in this frame, and the y axis is perpendicular to the production plane. With respect to this new reference frame, the density matrix elements are given by

$$\rho_{m'm} = \sum_{\text{All } \lambda} d^{s_3}_{m'\lambda_3'}(\psi_3)\; d^{s_3}_{m\lambda_3}(\psi_3)\rho_{\lambda_3'\lambda_3} ,$$

where ψ_3 is the angle between the directions of particles 1 and 4 as seen in the rest frame of particle 3, and

$$\tan \psi_3 = \frac{m_3 \sqrt{1 - \cos^2 \theta}}{E_3 \left(\cos\theta - \frac{qE_1}{kE_3}\right)} ,$$

where the m_i and E_i are the masses and c.m. energies, respectively, of the particles.

Similar expressions hold when particle 4 is the resonance, with

$$\tan \psi_4 = - \frac{m_4 \sqrt{1 - \cos^2 \theta}}{E_4 \left(\cos \theta - \frac{qE_2}{kE_4}\right)} .$$

APPENDIX D

ROTATION FUNCTIONS.

The functions $d^{j}_{\lambda\mu}(x)$, where $x = \cos\theta$, are evaluated by first writing these functions in terms of Jacobi polynomials,

$$d^{j}_{\lambda\mu}(x) = \left[\frac{(j+\lambda)!\ (j-\lambda)!}{(j+\mu)!\ (j-\mu)!} \right]^{\frac{1}{2}} \left[\cos\frac{\theta}{2} \right]^{\lambda+\mu} \left[-\sin\frac{\theta}{2} \right]^{\lambda-\mu} P_{j-\lambda}^{\lambda-\mu,\lambda+\mu}(\cos\theta),$$

where $\lambda-\mu$ and $\lambda+\mu \geq 0$. The Jacobi polynomials obey two recurrence relations,

$$\tfrac{1}{2}\,(2+\alpha+\beta+2n)\,(x+1)\,P_n^{\alpha,\beta+1}(x)$$

$$= (n+1)\,P_{n+1}^{\alpha,\beta}(x) + (1+\beta+n)\,P_n^{\alpha,\beta}(x)$$

and

$$\tfrac{1}{2}\,(2+\alpha+\beta+2n)\,(x-1)P_n^{\alpha+1,\beta}(x)$$

$$= (n+1)\,P_{n+1}^{\alpha,\beta}(x) - (1+\alpha+n)\,P_n^{\alpha,\beta}(x).$$

By application of these relations the Jacobi polynomials can be reduced to Legendre polynomials, since

$$P_n^{0,0}(x) = P_n(x).$$

The resulting expressions for the rotation functions therefore contain no derivatives of Legendre polynomials.

This procedure gives, for the function of interest here,

$$d^j_{\frac{1}{2},\pm\frac{1}{2}}(x) = \frac{1}{\left[2(1\pm x)\right]^{\frac{1}{2}}} \left\{ P_{\ell+1}(x) \pm P_\ell(x) \right\} ,$$

$$d^j_{\frac{3}{2},\pm\frac{1}{2}}(x) = \frac{\left(\frac{1}{2}(\ell+2)\ell\right)^{\frac{1}{2}}}{(2\ell+3)\ (2\ell+1)} \quad \frac{1}{(1\pm x)\ (1\mp x)^{\frac{1}{2}}}$$

$$\times \left\{ (2\ell+1)\{P_{\ell+2}(x) - P_\ell(x)\} \pm (2\ell+3)\{P_{\ell+1}(x) - P_{\ell-1}(x)\} \right\},$$

$$d^j_{\frac{5}{2},\pm\frac{1}{2}}(x) = \frac{\left[\frac{1}{2}(\ell+3)\ (\ell+2)\ell(\ell-1)\right]^{\frac{1}{2}}}{(2\ell+5)\ (2\ell+3)\ (2\ell+1)\ (2\ell-1)} \quad \frac{1}{(1\pm x)^{3/2}(1\mp x)}$$

$$\times \left\{ (2\ell-1)\{(2\ell+1)P_{\ell+3}(x) - 2(2\ell+3)P_{\ell+1}(x) + (2\ell+5)P_{\ell-1}(x) \right.$$

$$\left. \pm \ (2\ell+5)\{(2\ell-1)P_{\ell+2}(x) - 2(2\ell+1)P_\ell(x) + (2\ell+3)P_{\ell-2}(x)\} \right\},$$

where $j = \ell + \frac{1}{2}$.

The other $d^j_{\lambda\mu}(x)$ may be obtained from the relations

$$d^j_{\lambda\mu}(x) = (-1)^{\lambda-\mu} d_{\mu\lambda}(x) = d^j_{-\mu,-\lambda}(x).$$

The Legendre polynomials appearing in these expressions are evalutated using the recurrence relation

$$(n+1) P_{n+1}(x) = (2n+1) x P_n(x) - n P_{n-1}(x)$$

given that

$$P_0(x) = 1,$$

$$P_1(x) = x.$$

APPENDIX E

HELICITY AMPLITUDES.

We distinguish between the incoming meson, target baryon, outgoing meson and outgoing baryon by the label i = 1, 2, 3 and 4, respectively. The c.m. coordinate system is defined such that particle 1 is travelling along the +z direction and particle 3 is travelling at an angle θ to this direction in the x-z plane. The quantities m_i, E_i and λ_i denote the mass, c.m. energy and helicity, respectively, of particle i, and k and q are the magnitudes of the c.m. 3-momenta in the initial and final states, respectively.

In addition to the notation introduced in the text, the following expressions are used

$$C_{\pm} = \frac{(E_4+m_4)\ (E_2+m_2) \pm kq}{\sqrt{(E_4+m_4)\ (E_2+m_2)}}$$

$$H_{\pm} = \frac{(E_4+m_4)\ k \pm (E_2+m_2)\ q}{\sqrt{(E_4+m_4)\ (E_2+m_2)}}$$

$$E_{\pm} = (E_1+E_3)\ C_{\pm} + (k \pm q)\ H_{\pm} \quad .$$

We also define

$$P_P = \alpha'_P \Gamma(-\alpha_P) \frac{1 + e^{-i\pi\alpha_P}}{2} \left(\frac{s + \frac{1}{2}t - \frac{1}{2}\Sigma}{s_0} \right)^{\alpha_P}$$

$$P_A = \alpha'_A \Gamma(-\alpha_A) \frac{1 - e^{-i\pi\alpha_A}}{2} \left(\frac{s + \frac{1}{2}t - \frac{1}{2}\Sigma}{s_0} \right)^{\alpha_A}$$

$$P_V = \alpha'_V \Gamma(1 - \alpha_V) \frac{1 - e^{-i\pi\alpha_V}}{2} \left(\frac{s + \frac{1}{2}t - \frac{1}{2}\Sigma}{s_0} \right)^{\alpha_V - 1}$$

$$P_T = \alpha'_T \Gamma(1 - \alpha_T) \frac{1 + e^{-i\pi\alpha_T}}{2} \left(\frac{s + \frac{1}{2}t - \frac{1}{2}\Sigma}{s_0} \right)^{\alpha_T - 1}$$

where the labels P, A, V and T refer to 0^-, 1^+, 1^- and 2^+ exchanges, respectively, the trajectories being defined by

$$\alpha(t) = \alpha_0 + \alpha' t,$$

with s_0 the scaling factor, and

$$\Sigma = \sum_{i=1}^{4} m_i^2 .$$

The g's and h's with subscripts which are combination of D,F, S and G are the appropriate SU(3) Clebsch-Gordan coefficients at the

baryon and meson vertices, respectively. These are given in Table 1.

The helicity dependence of the amplitudes is shown in Table 4. With this notation, the following expressions are obtained for $0^-\frac{1}{2}^+ \to 1^-\ \frac{3}{2}^+$. Defining

$$A_5 = \frac{3gh}{m_M}\, g_G\left(1 + \frac{2m}{\mu}\right)(h_F P_P + h_D P_A)$$

$$A_6 = \frac{3gh}{4m_B^2 m_M}\, g_G\left(1 + \frac{2m}{\mu}\right)(h_D P_V + h_F P_T)$$

and

$$D_1 = \frac{E_2 q - E_4 k\cos\theta}{m_4} C_+ \sin\tfrac{1}{2}\theta - \tfrac{1}{2} k \sin\theta\, C_- \cos\tfrac{1}{2}\theta$$

$$D_2 = \frac{E_2 q - E_4 k\cos\theta}{m_4} C_- \cos\tfrac{1}{2}\theta + \tfrac{1}{2} k \sin\theta C_+ \sin\tfrac{1}{2}\theta$$

$$D_3 = \frac{(E_1+E_3+E_4)q + E_4 k\cos\theta}{m_4} C_+ \sin\tfrac{1}{2}\theta + \tfrac{1}{2} k \sin\theta C_- \cos\tfrac{1}{2}\theta$$

$$D_4 = \frac{(E_1+E_3+E_4)q + E_4 k\cos\theta}{m_4} C_- \cos\tfrac{1}{2}\theta - \tfrac{1}{2} k \sin\theta C_+ \sin\tfrac{1}{2}\theta,$$

we obtain

$$\phi_1 = \tfrac{1}{2} A_5 k^2 \sin^2\theta C_- \cos \tfrac{1}{2}\theta$$

$$- A_6 \left\{(s - m_3^2 - m_4^2) k^2 \sin^2\theta \right.$$

$$\left. + \left\{(2s + t - \Sigma)t + (m_1^2 - m_3^2)(m_2^2 - m_4^2)\right\}\right] C_- \cos \tfrac{1}{2}\theta$$

$$\phi_2 = - \frac{1}{\sqrt{2}} A_5 \frac{E_1 q - E_3 k \cos\theta}{m_3} k \sin\theta C_- \cos \tfrac{1}{2}\theta$$

$$+ \frac{1}{\sqrt{2}} A_6 \left[(2s + t - \Sigma) \frac{E_1 q - E_3 k \cos\theta}{m_3}\right.$$

$$+ t \frac{(E_2+E_3+E_4)q + E_3 k \cos\theta}{m_3}$$

$$- (m_1^2 - m_3^2) \frac{(E_2+E_3+E_4)q + E_3 k \cos\theta}{m_3}$$

$$\left. + (m_2^2 - m_4^2) \frac{E_1 q - E_3 k \cos\theta}{m_3}\right] k \sin\theta C_- \cos \tfrac{1}{2}\theta$$

$$\phi_3 = - \tfrac{1}{2} A_5 k^2 \sin^2\theta C_- \cos \tfrac{1}{2}\theta$$

$$+ A_6 (s - m_3^2 - m_4^2) k^2 \sin^2\theta C_- \cos \tfrac{1}{2}\theta$$

$$\phi_4 = \frac{1}{\sqrt{3}} A_5 k \sin\theta D_2$$

$$+ \frac{1}{\sqrt{3}} A_6 \Big\{ - (2s + t - \Sigma)\, k \sin\theta D_2$$

$$- t\, k \sin\theta D_4$$

$$- (m_1^2 - m_3^2) D_2$$

$$+ (m_2^2 - m_4^2) D_4$$

$$- \Big[(2s + t - \Sigma)t + (m_1^2 - m_3^2)(m_2^2 - m_4^2) \Big] C_+ \sin \tfrac{1}{2}\theta \Big\}$$

$$\phi_5 = -\sqrt{\frac{2}{3}} A_5 \frac{E_1 q - E_3 k \cos\theta}{m_3} D_2$$

$$+\sqrt{\frac{2}{3}} A_6 \Big\{ (2s + t - \Sigma) \frac{E_1 q - E_3 k \cos\theta}{m_3} D_2$$

$$- t \frac{(E_2+E_3+E_4)q + E_3 k \cos\theta}{m_3} D_4$$

$$- (m_1^2 - m_3^2) \frac{(E_2+E_3+E_4)q + E_3 k \cos\theta}{m_3} D_2$$

$$- (m_2^2 - m_4^2) \frac{E_1 q - E_3 k \cos\theta}{m_3} D_4$$

$$+ \left[(2s + t - \Sigma)t + (m_1^2 - m_3^2)(m_2^2 - m_4^2) \right] \frac{E_3 E_4 + q^2}{m_3 m_4} C_- \cos\tfrac{1}{2}\theta \Bigg]$$

$$\phi_6 = - \frac{1}{\sqrt{3}} A_5 k \sin^2\theta D_2$$

$$+ \frac{1}{\sqrt{3}} A_6 \left[(2s + t - \Sigma) D_2 + tD_4 + (m_1^2 - m_3^2) D_2 - (m_2^2 - m_4^2) D_4 \right] k \sin\theta$$

$$\phi_7 = \frac{1}{\sqrt{3}} A_5 k \sin\theta D_1$$

$$+ \frac{1}{\sqrt{3}} A_6 \left[-(2s + t - \Sigma) D_1 - tD_3 - (m_1^2 - m_3^2) D_1 + (m_2^2 - m_4^2) D_3 \right] k \sin\theta$$

$$\phi_8 = -\sqrt{\frac{2}{3}} A_5 \frac{E_1 q - E_3 k \cos\theta}{m_3} D_1$$

$$+\sqrt{\frac{2}{3}} A_6 \left[(2s + t - \Sigma) \frac{E_1 q - E_3 k \cos\theta}{m_3} D_1 \right.$$

$$- t \frac{(E_2+E_3+E_4)q + E_3 k \cos\theta}{m_3} D_3$$

$$- (m_1^2 - m_3^2) \frac{(E_2+E_3+E_4)q + E_3 k \cos\theta}{m_3} D_1$$

$$- (m_2^2 - m_4^2) \frac{E_1 q - E_3 k \cos\theta}{m_3} D_3$$

$$+ \left[(2s + t - \Sigma)t + (m_1^2 - m_3^2)(m_2^2 - m_4^2) \right] \frac{E_3 E_4 + q^2}{m_3 m_4} C_+ \sin\tfrac{1}{2}\theta \Bigg]$$

$$\phi_9 = - \frac{1}{\sqrt{3}} A_5 k \sin\theta D_1$$

$$+ \frac{1}{\sqrt{3}} A_6 \Big[(2s + t - \Sigma)k \sin D_1$$

$$+ t\, k \sin\theta D_3$$

$$+ (m_1^2 - m_3^2)k \sin\theta D_1$$

$$- (m_2^2 - m_4^2)k \sin\theta D_3$$

$$- \left[(2s + t - \Sigma)t + (m_1^2 - m_3^2)(m_2^2 - m_4^2) \right] C_- \cos\tfrac{1}{2}\theta \Bigg]$$

$$\phi_{10} = -\tfrac{1}{2} A_5 k^2 \sin^2\theta C_+ \sin\tfrac{1}{2}\theta$$

$$+ A_6 (s - m_3^2 - m_4^2) k^2 \sin^2\theta C_+ \sin\tfrac{1}{2}\theta$$

$$\phi_{11} = \frac{1}{\sqrt{2}} A_5 \frac{E_1 q - E_3 k\cos\theta}{m_3} k \sin\theta C_+ \sin\tfrac{1}{2}\theta$$

$$+ \frac{1}{\sqrt{2}} A_6 \Bigg\{ -(2s + t - \Sigma) \frac{E_1 q - E_3 k\cos\theta}{m_3}$$

$$- t \frac{(E_2+E_3+E_4)q + E_3 k\cos\theta}{m_3}$$

$$+ (m_1^2 - m_3^2) \frac{(E_2+E_3+E_4)q + E_3 k\cos\theta}{m_3}$$

$$- (m_2^2 - m_4^2) \frac{E_1 q - E_3 k\cos\theta}{m_3} \Bigg\} k \sin\theta C_+ \sin\tfrac{1}{2}\theta$$

$$\phi_{12} = \frac{1}{2} A_5 k^2 \sin^2\theta C_+ \sin\tfrac{1}{2}\theta$$

$$- A_6 \Big\{ (s - m_3^2 - m_4^2) k^2 \sin^2\theta$$

$$+ \Big[(2s + t - \Sigma)t + (m_1^2 - m_3^2)(m_2^2 - m_4^2) \Big] \Big\} C_+ \sin\tfrac{1}{2}\theta .$$

APPENDIX F

CALCULATIONAL TECHNIQUES.

The computer program described here is designed to aid the analysis of scattering data. The essential function of the program is to partial-wave analyze the scattering amplitude, modify the partial waves in a prescribed manner, re-sum the series and compare the theoretical results with the experimental data.

Frequently in high-energy physics the theory is only able to provide a scattering amplitude in terms of functions involving a number of unknown parameters. Since these parameters are adjusted to agree with experimental data by a fitting procedure which involves many passes through the program, the technique for calculating the partial waves must be fast and accurate. This program satisfies this requirement and may be added to any of the standard fitting routines, e.g. MINUITS (CERN Program Library No: D506), with no difficulty.

Once the optimum fit to the data has been obtained, the program produces a numerical and, if required, a visual summary of the results. Included in the program is a CALCOMP package[62] which can produce cartesian, log-linear and log-log plots of the results.

The program is currently in use on the University of London CDC 6600 to calculate the differential cross sections for a wide range of meson-baryon scattering reactions[51].

METHOD OF SOLUTION

Typically in high-energy physics we are concerned with the evaluation of the differential cross section[63] for 2-body scattering processes. This may be written

$$\frac{d\sigma}{dt} = \frac{\pi}{k^2} \frac{1}{(2s_1+1)\,(2s_2+1)} \sum_i \left| \frac{\phi_i}{8\pi\sqrt{s}} \right|^2$$

where s and t are the usual Mandelstam variables, s_1 and s_2 are the incident and target particle spins respectively, k is the centre-of-mass 3-momentum and the ϕ_i are the s-channel helicity amplitudes.

The helicity amplitudes can be decomposed in the helicity representation[64]

$$\langle \lambda_3\lambda_4|\phi(s,t)|\lambda_1\lambda_2 = \sum_j (2j+1)\langle \lambda_3\lambda_4 |T^j(s)|\lambda_1\lambda_2\rangle\, d^j_{\lambda\mu}(\cos\theta)$$

where j is the total angular momentum, λ_i are the helicity labels of particles 1-4, $d^j_{\lambda\mu}(\cos\theta)$ are rotation matrices of the first kind, $\lambda = \lambda_1 - \lambda_2$ and $\mu = \lambda_3 - \lambda_4$, θ is the centre-of-mass scattering angle and $\langle \lambda_3\lambda_4|\, T^j(s)|\lambda_1\lambda_2\rangle$ are the partial-wave amplitudes.

By making use of the orthogonality property of the rotation functions $d^j_{\lambda\mu}(\cos\theta)$,

$$\int_{-1}^{1} d^{j}_{\lambda\mu}(\cos\theta)\; d^{j'}_{\lambda\mu}(\cos\theta)\; d(\cos\theta) = \frac{2}{2j+1}\,\delta_{jj'},$$

we obtain the partial-wave amplitudes

$$\langle\lambda_3\lambda_4|T^{j}(s)|\lambda_1\lambda_2\rangle = \tfrac{1}{2}\int_{-1}^{1}\langle\lambda_3\lambda_4|\emptyset(s,t)|\lambda_1\lambda_2\rangle\, d^{j}_{\lambda\mu}(\cos\theta)\, d(\cos\theta)$$

In the absorption model the partial waves corresponding to the exchange of a Regge pole are modified according to the prescription

$$\langle\lambda_3\lambda_4|T'^{j}(s)|\lambda_1\lambda_2\rangle = S^{j}\langle\lambda_3\lambda_4|T^{j}(s)|\lambda_1\lambda_2\rangle$$

where S^{j} is the S-matrix element for elastic scattering between the incident and target particles. This is usually parameterized by a Gaussian form

$$S^{j} = 1 - c(s)\; e^{-\ell(\ell+1)/\nu^2(s)\,K^2}$$

where $\ell = j-\frac{1}{2}$. The quantity ν is the radius of the interaction and c is related to the opacity of the target particle. The quantity ν is determined from the observed exponential slope of $(d\sigma/dt)_{elastic}$ and using the optical theorem c is obtained from the relation

$$c = \frac{\sigma_{TOT}}{2\pi\nu^2}$$

The program spends most of the time integrating by Gaussian quadrature to obtain the partial-wave amplitudes. Only a small fraction of the time is spent modifying the partial-wave amplitudes and resumming the series. Thus, the integration must be as efficient as possible.

The principle of an N-point Gaussian quadrature[65] is that

$$\int_{-1}^{1} f(x)\ dx = \sum_{m=1}^{N} W_m\ f(x_m)$$

This integrates exactly a polynomial of degree 2N-1. In this case

$$\int_{-1}^{1} \langle \lambda_3\lambda_4 |\ \emptyset(s,t)|\lambda_1\ \lambda_2\rangle\ d^j_{\lambda\mu}(\cos\theta)\ d(\cos\theta) = \tfrac{1}{2}\sum_{m=1}^{N} \langle\lambda_3\lambda_4|\emptyset(s,\cos\theta_m)|\lambda_1\lambda_2\rangle$$

$$d^j_{\lambda\mu}(\cos\theta_m)\ W_m$$

where W_m is the quadrature weight associated with the point X_m. Clearly the rotation matrices are independent of energy and depend only on the value of the angle $\cos\theta_m$. These values of $\cos\theta_m$ depend only on the order of the Gaussian quadrature. Thus, the integration can be written in terms of new weights

$$W'_m = \tfrac{1}{2}\, d^j_{\lambda\mu}\ (\cos\theta_m)\ W_m\ .$$

These "new weights" need only be evaluated at the first entry to the program, thus saving an immense amount of computing time. From the symmetry properties of the $d^j_{\lambda\mu}$ functions the number of rotation matrices required is less than or at most equal to the number of independent s-channel helicity amplitudes. In the former case this technique brings about an additional saving in time.

It is important in order to minimize computing time to reduce the number of calls to angle dependent routines. This is accomplished by a judicious nesting of loops corresponding to the indices j for the total angular momentum and i for the independent helicity amplitudes.

DESCRIPTION OF THE CODE.

The program consists of the main program, FCN, which directs the flow of the calculations and fourteen sub-programs BLOCK DATA, DATIN, NEWWT, DJ, KIN, KAYS, PTWAVE, REGGE, GAMMA, AMP, RESUM, CALAMP, SORT and APLOT.

The code is organised so that it can be readily modified to treat many processes and exchanges.

A short description of each routine follows.

THE MAIN PROGRAM FCN.

The flow of this routine is shown in Fig. 27 . This is set up to be called by the minimization program. Here IFLAG=1 is the first entry to the program, IFLAG=2 is not used, IFLAG=3 is used for printing results and IFLAG=4 is the minimization call.

SUBPROGRAM BLOCK DATA.

This routine contains the data for the Gaussian quadrature in BLOCK DATA form. The program at present uses a 48-point Gaussian quadrature.

SUBROUTINE DATIN.

This routine is called by the Fortran statement CALL DATIN. This reads in all the data needed for the program, namely; experimental data points, types of exchanges allowed, coupling constants and absorption parameters.

SUBROUTINE NEWWT.

The statement used to call this routine is CALL NEWWT. As described previously , this routine calculates the "new weights" from the Gaussian quadrature weights which were entered at compilation time from BLOCK DATA.

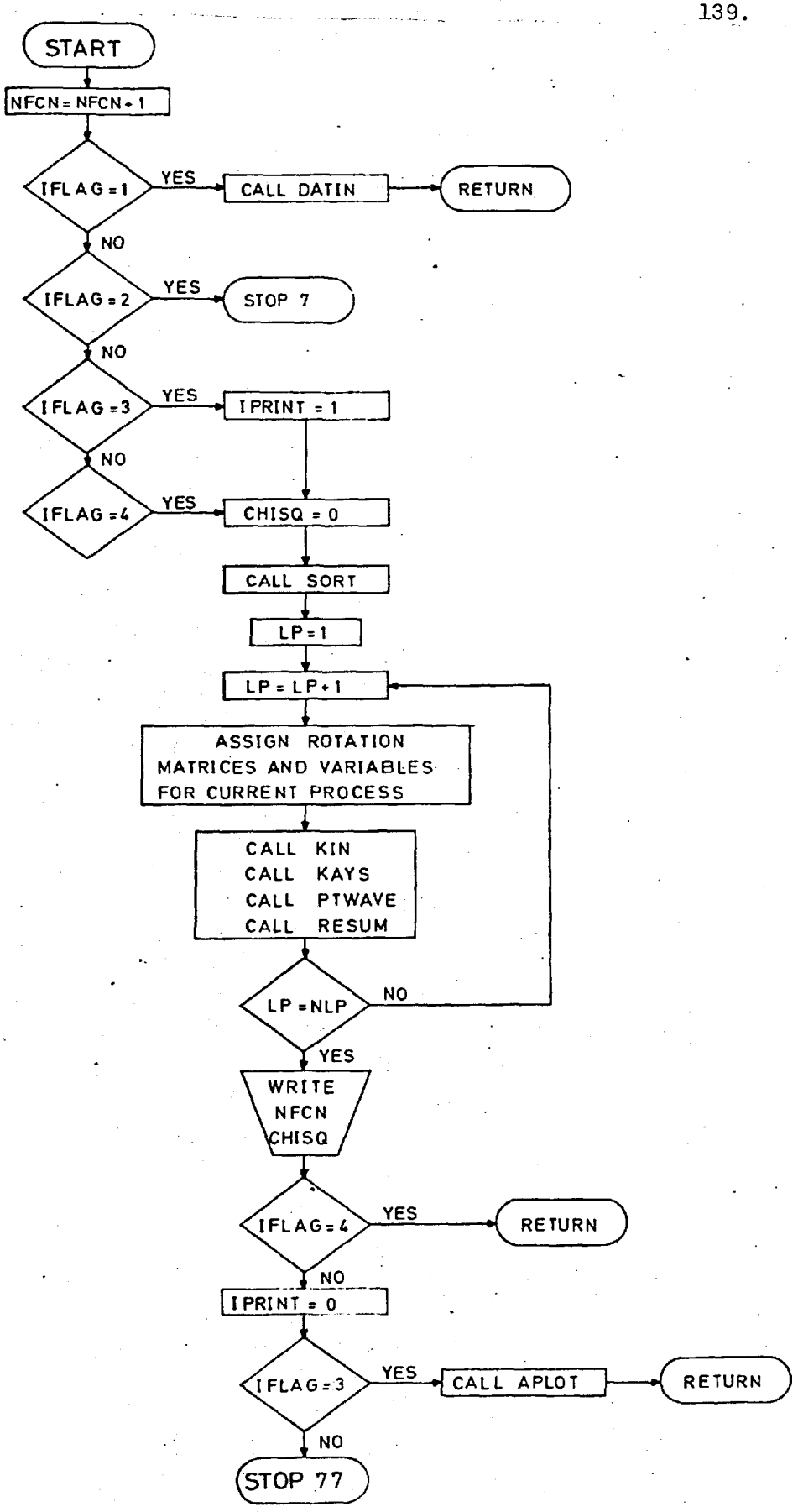
START
NFCN = NFCN + 1
IFLAG = 1
YES
CALL DATIN
RETURN
NO
IFLAG = 2
YES
STOP 7
NO
IFLAG = 3
YES
IPRINT = 1
NO
IFLAG = 4
YES
CHISQ = 0
CALL SORT
LP = 1
LP = LP + 1
ASSIGN ROTATION MATRICES AND VARIABLES FOR CURRENT PROCESS
CALL KIN
CALL KAYS
CALL PTWAVE
CALL RESUM
LP = NLP
NO
YES
WRITE NFCN CHISQ
IFLAG = 4
YES
RETURN
NO
IPRINT = 0
IFLAG = 3
YES
CALL APLOT
RETURN
NO
STOP 77

FIG. 27.

FUNCTION DJ

This routine calculates the necessary rotation matrices from Legendre polynomials. Calls to this routine are denoted by DJ(J,CT,N,JFLAG) where J is the total angular momentum, CT is the current value of cosθ , N labels the different rotation functions and JFLAG is a subtlety to reduce the number of evaluations of the Legendre polynomials.

SUBROUTINE KIN

The statement CALL KIN leads to the calculation of the kinematic quantities which are independent of the scattering angle.

SUBROUTINE KAYS

This is called by the statement CALL KAYS. The elastic scattering S-matrix elements are evaluated in this routine.

SUBROUTINE PTWAVE

This subroutine, which is called by the statement CALL PTWAVE, partial-wave analyzes the scattering amplitude.

SUBROUTINE REGGE

The Fortran statement used to call this routine is CALL REGGE (CT) where CT is the value of cos θ. In this routine all the angle dependent Regge pole factors are calculated.

FUNCTION GAMMA

This function subroutine calculates the gamma function of complex argument U,Γ (U), by means of Chebyshev polynomials.

FUNCTION AMP

This is called by the statement CALL AMP(CT) , where CT is the current value of cos θ. This routine calculates the helicity amplitudes.

SUBROUTINE RESUM

CALL RESUM is the statement used to call this routine. In this routine the modified partial-wave amplitudes are resummed to calculate , for example, the differential cross section. As a check on the convergence of the series the unmodified partial waves are resummed so that this sum may be compared with the original amplitude.

SUBROUTINE CALAMP

This routine is called by the Fortran statement CALL CALAMP (CT,F) where CT is the current value of cos θ and the array F contains, on return, the values of the helicity amplitudes.

SUBROUTINE SORT.

When used in conjunction with the minimization program MINUITS, this routine is called by the statement CALL SORT(X). The variables in the array of parameters X from the minimization program are associated with the variables used in the Regge pole program.

SUBROUTINE APLOT.

CALL APLOT is the statement used to call this routine, which is used, if required, to Calcomp plot the results of the program's calculations. An example of this[66] is shown in Fig.28.

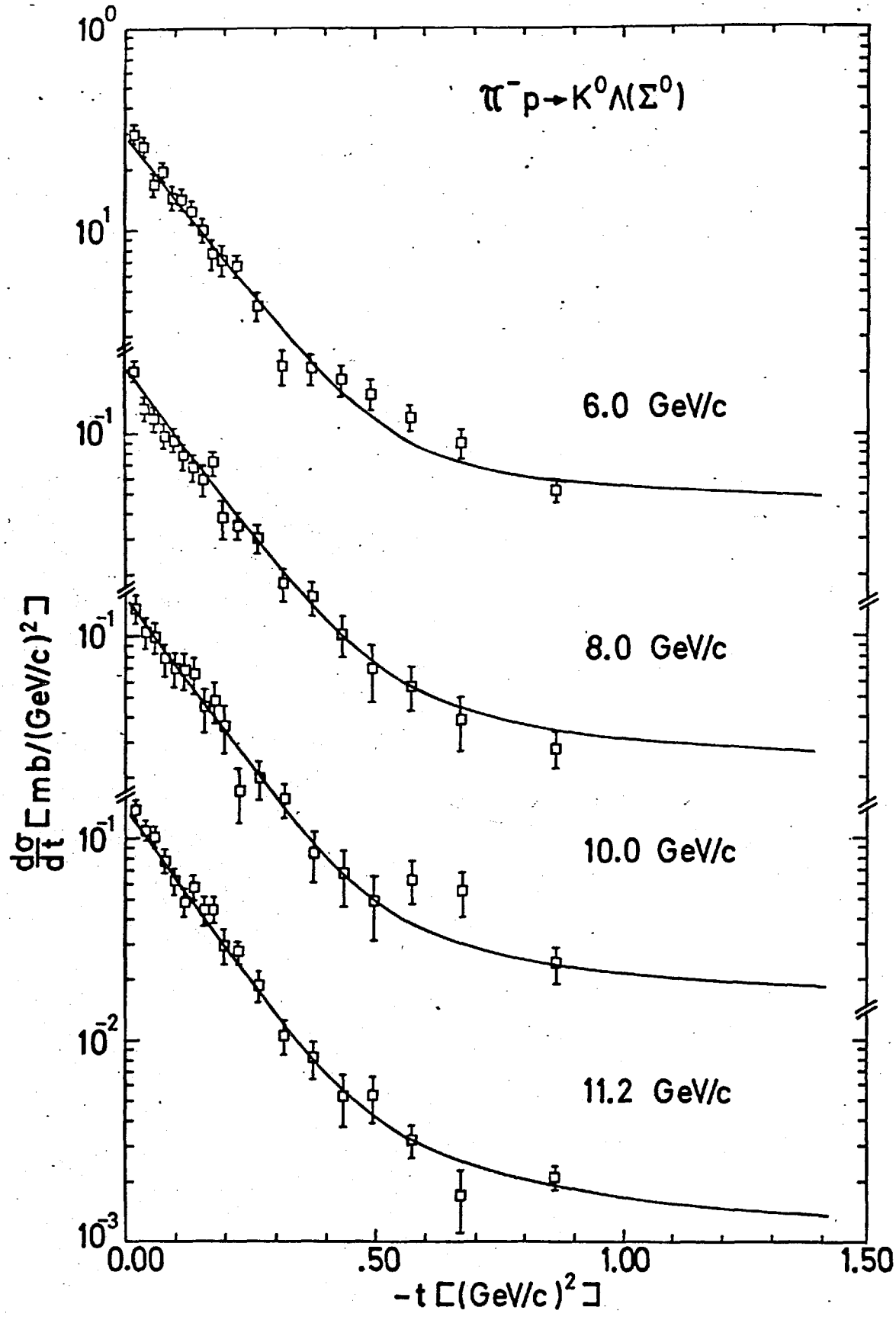
$\pi^- p \to K^0 \Lambda(\Sigma^0)$
6.0 GeV/c
8.0 GeV/c
10.0 GeV/c
11.2 GeV/c
$\frac{d\sigma}{dt}$ [mb/(GeV/c)^2]
$-t$ [(GeV/c)^2]
10^0
10^1
10^{-1}
10^{-1}
10^{-1}
10^{-2}
10^{-3}
0.00
.50
1.00
1.50

FIG. 28.

REFERENCES

1. J.D. Jackson, invited talk, Proceedings of the XIII International Conference on High-Energy Physics, Berkeley,1966.

2. C. Fu, Resonance Production in K^+P Interactions at 4.6 GeV/c and 9 GeV/c, Berkeley Preprint, UCRL - 19809.

3. J.D. Jackson, invited talk, Proceedings of the Lund International Conference on Elementary Particles, Lund, 1969.

4. S.T. Butler, Phys. Rev. 106, 272 (1957).

5. A. Dar, invited talk, Proceedings of the Second International Conference on High-Energy Physics and Nuclear Structure, Rehovoth, 1967.

6. N.J. Sopkovich, Nuovo Cimento, 26, 186 (1962).

7. J.D. Jackson, Rev. Mod. Phys. 37, 484 (1965).

8. H.D.D. Watson, Phys. Letters 17, 72 (1965).

9. A. Salam, R. Delbourgo and J. Strathdee, Proc. Roy. Soc. 284A, 146 (1965);
M.A. Beg and A. Pais, Phys. Rev. Letters 14, 267 (1965);
B. Sakita and K.C. Wali, Phys. Rev. Letters 14, 404 (1965);
Phys. Rev. 139, B1355 (1965);
R. Delbourgo, M.A. Rashid, A. Salam and J. Strathdee, Seminar on High-Energy Physics and Elementary Particles, Trieste (International Atomic Energy Agency, VIENNA , 1965).

10. H. Högaasen and J. Högaasen, Nuovo Cimento 39, 941 (1965).

11. T. Regge, Nuovo Cimento 14, 951 (1959); 18, 947 (1960).

12. G. Höhler, J. Baacke, H. Schlaile and P. Sonderegger, Phys. Letters 20, 79 (1966).

13. V. Barger and M. Ebel, Phys. Rev. 138, B1148 (1965).

14. See, e.g. J.L. Schonfelder and F. Riordan, The K-matrix, Absorption Corrections and Regge Poles; University of Birmingham Report, 1970; C. Risk, The Derivation of the Absorption Model from Feynman Diagrams, Lawrence Radiation Laboratory Report No: UCRL - 19453.

15. J.T. Donohue, Phys. Rev. 163, 1549 (1967).

16. M. Gell-Mann, Phys. Rev. 125, 1067 (1962).

17. G. Ebel, H. Pilkuhn and F. Steiner, Proceedings of the Lund International Conference on Elementary Particles, Lund, 1969.

18. Particle Data Group, Rev. Mod. Phys. 42, 87 (1970).

19. R.H. Dalitz, Strange Particles and Strong Interactions, Oxford, 1962.

20. H.D.D. Watson, J.H.R. Migneron, Phys. Letters 19, 424 (1965). J.H.R. Migneron and K. Moriarty, Phys. Rev. Letters 18,978 (1967); J.H.R. Migneron and H.D.D. Watson, Phys. Rev. 166,1654 (1968).

21. H.D.D. Watson, R. Migneron, K. Moriarty, D. Fincham and A.P. Hunt, Nuovo Cimento 62A, 127 (1969).

22. D.G. Fincham, A.P. Hunt, J.H.R. Migneron and K. Moriarty, Nucl. Phys. B13, 161 (1969).

23. D.G. Fincham, J.H.R. Migneron and K.J.M. Moriarty, Nuovo Cimento 57A, 588 (1968).
F.D. Gault, B.J. Hartley, J.H.R. Migneron and K.J.M. Moriarty, Nuovo Cimento 62, 269 (1969).

24. B. Werner, R. Davis, R. Ammar, W. Kropac, H. Yarger, Y. Cho, M. Derrick, D. Johnson, B. Musgrove, T. Wangler and D. Griffiths, Nucl. Phys. B23, 37 (1970).

25. Aachen-Berlin-Birmingham-Bonn-Hamburg-London (I.C.)-München Collaboration, Phys. Rev. 138, B897 (1965).

26. P. Slatterly, H. Kraybill, B. Forman and T. Ferbel, University of Rochester Report No: UR-875-153;
Aachen-Berlin-CERN Collaboration, Phys. Letters 27,174 (1968);
J.A. Gaidos, R.B. Williams, J.W. Lamsa, C.R. Ezell and F.T. Meiere, Purdue University Report No: COO-1428-144;
J. Bellam, A. Brody, G. Chadwick,Z.G.T. Guiragossian, W.B. Johnson, R.R. Larsen, D.W.G.S. Leight and E. Pickup, private communication to G. Wolf, Phys. Rev. 182, 1538 (1969).

27. R.S. Holmes, J.C. Berlinghieri, M. Farber, T. Ferbel, P. Slattery, B. Werner and H. Yuta, University of Rochester Report No: UR-875-313.

28. Bruxelles-CERN Collaboration, Nuovo Cimento 49A, 9 (1967); 61A, 397 (1969).

29. Aachen-Berlin-CERN Collaboration, Phys. Letters 19, 608 (1965).

30. M. Froissart, Phys. Rev. 123, 1053 (1961).

31. V. Barger, Regge Analysis of High-Energy Scattering Data, invited talk presented at the Regge Pole Conference, University of California, Irvine 1969.

32. Saclay-Orsay-Pisa Collaboration, Nucl. Phys. B16, 335 (1970).

33. R.W. Moore, K.J.M. Moriarty and J.H.R. Migneron, J. Phys. A, 4, 244 (1971).

34. Particle Data Group, Rev. Mod. Phys. 42, 87 (1970). Recent experiments at 17 and 20 GeV/c have shown that the A_2 is not split, private communication from B. Hyams and S.J. Lindenbaum respectively.

35. G. McClellan, N. Mistry, P. Mostek, H. Ogren, A. Osborne, A. Silverman, J. Swartz, R. Talman and O. Diambrini-Palazzi, Phys. Rev. Letters 23, 718 (1969).

36. L. Bertocchi, Proceedings of the International Conference on Elementary Particles, Heidelberg, 1967.

37. M. Le Bellac, Phys. Letters 25B, 524 (1967).

38. J.V. Allaby, Yu. B. Bushnin, S.P. Denisov, A.N. Diddens, R.W. Dobinson, S.V. Donskov, G. Giacommelli, Yu. P. Gorin, A. Klovning, A.I. Petrukhin, YU. D. Prokoshkin, R.S. Shuvalov, C.A. Stahlbrandt and D.A. Stoyanova, Phys. Letters 30B, 500 (1969).

39. V. Barger and R.J.N. Phillips, Phys. Letters 31B, 643 (1970).

40. W.M. Bugg, Bulletin of the American Physical Society, 12, 470 (1967).

41. P. Sonderegger, invited paper presented at the 5th. Moriond Meeting, 1970.

42. D. Amati, S. Fubini and A. Stanghellini, Nuovo Cimento 26, 896 (1962)

43. S. Mandelstam, Nuovo Cimento 30, 1127 (1963);
30, 1148 (1963).

44. G.E. Hite, Rev. Mod. Phys. 41, 669 (1969).

45. B.J. Hartley, R.W. Moore and K.J.M. Moriarty,
Phys. Rev. 187, 1921 (1969);
Phys. Rev. D1, 954 (1970);
P.A. Collins, B.J. Hartley, R.W. Moore and K.J.M. Moriarty,
Nucl. Phys. B20, 381 (1970); Phys. Rev. D1, 3195 (1970).
P.A. Collins, B.J. Hartley, J.D. Jenkins, R.W. Moore and
K.J.M. Moriarty, Phys. Rev. D1, 2619 (1970).

46. G.L. Kane, F. Henyey, D.R. Richard, M. Ross and
G. Williamson, Phys. Rev. Letters 25, 1519 (1970);
M. Ross, F.S. Henyey and G.L. Kane, Nucl.Phys. B23, 269 (1970).

47. C.E. Jones and V. Teplitz, Phys. Rev. 159, 1271 (1967).

48. S. Mandelstam and L.L. Wang, Phys. Rev. 160, 1490 (1967).

49. R.C. Arnold, Phys. Rev. 153, 1523 (1968).

50. Aachen-Berlin-CERN Collaboration, Nucl. Phys. B24, 509 (1970).

51. A complete survey can be found in S.A. Adjei, P.A. Collins,
B.J. Hartley, R.W. Moore and K.J.M. Moriarty, A Parameter-Free
Reggeized Absorption Model for Meson-Baryon Scattering, ICTP/70/19.

52. S.A. Adjei, P.A. Collins, B.J. Hartley, R.W. Moore and
K.J.M. Moriarty, A Parameter-Free Reggeized Absorption Model for
Δ(1236) Production in Proton-Proton Reaction, ICTP/70/20.

53. For a fixed-pole model with U(6,6) symmetry see ref. 23b.

54. B. Petersson and N.A. Törnqvist, Nucl. Phys. B13, 629 (1969); N.A. Törnqvist, CERN Report No: TH.1094 (1969); P.A. Collins, B.J. Hartley, R.W. Moore and K.J.M. Moriarty, Phys. Rev. D1, 3134 (1970); Nucl. Phys. B22, 150 (1970).

55. S.A. Adjei, P.A. Collins, B.J. Hartley, R.W. Moore and K.J.M. Moriarty, A Veneziano Model for $K^-p \to K^{*-}\pi^+n$ and $K^-p \to \bar{K}^{*o}$ taking some account of spin, ICTP/70/13.

56. S.A. Adjei, P.A. Collins, B.J. Hartley, R.W. Moore and K.J.M. Moriarty, Phys. Rev. D3, 150 (1971); An Attempt at the Inclusion of spin in the Generalized Veneziano Model for $K^-p \to \bar{K}^o\pi^-p$ and $K^-p \to K^{*-}p$, ICTP/70/21.

57. S.A. Adjei, P.A. Collins, B.J. Hartley, R.W. Moore and K.J.M. Moriarty, Phys. Rev. D3, May (1971). Residue Recurrence Relations for the Veneziano Model, ICTP/70/3; A Daughterless Dual Model, ICTP/70/12.

58. S.A. Adjei, P.A. Collins, B.J. Hartley, R.W. Moore and K.J.M. Moriarty, A Veneziano Model with cuts for $\bar{K}N$ and KN Charge-Exchange Scattering, ICTP/70/1.

59. P.A. Collins, B.J. Hartley, R.W. Moore, K.J.M. Moriarty and G. Parry, A Veneziano Model with cuts for Higher-spin Production, ICTP/70/24.

60. S.A. Adjei, P.A. Collins, B.J. Hartley, R.W. Moore and K.J.M. Moriarty, An Efficient Partial-Wave Analyzer with Application to the Reggeized Absorption Model, invited paper presented by K.J.M. Moriarty, Institute of Physics and the Physical Society, Conference on Computational Physics, London, 1970.

61. C. Lovelace, Nucl. Phys. B12, 253 (1969).

62. R.C. Beckwith, 1968, private communication.

63. R.J. Eden, High-Energy Collisions of Elementary Particles, (Cambridge University Press, New York, 1967).

64. M. Jacob and G.C. Wick, Ann. Phys. (N.Y.) 7, 404 (1959).

65. A.H. Stroud and D. Secrest, Quadrature Formulas, (Prentice-Hall, Inc., Englewood Cliffs, N.J., 1966).

66. See Ref. 45c.